12-2016

Pharmacokinetics, Tissue Distribution, Synergistic Activity, and Antitumor Activity of Two Isomeric Flavones

Crystal L. Whitted
East Tennessee State University

Pharmacokinetics, Tissue Distribution, Synergistic Activity, and Antitumor Activity of Two Isomeric Flavones

---

A dissertation

presented to

the faculty of the Department of Pharmacology

East Tennessee State University

In partial fulfillment

of the requirements for the degree

Doctor of Philosophy in Biomedical Science Pharmaceutical Science Concentration

---

by

Crystal L. Whitted

December 2016

Dr. Victoria Palau, Chair

Dr. Sam Harirforoosh

Dr. Zac Walls

Dr. Gary Wright

Dr. Koyamangalath Krishnan

Keywords: Flavone A, Flavone B, Pharmacokinetic, Colon cancer, Anticancer

ABSTRACT

Pharmacokinetics, Tissue Distribution, Synergistic Activity, and Antitumor Activity of Two Isomeric Flavones

by

Crystal Whitted

Flavonoids are polyphenolic secondary metabolites found in plants that have bioactive properties including antiviral, antioxidant, and anticancer. Two isomeric flavones were extracted from G*naphalium elegans* and *Achyrocline bogotensis,* plants used by the people from the Andean region of South America as remedies for cancer. 5,7-dihydroxy-3,6,8-trimethoxy-2-phenyl-4H-chromen-4-one (5, 7–dihydroxy- 3, 6, 8 trimethoxy flavone/ flavone A) and 3,5-dihydroxy-6,7,8-trimethoxy-2-phenyl-4H-chromen-4-one (3, 5–dihydroxy-6, 7, 8–trimethoxy flavone/ flavone B) have shown antineoplastic activity against colon cancer cell lines dependent upon their differentiation status. Pharmacokinetic studies reported herein were used to determine dosing for antitumor assays, as well as determine target tissue concentration. These included the development of methods to extract the flavones from plasma or colon tissue and reverse phase high performance liquid chromatography methods for quantification. Quantification methods were linear (r^2 e 0.99) with plasma calibration curves ranging from 250 - 2,500 ng/mL and 2,500 - 100,000 ng/mL for both flavones and colon calibration curves ranging from 250 – 100,000 ng/g (flavone A) and 1,000-25,000 ng/g (flavone B). Intravenous administration of a 20 mg/kg dose in rats yielded half-lives of 83.68 ± 56.61 and 107.45 ± 53.31 minutes with clearance values of 12.99 ± 13.78 and 80.79 ± 35.06 mL/min/kg for flavones A and B, respectively. Analysis of colon tissue yielded concentrations of 1639 ± 601 ng/g (flavone A) and 5975 ± 2480 ng/g (flavone B), suggesting both may be good candidate for individual or adjunct therapy for colon

cancer due to distribution to the target tissue. Preliminary studies in colon cancer cells CaCo 2 and HCT 116 using either flavone in combination with 5-fluorouracil (5-FU) suggested synergistic activity of these compounds. The combination treatment increased induction of apoptosis by enhancing the DNA damaging mechanism of 5-FU. *In vivo*, preliminary xenograft experiments using HCT 116 cells showed smaller tumors in mice dosed with flavone B as compared to the 5-FU or combination treatment. Further experiments are warranted to confirm these observations.

TABLE OF CONTENTS

LIST OF TABLES

Table Page

LIST OF FIGURES

Figure Page

CHAPTER 1

INTRODUCTION

Flavonoids are polyphenolic secondary metabolites found in plants that have a common phenylbenzopyrone structure (C6-C3-C6) (Figure 1). Over 5,000 flavonoids have been discovered (Cai et al. 2003). These are divided into several subgroups depending on the presence of double bonded oxygen, a hydroxyl group, a double bond in the C ring, or the carbon of the C ring to which the B ring attaches (Figure 2) (Liu et al. 2010; Middleton et al. 2000).

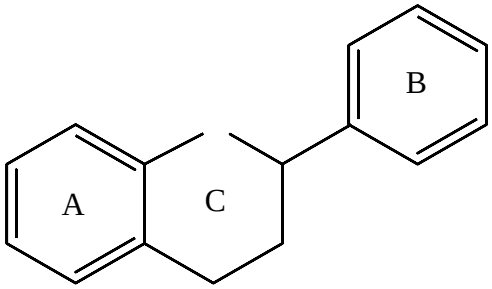

Figure 1.#

(Xiao et al. 2014). Another subgroup, flavonols are associated with a reduced risk of esophageal cancer in current smokers (Vermeulen et al. 2013) and inversely associated with the risk of bladder cancer (Zamora-Ros et al. 2014). Individual flavonoids such as eupatorin, apigenin, naringen, aromadendrin, fisetin, nobiletin, and quercerin display antineoplastic properties *in vitro* (Chiang et al. 2006; Choudhury et al. 2013; Doleckova et al. 2012; Khan et al. 2008; Surichan et al. 2012; Wesolowska et al. 2007; Wu et al. 2005), while other flavonoids such as tectochrysin, anthocyanin, kaempferol, and quercertin for example, display antitumor properties *in vivo* (Ha et al. 2015; Park et al. 2015; Song et al. 2015; Yang et al. 2015).

Our laboratory investigates flavonoids from plants belonging to the family Compositae (Asteraceae) including the genera Gnaphalium and Achyrocline. These are annual or perennial herbs with worldwide distribution, and some are used for traditional folk medicine (Zheng et al. 2013). In the Andean region of South America, G*naphalium elegans* and *Achyrocline bogotensis* are used to make hot beverages commonly recommended as a remedy for cancer. Investigation into the compounds that are possibly responsible for the anticancer activity of these plants has yielded a pair of isomeric flavones, 5,7-dihydroxy-3,6,8-trimethoxy-2-phenyl-4H-chromen-4-one (5, 7–dihydroxy- 3, 6, 8 trimethoxy flavone/ flavone A) and 3,5-dihydroxy-6,7,8-trimethoxy-2-phenyl-4H-chromen-4-one (3, 5–dihydroxy-6, 7, 8–trimethoxy flavone/ flavone B) (Figure 3) (Torrenegra et al. 1980; Torrenegra et al. 1982). *In vitro,* flavone A and flavone B have differential antineoplastic activity against colon, pancreatic, breast, and prostate cancer cell lines with little cytotoxicity to normal colon fibroblast cells (Thomas et al. 2012).

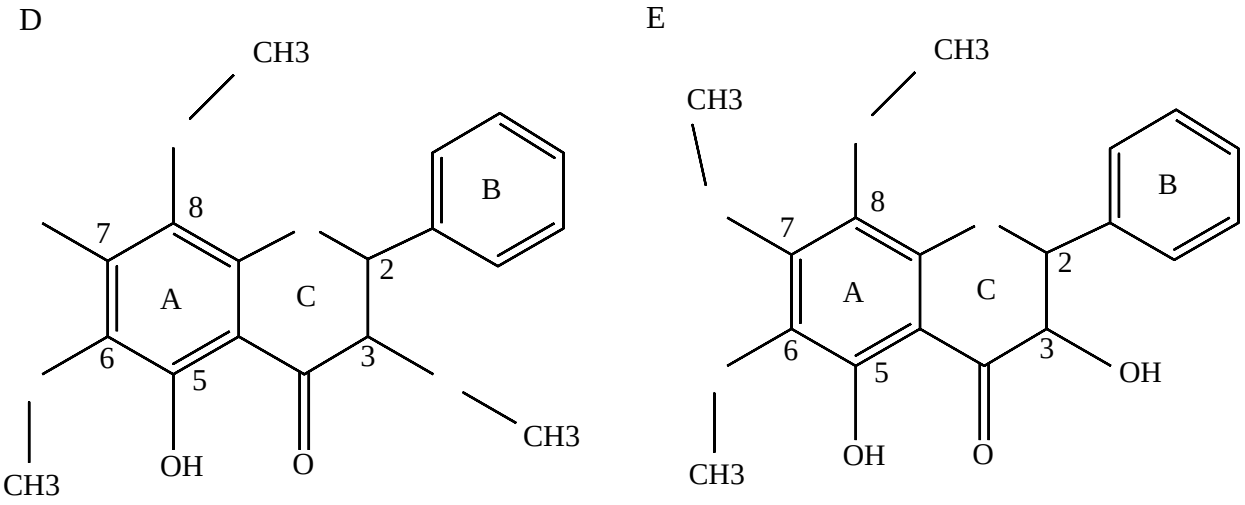

Figure 3. Flavone structures (A) 5,7-dihydroxy-3,6,8-trimethoxy-2-phenyl-4H-chromen-4-one (5, 7–dihydroxy- 3, 6, 8 trimethoxy flavone/ flavone A) from G*naphalium elegans* (B) 3,5-dihydroxy-6,7,8-trimethoxy-2-phenyl-4H-chromen-4-one (3, 5–dihydroxy-6, 7, 8–trimethoxy flavone/ flavone B) from *Achyrocline bogotensis.*

The mechanisms used by several flavonoids to achieve their anticancer effect involve the induction of apoptosis (Chiang et al. 2006; Das et al. 2012; Ha et al. 2015; Hwang et al. 2005). This can be accomplished by activating either the extrinsic or intrinsic pathway. The role of the extrinsic pathway is to remove unwanted cells during development, and train the immune system, as well as trigger immune-system-mediated tumor removal (Boatright and Salvesen 2003). The extrinsic pathway is activated by a ligand binding a death receptor such as the Fas or TRAIL receptor, followed by binding of the Fas-associated protein with death domain (FADD) to caspase 8. Subsequently, FADD is capable of activating caspase 8/10 which results in the activation of the executioner caspase 3/7. The intrinsic pathway eliminates cells damaged by ionizing radiation and chemotherapeutic drugs, as well as those with mitochondrial damage. Certain developmental cues or decreased levels of active pro-survival proteins such as ERK, S6, and BAD can also trigger the intrinsic pathway. Once the pathway is triggered, the mitochondrial membrane is permeabilized by proapoptotic BAX or BAK, releasing cytochrome *c*. Caspase 9 is

then activated followed by the activation of caspase 3/7 (Boatright and Salvesen 2003; Cohen 1997; Nagata 1997). Although both flavone A and flavone B induce apoptosis, they use different apoptotic pathways (LeJeune et al. 2015). Flavone A activates the intrinsic apoptotic pathway by downregulating the active, phosphorylated forms of ERK, S6, and BAD. Dephosphorylated BAD is then targeted to the mitochondria where it binds to BCL2 and BCL-$_{XL}$ and trigger apoptosis (Chattopadhyay et al. 2001). Flavone B is able to activate the extrinsic pathway of apoptosis via the concomitant increase of pERK and pc-JUN ultimately causing cell death (LeJeune et al. 2015).

Although *in vitro* activity of flavone A and flavone B have been investigated, no studies have been performed with either flavone *in vivo.* In order to determine a suitable dose for the *in vivo* studies, the pharmacokinetics of a drug must be known. Pharmacokinetics is the study of how the body acts on a drug (Shargel et al. 2005). This includes different aspects of metabolism, absorption, distribution, and excretion of a drug. It is studied by taking blood samples at various times prior and post dosing to determine the concentration of the drug in plasma. The plasma concentration time profile can be used to determine parameters such as half-life ($t_{1/2}$), volume of distribution (Vz), clearance (CL), and area under the curve (AUC). Tissue samples can be collected to determine distribution of the drug, while urine, and feces samples can help determine the rate and route of excretion.

The pharmacokinetic parameter half-life is the amount of time required for the concentration of drug to decrease by half in plasma (Shargel et al. 2005). This information is necessary to determine the frequency in which a drug needs to be administered. As the drug travels through the body, a certain percentage may be distributed to the tissues. The volume of distribution is used to determine the amount of drug that distributed throughout the body. Tissue

samples collected post dosing an animal can help determine which organs a drug is distributed to and in what percent of the total drug concentration administered. The distribution patterns of a drug can influence the effectiveness of drug used against a certain disease.

As the drug travels through the body it is broken down by metabolism and excreted by the kidneys. Clearance is the rate at which this process occurs. Measuring the concentrations of the drug in the urine and feces can help determine how much of the drug is cleared by excretion and what percent of the drug is metabolized. Another parameter that is helpful in understanding how the body affects the drug is the systemic exposure or the total concentration of drug in plasma from administration to a set time post dosing or total elimination.

There are several different models to describe the pharmacokinetic of a drug (Shargel et al. 2005). The simplest model is a one compartment open model which considers the body as one container. The two compartment open model considers the blood, extracellular fluid, and highly perfused tissues as one compartment while the tissues in which the drug equilibrates more slowly is the second compartment. The three compartment open model adds bone and fat as a third compartment to the two compartment model. Each pharmacokinetic parameter is calculated slightly differently depending on the model in which the drug plasma concentration time profile fits. These calculations can also be made using a noncompartment model which uses no assumptions for a specific compartment model to analyze data.

In the studies described in chapters 2 and 3, rats were used to determine pharmacokinetic parameters such as half-life, volume of distribution, clearance, area under the curve, and target tissue concentration due to sensitivity of the HPLC method and their larger blood volume compared to mice. Using rats allowed for the collection of blood samples at more time points to

give us a better picture of the effect of the body on the flavones. Since flavone A and flavone B have been reported to have antineoplastic activity against colon cancer *in vitro (Thomas et al. 2012),* colon tissues were collected to determine if the flavones distribute to the target organs which would influence the effectiveness of these drugs as anticancer therapies and are discussed in chapter 3.

The *in vitro* antitumor activity of these flavones against colon cancer is important because it suggests possible activity *in vivo*. Colorectal cancer is the third most common type of cancer found in both men and women in the United States. The American Cancer Society (ACS) projects that 95,270 new cases of colon cancer will be diagnosed in 2016 and will result in 40,000 deaths (American Cancer Society 2016). Colon cancer can be detected at an early stage to have a 90% five-year survival rate after treatment. However, 60% of colon cancer patients are diagnosed after the cancer has spread to other organs, when the five year survival rate is found to drop to 13% (American Cancer Society 2015).

The drastic difference in the five-year survival rates for colon cancer is due in part to the ability to surgically remove cancerous tissue confined to the colon. However, once it has spread to other part of the body, alternative forms of treatment including chemotherapy and radiation are used to treat the disease (American Cancer Society 2016). The most commonly used chemotherapy drug for colon cancer is the thymidylate synthase inhibitor, 5-fluorouracil (5-FU). A metabolite of 5-FU, 5-fluoro-dUMP (FdUMP), binds with thymidylate synthase (TS) and 5,10-methylene-tetrahydrofolate (CH2-THF) preventing the conversion of dUMP to dTMP. Without dTTP being added to the nucleotide pool, dUTP gets inserted into DNA instead. The dTTP depletion also causes another 5-FU metabolite, 5-deoxyuridine triphosphate (FdUTP), to also be incorporated into the DNA (Geng et al. 2011; Ghoshal and Jacob 1997; Peters et al.

2002). Unfortunately, the effect of 5-FU is not specific to cancer cells, and may result in several side effects. This drug has a 10-20% response rate in colon cancer patients (Gu et al. 2013; Longley et al. 2003; Rashid et al. 2014; Zhang et al. 2008).

The low five-year survival rate and low response rate of current therapies for colon cancer warrant an urgent need for the development of new therapies. One strategy for increasing the effectiveness of 5-FU is to add a secondary therapy with a different mechanism of action, in order to increase the antineoplastic activity of the drug. Chapter 4 discusses the effect of using flavone A or flavone B in combination with 5-FU against colon cancer *in vitro* and the mechanism by which cell death is suggested to occur.

The pharmacokinetic studies discussed in chapter 3 determined that both flavone A and flavone B distributed to the colon of the rats. These results indicated that both flavones were good candidates for *in vivo* antitumor assays seeking to investigate the effect of the flavone on colon cancer tumors. Over the years many different mouse models have been developed in order to study different aspects of cancer. These models include xenografts of tumor cells, and transgenic mice (Herreros-Villanueva et al. 2012). Some of these models are good for testing the effect of a drug on tumor growth while others are better for testing tumor prevention or genetic modifications in tumorigenic cells.

There are two different types of xenograft models, heterotopic and orthotopic (Herreros-Villanueva et al. 2012). The heterotopic model implants cancer cells between the muscle and dermis of an immune compromised mouse. This can be done on the flank, shoulder, or foot pad of the mouse. This is the most commonly used model for preclinical testing of anticancer drugs due to the short time period required, and reproducibility. Furthermore, in this model the tumor

is visible and can be easily measured to determine changes in tumor growth over time, or by fluorescent imaging if the cancer cells used for the xenograft, have been fluorescently tagged.

The heterotopic xenograft model does have the disadvantage in that the cancer cells are not located in the target organ. This causes changes in the microenvironment that can affect the effectiveness of the drug. Differences in drug distribution can also cause changes in the effect of a drug as a drug might get distributed to the subcutaneous tumor but not the target organ. Another disadvantage of this model is that subcutaneous tumors rarely metastasize (Becher and Holland 2006; Killion et al. 1998; Niedergethmann et al. 2007).

The orthotopic xenograft model injects cancer cells into the respective organ. The advantage of this model is that the microenvironment and distribution of the drug are the same for the tumor and target organ. In addition, these tumors are able to metastasize and site specific studies for genes changes and drug therapy can be replicated. Unfortunately, this type of xenograft is labor intensive, technically challenging, as well as expensive. This method takes longer as there is a healing and recovery time. Since the tumors are not on the surface of the animal, low throughput imaging is required to monitor changes in tumor volume (Niedergethmann et al. 2007). Of the two xenograft models, the heterotopic option is good to use in preclinical studies investigating the antitumor activity of a drug. However, the orthotopic xenograft is better in studies investigating changes in gene expression and tumor metastasis in response to therapy (Niedergethmann et al. 2007).

In this dissertation, the heterotopic xenograft model was used to determine the *in vivo* antitumor activity of flavone B against colon cancer as well as the synergistic activity of flavone B with 5-fluorouracil and is described in chapter 4.

CHAPTER 2

DEVELOPMENT OF REVERSED-PHASE HIGH PERFORMANCE LIQUID CHROMATOGRAOHY METHODS FOR QUANTIFICATION OF TWO ISOMERIC FLAVONES AND THE APPLICATION OF METHODS TO PHARMACOKINETICS STUDIES IN RATS

Crystal L. Whitted[1], Victoria E. Palau[1,2], Ruben D. Torrenegra[3], and Sam Harirforoosh[1*]

[1]Department of Pharmaceutical Sciences, Gatton College of Pharmacy, East Tennessee State University, Johnson City, Tennessee, United States

[2]Department of Internal Medicine, Quillen College of Medicine, East Tennessee State University, Johnson City, Tennessee, United States

[3] Department of Environmental Science and Technology, Universidad de Ciencias Aplicadas y Ambientales, Bogota, Colombia

[*]Correspondence: Dr. Sam Harirforoosh, Department of Pharmaceutical Sciences, Gatton College of Pharmacy, East Tennessee State University, Box 70594, Johnson City, TN 37614-1708

E-mail: harirfor@etsu.edu

Fax: +1 423 439 6350

http://dx.doi.org/10.1016/j.jchromb.2015.07.039

Abstract

Isomers 5,7-dihydroxy-3,6,8-trimethoxy-2-phenyl-4H-chromen-4-one (5,7–dihydroxy-3,6,8 trimethoxy flavone) (flavone A) and 3,5-dihydroxy-6,7,8-trimethoxy-2-phenyl-4H-chromen-4-one (3,5–dihydroxy-6,7,8–trimethoxy flavone) (flavone B) have recently demonstrated differential antineoplastic activities against pancreatic cancer *in vitro.* These studies also indicated that these compounds target highly tumorigenic cells while sparing normal cells. The *in vivo* antitumor activities of these flavones have not been determined, and detection protocols for these compounds are needed to conduct pre-clinical assays following intravenous dosing. Here, we report methods developed using acetonitrile to extract two flavone isomers and corresponding internal standards, celecoxib and diclofenac, from rat plasma. Separation was achieved using a Shimadzu liquid chromatography system with a C18 column and mobile phase acetonitrile/water (60:40 and 70:30 for flavones A and B, respectively) containing 0.2% acetic acid and 0.05% triethylamine at a flow rate of 0.4 mL/minute and detection at 245 nm. Calibration curves ranging from 250-2,500 ng/mL and 2,500-100,000 ng/mL for both flavones were linear (r^2 *e* 0.99) with the lower limits of quantification being 250 ng/mL. Recovery of concentrations 250, 1,000, 2,500, 5,000, and 100,000 ng/mL ranged from 87-116% and 84-103% (n=3) for flavone A and B, respectively. Stability of both flavones after a freezing/thawing cycle yielded a mean peak ratio e 0.92 when compared to freshly extracted samples. Intravenous administration of a 20 mg/kg dose in rats yielded half-lives of 83.68 ± 56.61 and 107.45 ± 53.31 minutes with clearance values of 12.99 ± 13.78 and 80.79 ± 35.06 mL/min/kg for flavones A and B, respectively.

Keywords: 5, 7–dihydroxy- 3, 6, 8 trimethoxy flavone, 3, 5–dihydroxy-6, 7, 8–trimethoxy flavone, flavonoids, cancer, HPLC, pharmacokinetics

1. Introduction

Throughout history people have used plants for medicinal purposes. In the Andean mountains of South America, people often rely on a group of plants commonly known as vira- viras to treat different ailments (Thomas et al. 2012). Many of the bioactive compounds found in these plants are part of a class of polyphenolic secondary metabolites called flavonoids, a large family of compounds characterized by a C6-C3-C6 phenylbenzopyrone backbone. They are further subclassified as flavones, isoflavones, flavanones, flavonols, anthocyanidins, and chalcones. Over 5,000 flavonoids have been discovered, but the potential health benefit of only a few have been studied (Cai et al. 2003). Pharmacological properties of flavonoids include antioxidant (Benariba et al. 2013; Choudhary et al. 2008), antiviral (Lin et al. 2013; Zandi et al. 2012), antidiabetic (Konate et al. 2014), as well as protective properties of the gastrointestinal tract (Mota et al. 2009), and cardiovascular system (Middleton et al. 2000). Anticancer studies have shown some flavonoids to prevent or inhibit the development of cancer in rodents (Ito et al. 2000; Kandaswami et al. 2005; Lambert 2013; Record et al. 1997; Yang et al. 2001). The antineoplastic properties of flavonoids are due to their effect on cell growth, inhibition of kinase activity, induction of apoptosis, suppression of the secretion of matrix metalloproteinases, and/or tumor invasive behavior (Chiang et al. 2006; Dole•ková et al. 2012; Kandaswami et al. 2005).

Gnaphalium elegans and *Achyrocline bogotensis* are two of the species identified generically as vira– viras that are traditionally used in the treatment of various cancers. A pair of isomeric flavones, 5, 7–dihydroxy- 3, 6, 8 trimethoxy flavone (flavone A) and 3, 5–dihydroxy-6, 7, 8–trimethoxy flavone (flavone B) were isolated from bioactive fractions of *G. elegans* and *A. bogotensis* respectively (Thomas et al. 2012; Torrenegra et al. 1980; Torrenegra et al. 1982; Torrenegra et al. 1987). *In vitro* studies suggest that flavone A and flavone B have differential antineoplastic activity against cancer cell lines, which may depend upon cellular tumorigenic and

differentiation status. Indeed, flavones A and B target cancer cell lines derived from colon, pancreas, breast, and prostate that have been categorized as being highly tumorigenic. Among these, flavone A demonstrated preferential activity against the better differentiated cell lines, while flavone B was shown to be active against the poorly differentiated cells. Furthermore, flavones A and B demonstrated significant cytotoxic activity on cancer cell lines of the pancreas and the colon (Thomas et al. 2012).

Only 6% of the 46,420 new cases of pancreatic cancer projected to be diagnosed during 2014 will survive another 5 years. Of the 96,830 new cases of colon cancer predicted to be diagnosed in 2014, only 40% will be detected at an early stage to have a 90% 5 year survival rate. However, once the cancer has spread to distant organs, the 5 year survival rate drops to13% (American Cancer Society 2014). Thus, new treatments for pancreatic and colon cancer are urgently needed. *In vivo* testing and mechanistic analysis are warranted to further understand the antineoplastic properties of these compounds.

In this study, we developed methods to quantify the concentration of flavone A or flavone B in rat plasma, using high performance liquid chromatography (HPLC) analysis with celecoxib or diclofenac as internal standards, respectively. These methods were used to determine the pharmacokinetic parameters of flavone A and flavone B in rats administered a 20 mg/kg dose via intravenous injection.

2. Experimental

2.1 Chemicals and standards

5,7–dihydroxy- 3,6,8 trimethoxy flavone (flavone A) and 3,5–dihydroxy-6, 7,8–trimethoxy flavone (flavone B) were extracted as described previously (Thomas et al. 2012). NMR analysis was done to verify that compounds were e 99% pure in a Bruker 400MHz spectrometer (Billerica MA). The results were compared to spectra previously obtained (Torrenegra et al.

1980; Torrenegra et al. 1982). Celecoxib was purchased from Toronto Research Chemicals (Toronto, ON, CA). Diclofenac sodium was purchased from MP Biomedicals, LLC (Solon, OH). HPLC grade acetonitrile, acetic acid, triethylamine and water were purchased from Fisher Scientific (Pittsburgh, PA). Polyethylene glycol 400 was purchased from Electron Microscopy Sciences (Hatfield, PA).

2.2 Stock solution and standards

Stock solutions of flavone A (100 µg/mL) and celecoxib (25 µg/mL) were prepared with acetonitrile/water/acetic acid/triethylamine (60:40:0.2:0.05). Stock solutions of flavone B (100 µg/mL) and diclofenac (25 µg/mL) were prepared with acetonitrile/water/acetic acid/trimethylamine, (70:30:0.2:0.05). All solutions were stored protected from light at 4 °C.

2.3 Sample preparation

Calibration curves for flavone A was prepared by spiking 100 µL of blank plasma with 100 µL flavone A, 100 µL celecoxib (25 µg/mL), and 200 µL of organic solvent (acetonitrile). The samples were vortex mixed for 5 seconds before centrifugation for 15 minutes at 4,400 rpm. The supernatant was removed to a clean tube and evaporated using a Labconco vacuum concentrator (Kansas City, MO). 200 µL of mobile phase was used to reconstitute the residue and 100 µL of sample was injected into the HPLC column. Calibration curves for flavone B were prepared in similar manner with diclofenac as the internal standard. Analysis was conducted in triplicate.

2.4 HPLC conditions and quantitation

Assays were performed with a Shimadzu liquid chromatography system (Shimadzu Scientific Instruments Inc., Columbia, Maryland, USA) consisting of a DGU-20A Prominence degasser, of

LC020AB solvent delivery system, SIL-20A$_{HT}$ auto sampler, CBM-20A communication bus module, SPD-M20A diode array detector, and CTO-20A column oven with a C18 (100 × 4.6 mm, 2.6 µm; ACE, Aberdeen, Scotland) column. Mobile phases used were acetonitrile/water/acetic acid/triethylamine 60:40:0.2:0.05 (for flavone A HPLC assay) and 70:30:0.2:0.05 (for flavone B HPLCassay). Detection was at 245 nm with a temperature of 30˚C. Flow rate was 0.4 mL/minute with run times of 11 and 10 minutes respectively. LC solutions program was used to collect and analyze the data. Plotting the peak area ratios of flavone against internal standard in Excel were used to make the calibration curves.

2.5 Accuracy and precision

Calibration curves were used to determine the accuracy and precision of the methods. The coefficient of variation (CV) of three replicates performed on the same day was used to determine the precision for intra-day analysis and the CV of replicates performed on three consecutive days was used for the precision of inter-day analysis. Accuracy was determined by how close the calculated concentration was to the known concentration. Data is presented as mean ± standard deviation.

2.6 Recovery

Five concentrations (250, 1,000, 2,500, 5,000 and 100,000 ng/mL) were used to determine the percent of flavone recovered by the extraction method. Recovery was determined by comparing the peak area ratio of extracted samples to the peak area ratio of non-extracted standard of the same concentration. Experiment was performed in triplicate.

2.7 Stability

Three concentrations (1,000, 5,000, and 100,000 ng/mL) were used to determine the stability of the flavones after freezing/thawing cycle. 100 µL of blank plasma was spiked with 100 µL flavone and put in -20 °C for 24 hours. After thawing, 100 µL of internal standard and 200 µL of acetonitrile were added to the sample. Extraction was completed as describe above. The peak area ratio of frozen samples was compared to the peak area ratio of freshly prepared samples. Experiments were performed in triplicate.

2.8 Animals and drug administration

Male Sprague-Dawley rats weighting 269-305g and fitted with jugular vein cannulas were purchased from Charles River (Raleigh, NC). Animals were housed in a 12 hour light-dark cycle and experiments were carried out within the Animal Care Committee of East Tennessee State University guidelines. During the experiment, rats were housed in metabolic cages. Flavones were mixed in polyethylene glycol 400 and administered by intravenous injection to deliver a 20 mg/kg dose of flavone A (n=6) or flavone B (n=6). Serial blood samples (250 µL) were collected at 0, 5, 15, 30, 60, 90, 120, 240, and 360 minutes post dosing. After 3 minutes of centrifugation at 10,000 rpm, plasma collected and stored at -20 ˚C.

2.9 Pharmacokinetic analysis

Outliers were determined using SPSS Statistics software version 21. The non-compartmental component of Phoenix WinNonlin (v.6.3) was used to calculate the pharmacokinetic parameters such as clearance (CL), area under the plasma concentration-time curve from zero to t (AUC_{0-t}), area under the plasma concentration-time curve from zero to infinity ($AUC_{0-\infty}$), half-life ($t_{1/2}$),

and volume of distribution (Vz) for both flavones. A Student's t-test was used to determine statistical differences between the pharmacokinetic parameter of flavone A and B.

3. Results

3.1 Specificity

Chromatograms of blank plasma, blank plasma spiked with celecoxib, and blank plasma spiked with celecoxib and flavone A are shown in Figure 1. Chromatograms of blank plasma, blank plasma spiked with diclofenac, and blank plasma spiked with diclofenac and flavone B are shown in Figure 2. The retention times for flavone A and celecoxib are 7.0 and 9.6 minutes, respectively. Retention times for diclofenac and flavone B are 5.0 and 6.8 minutes, respectively. Good separation was achieved and no interfering peaks were seen under these chromatographic conditions.

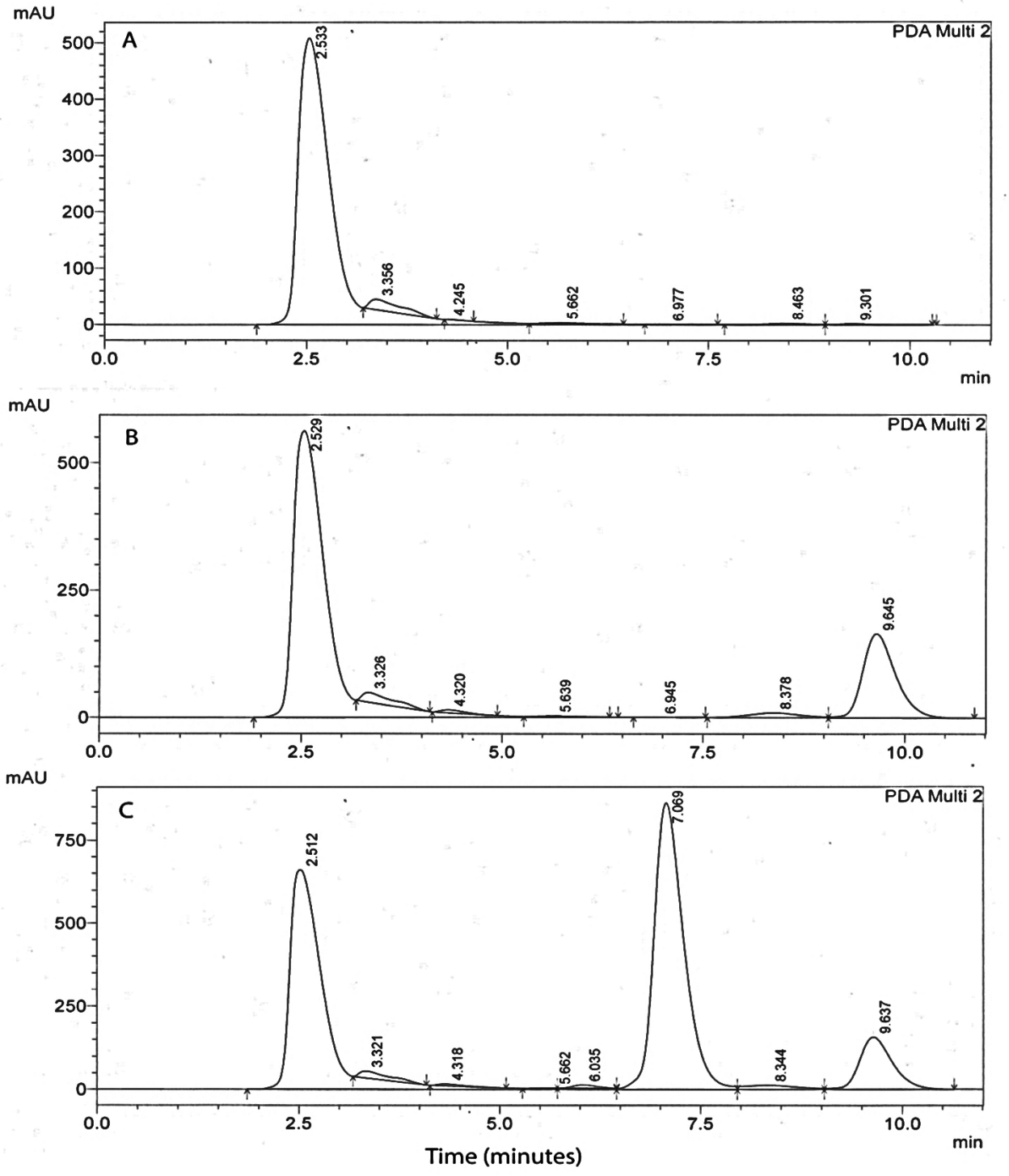

Figure 1. Elution of flavone A from plasma. HPLC chromatographs of (A) blank plasma; (B) plasma spiked with internal standard (celecoxib 25 µg/ ml); (C) plasma spiked with flavone A (100 µg/ml) and internal standard.

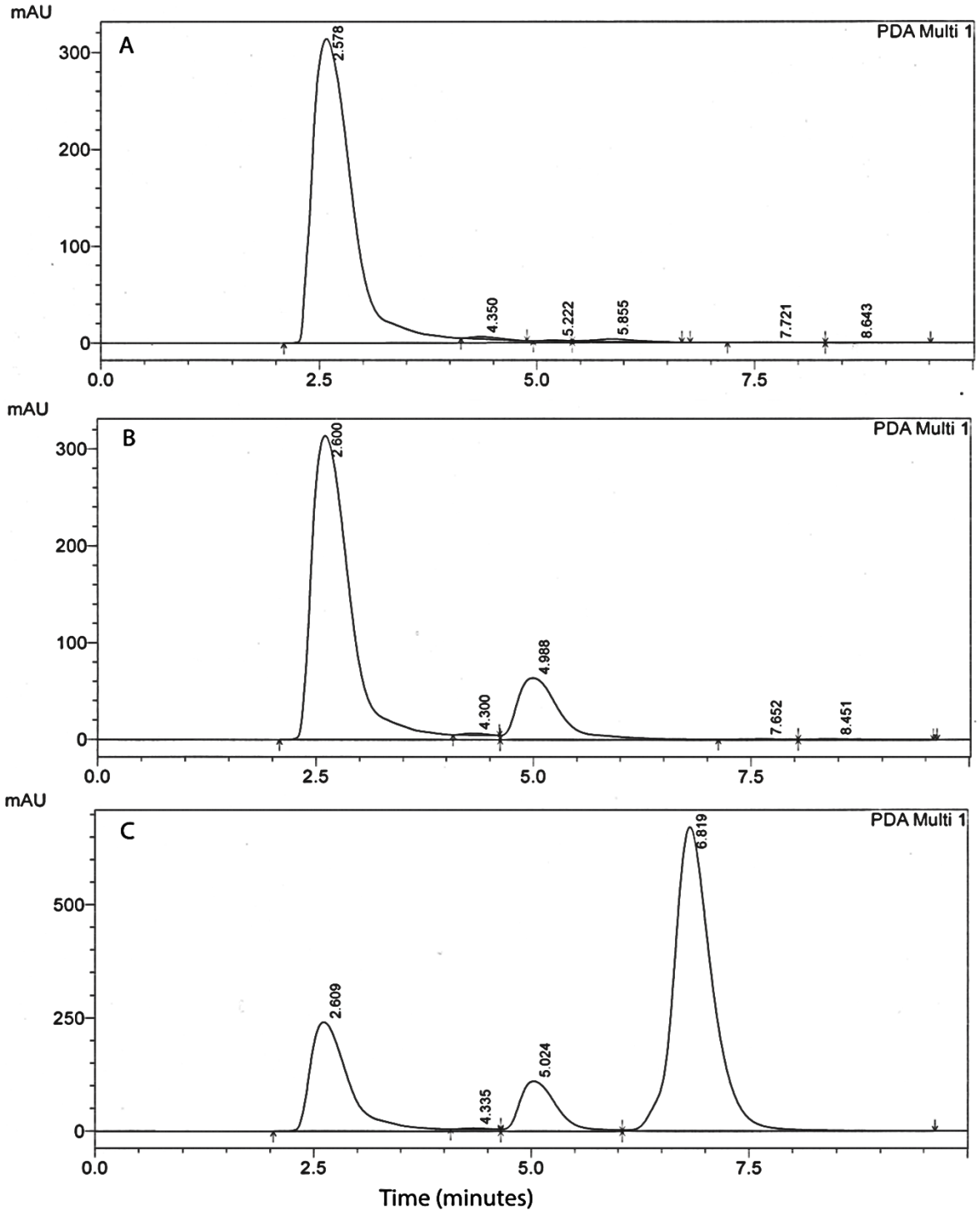

Figure 2. **Elution of flavone B from plasma.** HPLC chromatographs of (A) blank plasma; (B) plasma spiked with internal standard (diclofenac 25 µg/ml); (C) plasma spiked with internal standard and flavone B (100 µg/ml).

3.2 Linearity, lower limit, and precision

For both flavones, calibration curves were divided into 250-2,500 ng/mL and 2,500-100,000 ng/mL sections. The 2,500-100,000 ng/mL curve for flavone A has the representative calibration equation of y = 0.000048x + 0.03024 while the 250-2,500 ng/mL curve has the representative equation of y = 0.00005x + 0.01752 (Figure 3). Good linearity can be seen for flavone A with r^2 = 0.9991 and r^2 = 0.9917, respectively. For flavone B, the representative calibration equation for the 2,500-100,000 ng/mL curve was y = 0.00006x while the 250-2,500 ng/mL curve equation was y = 0.000148x + 0.00458 (Figure 4). These curves also had good linearity with r^2 = 0.9994 and r^2 = 0.9958, respectively. The lower limit of quantification (coefficient of variation < 40) for both flavone A and B in plasma was 250 ng/mL (Tables 2 and 4).

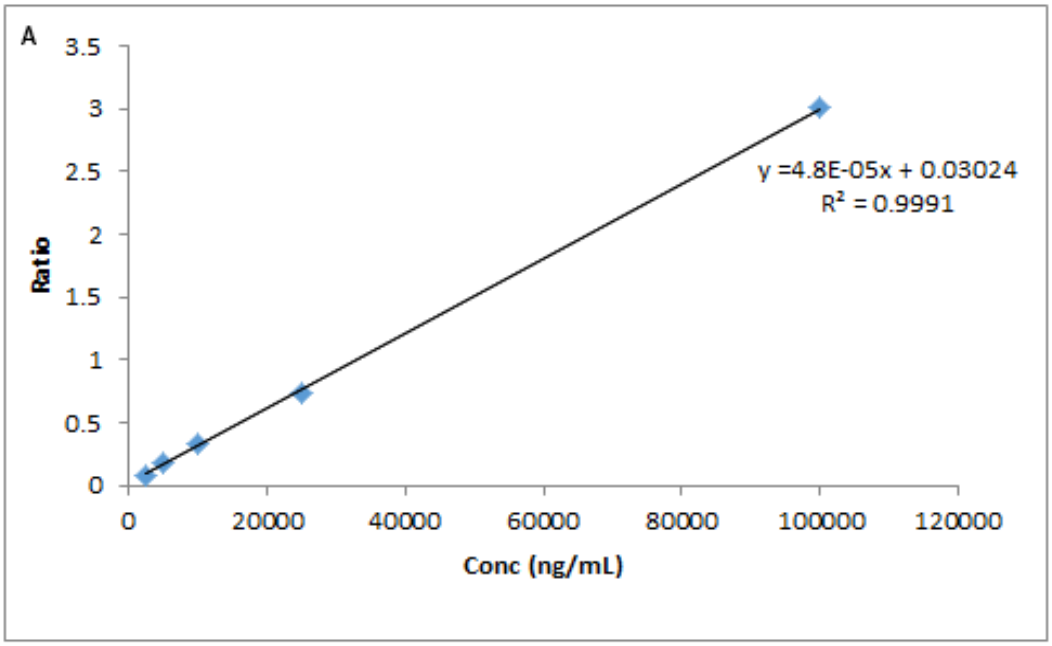

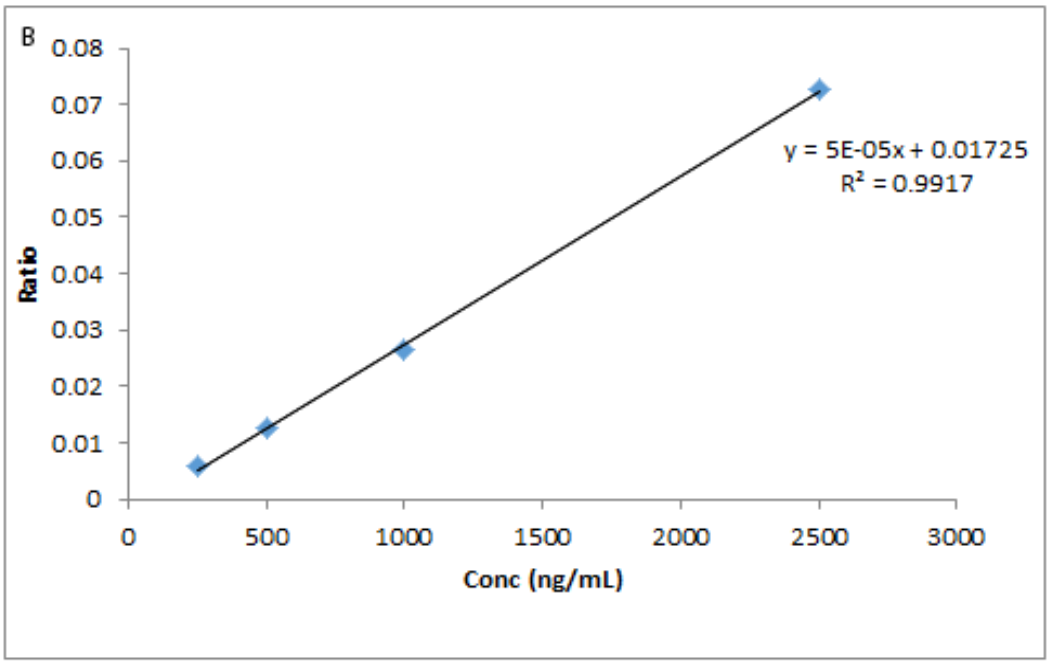

Figure 3. **Calibration curves for flavone A extracted from plasma.** Calibration curves were made by graphing the flavone/internal standard area under the curve extracted from plasma versus the known concentration of flavone A ranging from (A) 2,500-100,000 ng/mL or (B) 250-2,500 ng/mL.

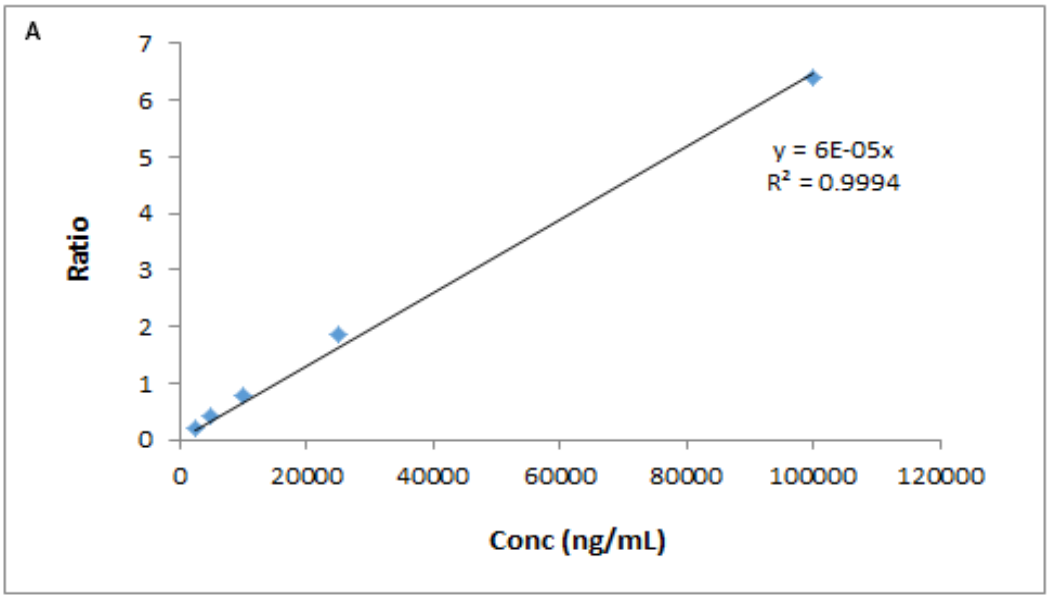

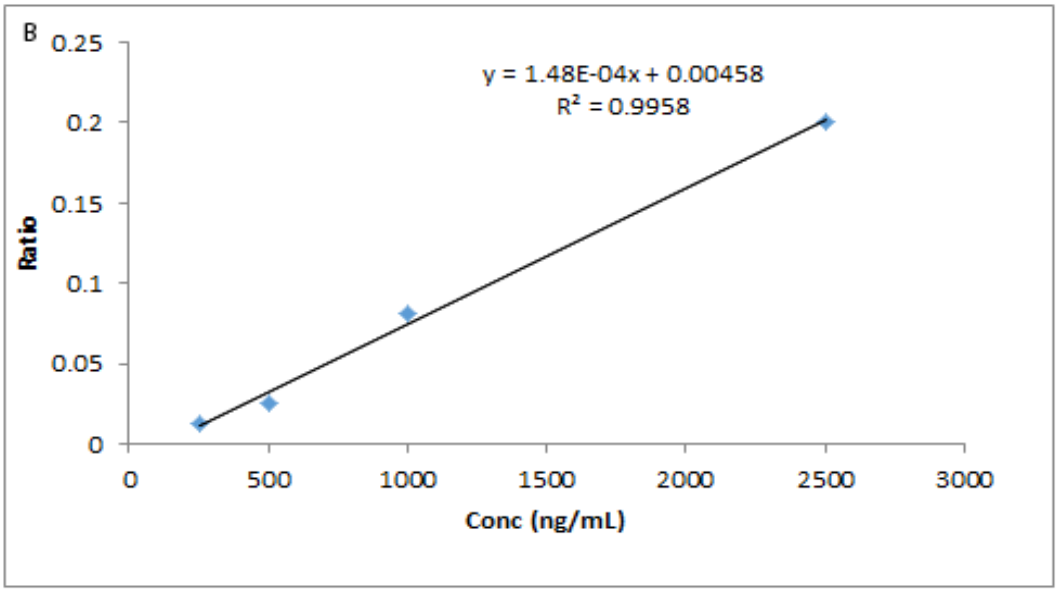

Figure 4. **Calibration curves for flavone B extracted from plasma.** Calibration curves were made by graphing the flavone/ internal standard area under the curve extracted from plasma versus the known concentration of flavone B ranging from (A) 2,500-100,000 ng/mL or (B) 250-2,500 ng/mL.

Intra-day precision was determined by three calibrations curves performed in the same day. Inter-day precision was determined by calibration curves performed on three consecutive days. Intra-day coefficient of variation for flavone A (Tables 1 and 2) and B (Tables 3 and 4) were d 20.23 and d 39.94, respectively. The accuracy ranged from 94-112% for flavone A and 83-124% for flavone B. Inter-day coefficient of variation for flavone A and B were d 22.44 and d 16.18 respectively. The accuracy ranged from 83-111% for flavone A and 89-103% for flavone B, respectively.

Table 1. Intra-day and inter-day precision and accuracy for 2500-100000 ng/mL flavone A extracted from rat plasma

Concentration (ng/mL)	Error intra-day (%)	Observed intra-day (n=3)	CV	Accuracy (%)
100000	2.51 ± 1.82	98830 ± 3277	3.31	98
25000	4.43 ± 4.72	24028 ± 1347	5.61	96
5000	8.28 ± 6.29	5126 ± 576	11.24	102
2500	17.38 ± 12.31	2774 ± 514	18.56	110
Concentration (ng/mL)	Error inter-day (%)	Observed inter-day (n=3)	CV	Accuracy (%)
100000	6.61 ± 4.28	103582 ± 8033	7.75	103
25000	9.17± 7.33	26843 ± 2481	9.24	107
5000	4.43 ± 3.85	4898± 308	6.29	97
2500	12.53 ± 2.69	2186 ± 67	3.07	87

Table 2. Intra-day and inter-day precision and accuracy for 250-2500 ng/mL flavone A extracted from rat plasma				
Concentration (ng/mL)	Error intra-day (%)	Observed intra-day (n=3)	CV	Accuracy (%)
2500	3.54 ± 1.83	2494 ± 117	4.71	99
1000	12.53 ± 11.32	1125 ± 113	10.06	112
500	11.25 ± 10.94	516 ± 85	16.57	103
250	12.61 ± 13.26	236 ± 48	20.23	94
Concentration (ng/mL)	Error inter-day (%)	Observed inter-day (n=3)	CV	Accuracy (%)
2500	5.92 ± 3.39	2509 ± 199	7.96	100
1000	15.07 ± 12.65	996 ± 223	22.44	99
500	11.75 ± 13.59	558± 68	12.17	111
250	16.54 ± 9.02	208 ± 23	11.03	83

Table 3. Intra-day and inter-day precision and accuracy for 2500-100000 ng/mL flavone B extracted from rat plasma				
Concentration (ng/mL)	Error intra-day (%)	Observed intra-day (n=3)	CV	Accuracy (%)
100000	3.71 ± 2.52	103140 ± 3497	3.39	103
25000	4.16 ± 2.35	23958 ± 588	2.46	96
5000	9.68 ± 3.36	4515 ± 168	3.73	90
2500	9.71 ± 2.22	2257 ± 56	2.48	90
Concentration (ng/mL)	Error inter-day (%)	Observed inter-day (n=3)	CV	Accuracy (%)
100000	3.11 ± 3.18	104648 ± 2355	2.28	103
25000	4.89 ± 2.64	25450 ± 1999	7.84	102
5000	10.88 ± 4.61	4781 ± 334	6.98	96
2500	10.51 ± 9.30	2223 ± 149	6.7	89

Table 4. Intra-day and inter-day precision and accuracy for 250-2500 ng/mL flavone B extracted from rat plasma				
Concentration (ng/mL)	Error intra-day (%)	Observed intra-day (n=3)	CV	Accuracy %
2500	8.28 ± 2.11	2535 ± 255	10.07	101
1000	7.43 ± 5.77	1068 ± 67	6.28	106
500	24.31 ± 17.38	621 ± 87	13.98	124
250	20.95 ± 29.27	209 ± 83	39.94	83
Concentration (ng/mL)	Error inter-day (%)	Observed inter-day (n=3)	CV	Accuracy %
2500	4.56 ± 3.42	2527 ± 160	6.35	101
1000	4.51 ± 4.83	1027 ± 65	6.35	102
500	10.86 ± 9.03	487 ± 79	16.18	97
250	9.20 ± 9.42	259 ± 35	13.4	103

3.3 Recovery

Recovery was determined by comparing the peak area ratio of extracted sample to peak area ratio for non-extracted standards of specific concentration (250, 1,000, 2,500, 5,000, and 100,000 ng/mL). This experiment was performed in triplicate with mean recovery ranging 87-116% for flavone A and 84-102% for flavone B, respectively (Tables 5 and 6).

Table 5. Recovery of flavone A extracted from rat plasma		
Concentration (ng/mL)	Recovery (%)	RSD (%)
100000	87	4.01
5000	102	6.02
2500	106	8.70
1000	116	10.04
250	92	25.40

Table 6. Recovery of flavone B extracted from rat plasma		
Concentration (ng/mL)	Recovery (%)	RSD (%)
100000	92	3.10
5000	102	1.78
2500	84	15.20
1000	103	7.92
250	101	4.11

3.4 Stability

Stability was determined by comparing the peak area ratio of spiked plasma that had been frozen with peak area ratio of samples that had been freshly prepared for concentrations 1,000, 5,000, and 100,000 ng/mL. This experiment was performed in triplicate with mean peak ratio ranging from 0.93-1.04 for flavone A and 0.92-1.09 for flavone B, respectively (Table 7).

Table 7. Stability of flavone A and flavone B in rat plasma after freeze/thaw cycle (n=3)					
Flavone A			**Flavone B**		
Concentration (ng/mL)	Mean peak area ratio	RSD (%)	Concentration (ng/mL)	Mean peak area ratio	RSD (%)
100000	1.01	4.82	100000	1.05	3.61
5000	0.93	18.68	5000	1.09	3.53
1000	1.04	25.84	1000	0.92	5.29

3.5 Pharmacokinetics of flavones A and B following a single intravenous injection

The plasma concentration-time profile for flavone A after the administration of a 20 mg/kg dose via intravenous injection is shown in Figure 5A. The pharmacokinetic parameters are listed in Table 8. Flavone A has a short half-life of 83.68 ± 56.61 minutes and clearance of 12.99 ± 13.78 mL/min/kg. The plasma concentration-time profile and pharmacokinetic parameters for flavone B after the intravenous administration of a 20 mg/kg dose are shown in Figure 5B and table 9.

The half-life of flavone B is calculated to be 107.45 ± 53.31 minutes with a clearance of 80.79 ± 35.06 mL/min/kg.

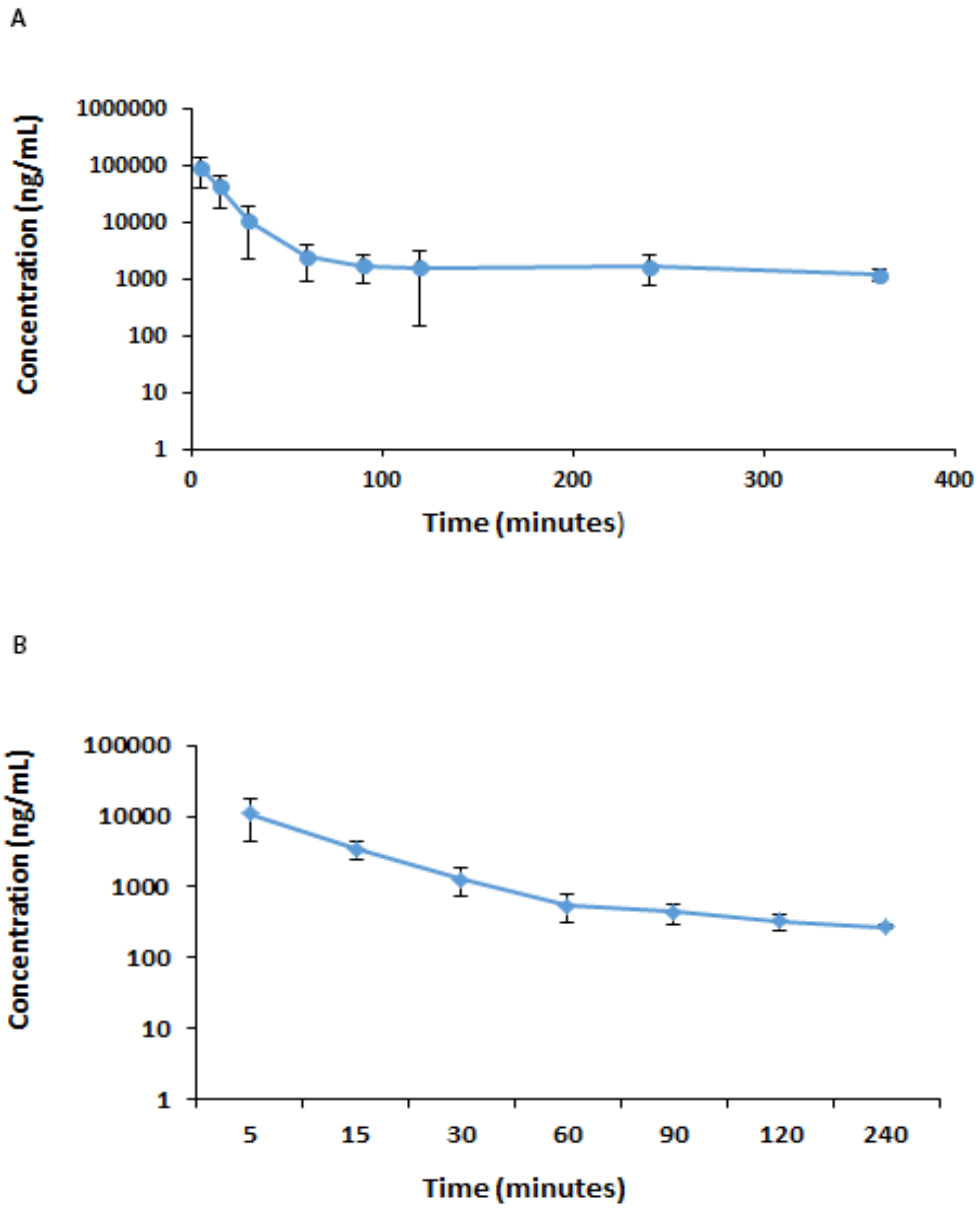

Figure 5. Area under the plasma concentration-time (AUC) curves. AUC following intravenous administration of 20 mg/kg doses of (A) flavone A or (B) flavone B.

Table 8. Pharmacokinetic parameters of flavone A after administration of a 20 mg/kg dose via intravenous injection (n=6)	
Parameters	Values
$t_{1/2}$ (min)	83.68 ± 56.61
Vz (mL/kg)	986.77 ± 591.30
CL (mL/min/kg)	12.99 ± 13.78
AUC_{0-360} (µg*min/mL)	2358.14 ± 1200.70
$AUC_{0-\infty}$ (µg*min/mL)	2492.82 ± 1244.27

Legend: $t_{1/2}$ - half-life, V_Z – volume of distribution, CL – total clearance, AUC_{0-t} – area under the plasma concentration-time curve from 0 to 360 minutes, $AUC_{0-\infty}$ - area under the plasma concentration-time curve from time 0 to infinity.

Table 9. Pharmacokinetic parameters of flavone B after administration of a 20 mg/kg dose via intravenous injection (n=6)	
Parameters	Values
$t_{1/2}$ (min)	107.45 ± 53.31
Vz (mL/kg)	11463.50 ± 5936.69
CL (mL/min/kg)	80.79 ± 35.06
AUC_{0-240} (µg*min/mL)	245.47 ± 112.47
$AUC_{0-\infty}$ (µg*min/mL)	289.14 ± 121.58

Legend: $t_{1/2}$ - half-life, V_Z – volume of distribution, CL – total clearance, AUC_{0-t} – area under the plasma concentration-time curve from 0 to 240 minutes, $AUC_{0-\infty}$ - area under the plasma concentration-time curve from time 0 to infinity.

4. Discussion

Our previous studies have shown that isomeric flavones A and B have significant antineoplastic activity against highly tumorigenic pancreatic and colon cancer cell lines with varying differentiation status (Thomas et al. 2012). In the current study, we developed simple HPLC methods to determine the concentration of either flavone A or B in rat plasma. The methods described in this paper provide good separation of the flavones from the plasma peaks and internal standards. To optimize our methods, several ratios of acetonitrile and water of differing pH were used to achieve separation from the plasma peak. Also, a variety of compounds were tested to determine the most appropriate internal standards, including flavonoids, vitamins, statins, and nonsteroidal anti-inflammatory drugs. Most compounds, especially the flavonoids, overlapped with the drug or the plasma peak. Celecoxib and diclofenac gave the best peaks without overlapping, as well as good run times close to 10 minutes (Figures 1 and 2).

The described assays provide satisfactory and reproducible quantification of the flavones in concentrations ranging from 250-100,000 ng/mL (Tables 1-4). The assays were linear for both flavone A and flavone B (Figure 3). The extraction method used yielded satisfactory, consistent recovery for both flavones at all concentrations (Tables 5 and 6). Freezing and thawing of spiked plasma samples showed that both flavones were not degraded during the process (Table 7).

Both flavone A and B have short half-lives (< 120 minutes) that are commonly seen in flavonoids (Talbi et al. 2014; Yang et al. 2014; Zhang et al. 2014; Zhu et al. 2015). The area under plasma concentration-time profiles shows that flavone B disappears from the plasma at a faster rate than flavone A (Figure 5). The concentrations of flavone B were below the limits of detection (250 ng/mL) by 360 minutes, whereas flavone A was still detectable at that time. This difference in plasma levels was also seen in the AUC_{0-}. values ($p = 0.0015$) depicted in tables 8

and 9. These observations correspond with the higher volume of distribution ($p = 0.0015$) and higher clearance ($p = 0.0013$) values of flavone B compared to those of flavone A. Part of the observed rapid disappearance of flavone B in plasma could be explained by the higher lipophilic nature of this flavone (Thomas et al. 2012). This is further supported by reports that flavonoids can be incorporated into the erythrocyte cell membrane causing an echinocytic form of these cells, and into epithelial cell membranes (Bonarska-Kujawa et al. 2014; Pawlikowska-Pawlega et al. 2014). The lipophilic nature of the compounds may also favor their rapid distribution into tissues.

5. Conclusion

Extraction methods were developed for flavones A and B from rat plasma that have been validated in terms of recovery, linearity, precision, and accuracy. The HPLC methods developed for flavones A and B have good separation and detection for the ranges of 250-100,000 ng/mL. Pharmacokinetic analysis of flavone A and B reveal them to have short half-lives comparable to other flavonoids.

Conflict of interest

All authors declare that there are no conflicts of interest.

Acknowledgements

This work was funded by a grant from the East Tennessee State University Research Development Committee Major Grants Program. We would like to thank Mr. Dustin L. Cooper for his technical assistance.

References

[1] C.M. Thomas, R.C. Wood, 3rd, J.E. Wyatt, M.H. Pendleton, R.D. Torrenegra, O.E. Rodriguez, S. Harirforoosh, M. Ballester, J. Lightner, K. Krishnan, V.P. Ramsauer, PloS one, 7 (2012) e39806.

[2] H. Cai, R.D. Verschoyle, W.P. Steward, A.J. Gescher, Biomedical chromatography : BMC, 17 (2003) 435-439.

[3] M.I. Choudhary, S. Hareem, H. Siddiqui, S. Anjum, S. Ali, R. Atta Ur, M.I. Zaidi, Phytochemistry, 69 (2008) 1880-1885.

[4] N. Benariba, R. Djaziri, W. Bellakhdar, N. Belkacem, M. Kadiata, W.J. Malaisse, A. Sener, Asian Pacific Journal of Tropical Biomedicine, 3 (2013) 35-40.

[5] K. Zandi, B.T. Teoh, S.S. Sam, P.F. Wong, M.R. Mustafa, S. Abubakar, BMC Complement Altern Med, 12 (2012) 214.

[6] Y.T. Lin, Y.H. Wu, C.K. Tseng, C.K. Lin, W.C. Chen, Y.C. Hsu, J.C. Lee, PloS one, 8 (2013) e54466.

[7] K. Konate, K. Yomalan, O. Sytar, P. Zerbo, M. Brestic, V.D. Patrick, P. Gagniuc, N. Barro, Evidence-based complementary and alternative medicine : eCAM, 2014 (2014) 867075.

[8] K.S. Mota, G.E. Dias, M.E. Pinto, A. Luiz-Ferreira, A.R. Souza-Brito, C.A. Hiruma-Lima, J.M. Barbosa-Filho, L.M. Batista, Molecules, 14 (2009) 979-1012.

[9] E. Middleton, Jr., C. Kandaswami, T.C. Theoharides, Pharmacological reviews, 52 (2000) 673-751.

[10] J.D. Lambert, The American journal of clinical nutrition, 98 (2013) 1667S-1675S.

[11] C.S. Yang, J.M. Landau, M.T. Huang, H.L. Newmark, Annual review of nutrition, 21 (2001) 381-406.

[12] C. Kandaswami, L.T. Lee, P.P. Lee, J.J. Hwang, F.C. Ke, Y.T. Huang, M.T. Lee, In vivo, 19 (2005) 895-909.

[13] I.R. Record, J.L. Broadbent, R.A. King, I.E. Dreosti, R.J. Head, A.L. Tonkin, International journal of cancer. Journal international du cancer, 72 (1997) 860-864.

[14] C. Ito, M. Itoigawa, H.T. Tan, H. Tokuda, X. Yang Mou, T. Mukainaka, T. Ishikawa, H. Nishino, H. Furukawa, Cancer letters, 152 (2000) 187-192.

[15] I. Dole•ková, L. Rárová, J. Grúz, M. Vondrusová, M. Strnad, V. Kryštof, Fitoterapia, 83 (2012) 1000-1007.

[16] L.C. Chiang, L.T. Ng, I.C. Lin, P.L. Kuo, C.C. Lin, Cancer letters, 237 (2006) 207-214.

[17] R.D. Torrenegra, S. Escarria, B. Raffelsberger, H. Achenbach, Phytochemistry, (1980) 2795–2796.

[18] R.D. Torrenegra, P. Pedrozo, C. Rojas, S. Carrizosa, Revista Latinoamericana de Quı´mica, (1987) 116–118.

[19] R.D. Torrenegra, S. Escarria, E. Tenorio, H. Achenbach, Rev Latinoam Quim, (1982) 75–76.

[20] American Cancer Society, in, American Cancer Society, Altanta, 2014.

[21] S. Zhu, H. Yan, K. Niu, S. Zhang, J Chromatogr Sci, 53 (2015) 909-914.

[22] W.M. Zhang, R.F. Li, M. Sun, D.M. Hu, J.F. Qiu, Y.H. Yan, J Chromatogr B Analyt Technol Biomed Life Sci, 965 (2014) 107-111.

[23] Y.F. Yang, Z. Li, W.F. Xin, Y.Y. Wang, W.S. Zhang, Chinese journal of natural medicines, 12 (2014) 632-640.

[24] A. Talbi, D. Zhao, Q. Liu, J. Li, A. Fan, W. Yang, X. Han, X. Chen, Molecules, 19 (2014) 5538-5549.

[25] D. Bonarska-Kujawa, S. Cyboran, R. Zylka, J. Oszmianski, H. Kleszczynska, BioMed research international, 2014 (2014) 783059.

[26] B. Pawlikowska-Pawlega, L.E. Misiak, A. Jarosz-Wilkolazka, B. Zarzyka, R. Paduch, A. Gawron, W.I. Gruszecki, Biochimica et biophysica acta, 1838 (2014) 2127-2138.

CHAPTER 3

QUANTIFICATION OF TWO ISOMERIC FLAVONES IN RAT COLON TISSUE USING REVERSE PHASE HIGH PERFORMANCE LIQUID CHROMATOGRAPHY

Introduction

Many flavonoids have been recognized for their antitumor properties (Kale et al. 2008; Kandaswami et al. 2005; Lopez-Lazaro 2002; Wang 2000). It is known that these activities are greatly determined by their chemical structure which subsequently dictates their ability to interact with cellular molecules (Lopez-Lazaro 2002). This differential effect has been observed with flavone isomers flavones 5,7–dihydroxy-3, 6, 8–trimethoxy flavone (flavone A) and 3, 5–dihydroxy-6, 7, 8–trimethoxy flavone (flavone B) (Thomas et al. 2012). Specifically, each isomer has been shown to target colon cancer cells with distinct phenotypical characteristics via different mechanisms of action (LeJeune et al. 2015). However, it is unknown whether either of these flavones distribute to the colon after intravenous administration of these compounds. Modifications were made to methods developed for extracting and quantifying these flavones in rat plasma using reverse phase high performance liquid chromatography. The modifications included preparation of the sample by homogenization in water and filtration using a polyvinylidene fluoride (PVDF) membrane, and the creation of calibration curves to determine the concentration of either flavone in colon tissue.

These methods allowed for the detection of flavone A and flavone B in rat colon. Our data indicate that flavone B was found in higher concentrations in the colon than flavone A, which may be the result of higher volume of distribution value of flavone B (Whitted et al. 2015) compared to that of flavone A.

Method and Results

Procedure to extract and purify flavones A and B

The compounds were obtained as described before (Thomas et al. 2012). Briefly, flavone A was purified from dried flowers of *Gnaphalium elegans* extracted with chloroform using a silica gel chromatography column. Flavone B was purified from leaves of *Achyrocline bogotensis*, using chloroform, followed by crystallizations in hexane. The physical and spectroscopic properties of these compounds allowed their proper identification.

Stock solution and standards

Stock solutions of flavone A at a concentration of 100 µg/mL, prepared as described previously (Whitted et al. 2015), and 25 µg/mL celecoxib (Toronto Research Chemicals; Toronto, ON, CA) were prepared with acetonitrile/water/acetic acid/triethylamine (60:40:0.2:0.05). Stock solutions of 100 µg/mL of flavone B, prepared as described previously(Whitted et al. 2015), and 25 µg/mL diclofenac (MP Biomedicals, LLC; Solon, OH) were prepared with acetonitrile/water/acetic acid/trimethylamine (70:30:0.2:0.05). All stock solutions were stored protected from light at 4ºC. HPLC grade acetonitrile, acetic acid, trimethylamine, and water were purchased from Fisher Scientific (Pittsburgh, PA). Flavone A or flavone B were mixed with polyethylene glycol 400 (Electron Microscopy Sciences; Hatfield, PA) for intravenous injection.

Sample preparation

Colon tissue was homogenized using a PowerGen 700 from Fisher Scientific (Pittsburgh, PA) in a 1:2 ratio with water (1 mg/ 2 mL). Serial concentrations for calibration curves (flavone

A: 250-100000 ng/g and flavone B: 1000-25000 ng/g) were prepared. Briefly, 100 µL of blank homogenate was spiked with 100 µL flavone, 100 µL internal standard (25 µg/mL celecoxib or diclofenac), and 200 µL of organic solvent (acetonitrile). The samples were vortex mixed before being centrifuged for 15 min at 3000 x g. The supernatant was removed and filtered with a polyvinylidene fluoride (PDVF) filter (0.45 µm) into a clean tube and evaporated using a Labconco vacuum concentrator (Kansas City, MO). Mobile phase (200 µL) was used to reconstitute the residue and 100 µL of sample was injected into the HPLC column. Analysis was conducted in triplicate.

HPLC conditions and quantitation

HPLC assays were performed using a Shimadzu liquid chromatography system (Shimadzu Scientific Instruments Inc., Columbia, Maryland, USA) with an ACE C18 (100×4.6 mm) (Aberdeen, Scotland) column. Mobile phases used for HPLC contained acetonitrile/water 60:40 (flavone A) and 70:30 (flavone B) with 0.2% acetic acid and 0.05% triethylamine. Detection wavelength was at 245 nm with a temperature of 30 ºC. Flow rate was 0.4 mL/min with run times of 11 and 10 min, respectively. LC solutions program was used to collect and analyze the data. Good separation was achieved (Figures 1 & 2) and the peak area ratios of flavone against internal standard were plotted in Excel to make the calibration curves (Figure 3). Representative equation for flavone A concentrations 250–100000 ng/g was y = 2E-05x + 0.0029 and flavone B concentrations 1000-25000 ng/g was y = 7E-05x + 0.0531 with r^2 e 0.99.

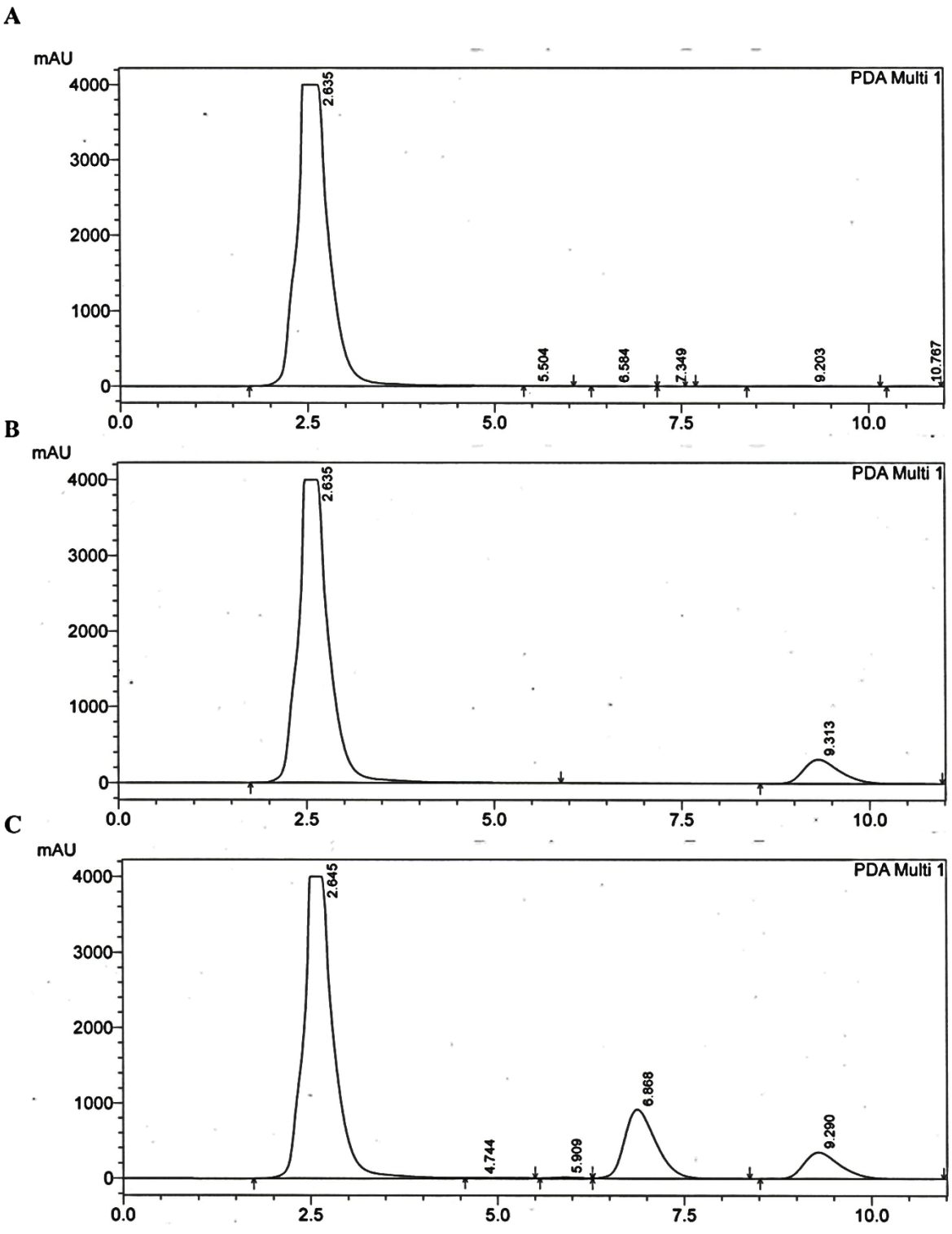

Figure 1. Elution of flavone A from colon**.** HPLC chromatographs of (A) blank colon; (B) colon spiked with internal standard (celecoxib 25 µg/mL); (C) colon spiked with flavone A (100 µg/mL) and internal standard.

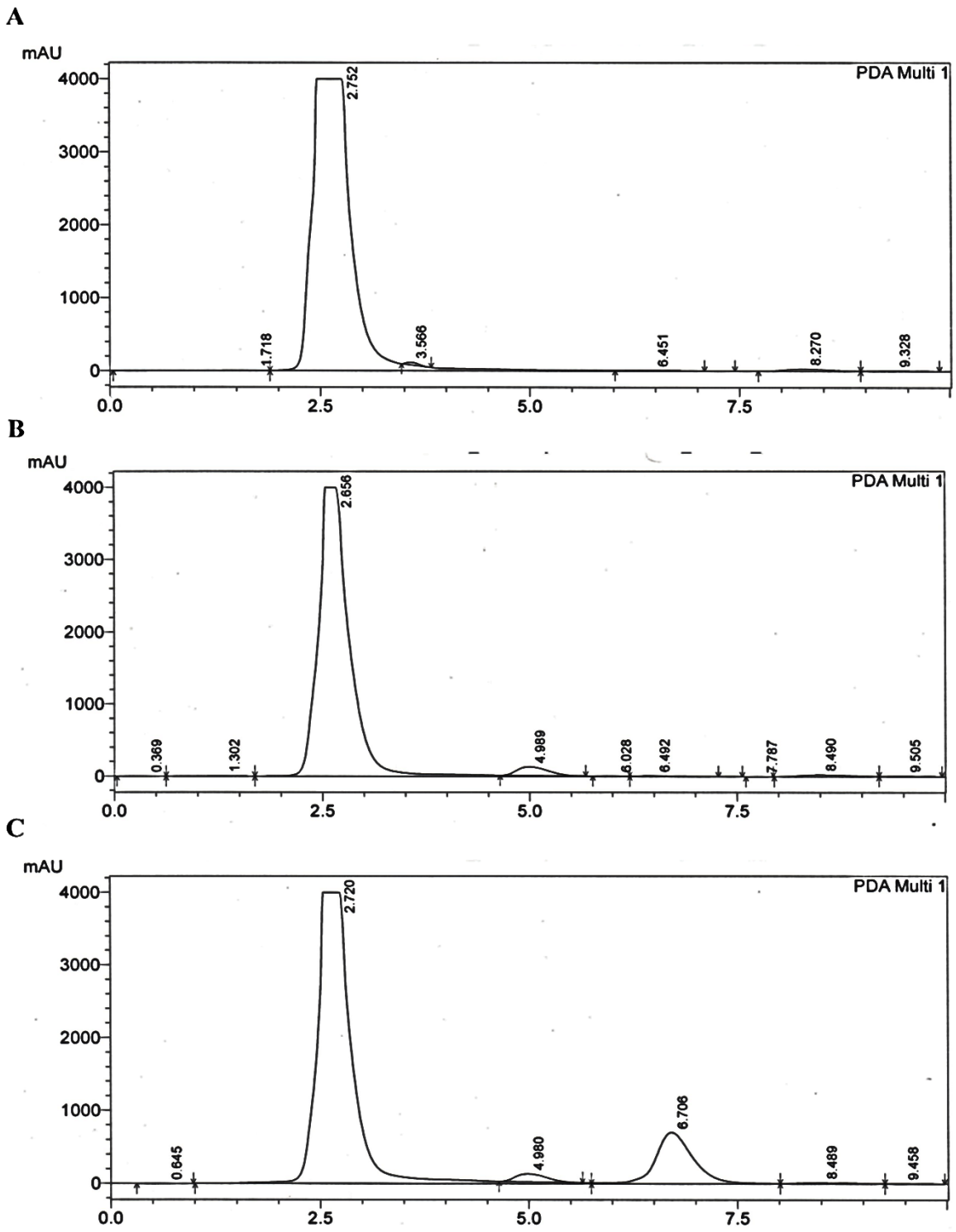

Figure 2. Elution of flavone B from colon**.** HPLC chromatographs of (A) blank colon; (B) colon spiked with internal standard (diclofenac 25 µg/mL); (C) colon spiked with flavone B (100 µg/mL) and internal standard.

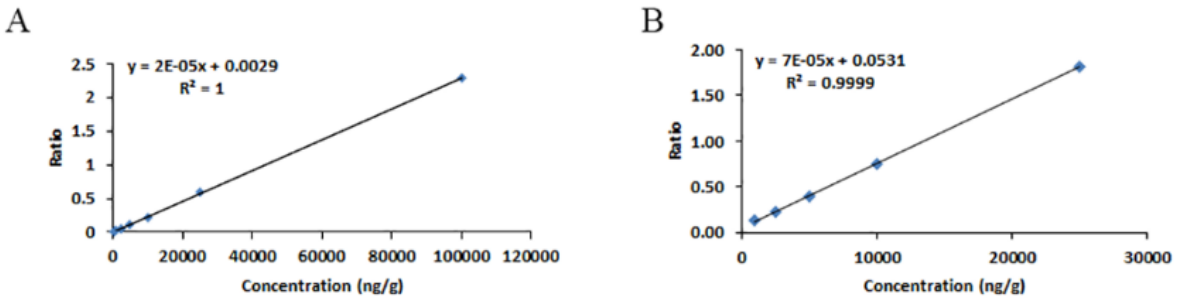

Figure 3. Calibration curves were made by graphing the ratio of flavone/internal standard area under the curve extracted from colon tissue versus the known concentration of flavone. Representative calibration curves for (A) flavone A and (B) flavone B are presented.

Precision and accuracy

Three calibration curves were used to determine the precision (coefficient of variation - CV) and accuracy of the methods. Data is presented as mean ± standard deviation (Tables 1 & 2).

Table 1. Precision and accuracy for 250-100000 ng/g flavone A extracted from rat colon tissue

Concentration (ng/g)	Error (%)	Observed (n=3)	CV	Accuracy (%)
100000	13.88 ± 2.14	113888 ± 2138	1.87	114
25000	16.32 ± 1.06	29081 ± 265	0.91	116
10000	11.83 ± 4.15	11182 ± 415	3.71	111
5000	9.93 ± 0.97	5496 ± 48	0.88	109
2500	13.92 ± 4.87	2848 ± 121	4.27	113
1000	11.45 ± 8.90	1114 ± 89	7.98	111
500	16.65 ± 21.51	558 ±129	23.21	111
250	21.02 ± 19.30	285 ± 68	24.03	113

Table 2. Precision and accuracy for 1000-25000 ng/g flavone B extracted from rat colon tissue				
Concentration (ng/g)	Error (%)	Observed (n=3)	CV	Accuracy (%)
25000	1.51 ± 0.50	25204 ± 410	1.62	101
10000	2.89 ± 0.52	10075 ± 345	3.43	101
5000	3.69 ± 3.42	4934 ± 271	5.51	98
2500	4.22 ± 2.55	2480 ± 142	5.73	99
1000	25.18 ± 27.00	1128 ± 378	33.56	113

Animals and drug administration

The methods described here were used to determine the concentrations of flavone A or flavone B in colon tissue collected from the male Sprague-Dawley rats used in a previous study (Whitted et al. 2015). Briefly, flavones were mixed in polyethylene glycol 400 and were administered by intravenous injection to deliver a 20 mg/kg dose of flavone A (n=6) or flavone B (n=6). Animals were euthanized under anesthesia 6 hours post dosing. Colon tissue was collected and flash frozen using dry ice and stored at -80 ºC until analyzed for the measurement of concentrations of flavones. Analysis yielded 1639 ± 601 ng/g of flavone A and 5975 ± 2480 ng/g of flavone B in colon tissue (Figure 4).

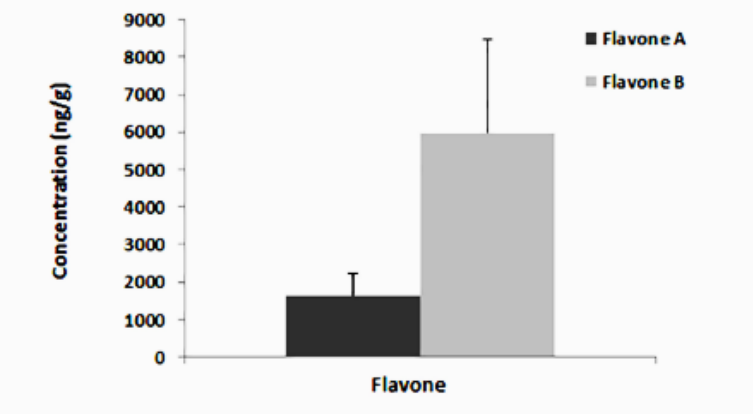

Figure 4. Distribution of flavones to target tissue. Male Sprague-Dawley rats received 20 mg/kg of either flavone A or flavone B via intravenous injection. The colon tissues were collected 6 hours after dosing and analyzed for the presence of flavone using a HPLC system.

Discussion

The modifications made to the methods for extracting flavone A and flavone B from rat plasma enabled the development of good methods for extracting and quantifying these flavones from rat colon tissue. The *in vitro* antineoplastic activity of these flavones against colon cancer cells in combination with both flavones distributing to rat colon tissue makes them good candidates for i*n vivo* experiment investigating their antitumor activity against colon cancer.

REFERENCES

Kale A, Gawande S, Kotwal S. 2008. Cancer phytotherapeutics: Role for flavonoids at the cellular level. Phytother Res. 22(5):567-577.

Kandaswami C, Lee LT, Lee PP, Hwang JJ, Ke FC, Huang YT, Lee MT. 2005. The antitumor activities of flavonoids. In vivo. 19(5):895-909.

LeJeune TM, Tsui HY, Parsons LB, Miller GE, Whitted C, Lynch KE, Ramsauer RE, Patel JU, Wyatt JE, Street DS et al. 2015. Mechanism of action of two flavone isomers targeting cancer cells with varying cell differentiation status. PloS one. 10(11):e0142928.

Lopez-Lazaro M. 2002. Flavonoids as anticancer agents: Structure-activity relationship study. Curr Med Chem Anticancer Agents. 2(6):691-714.

Thomas CM, Wood RC, 3rd, Wyatt JE, Pendleton MH, Torrenegra RD, Rodriguez OE, Harirforoosh S, Ballester M, Lightner J, Krishnan K et al. 2012. Anti-neoplastic activity of two flavone isomers derived from gnaphalium elegans and achyrocline bogotensis. PloS one. 7(6):e39806.

Wang HK. 2000. The therapeutic potential of flavonoids. Expert Opin Investig Drugs. 9(9):2103-2119.

Whitted CL, Palau VE, Torrenegra RD, Harirforoosh S. 2015. Development of reversed-phase high performance liquid chromatography methods for quantification of two isomeric flavones and the application of the methods to pharmacokinetic studies in rats. J Chromatogr B Analyt Technol Biomed Life Sci. 1001:150-155.

CHAPTER 4

THE EFFECT OF TWO ISOMERIC FLAVONES, 5-FLUOROURACIL, AND COADMINISTRATION AGAINST COLON CANCER

Introduction

The American Cancer Society lists colorectal cancer as the second leading cause of death in the United States and estimates that 49,190 death will result from colon cancer alone in 2016 (American Cancer Society 2016). Colon cancer has a 90% five-year survival rate if diagnosed early. Unfortunately, this is expected to only occur for 40% of the 95,270 new cases of colon cancer that are predicted to be diagnosed in 2016. Once the cancer has metastasized to distant organs, the five- year survival rate drops to 13% (American Cancer Society 2015).

Surgery is the most common treatment for localized colon cancer. Once the cancer has spread, chemotherapy is often used (American Cancer Society 2015). 5-fluorouracil (5-FU) has been used to treat a wide variety of cancers including that of the colon for the last 50 years (Rashid et al. 2014; Srimuangwong et al. 2012).

5-fluoro-dUMP (FdUMP), the main active metabolite of 5-FU, forms a complex with thymidylate synthase (TS) and 5,10-methylene-tetrahydrofolate (CH2-THF) preventing dUMP be converted to dTMP causing a depletion of dTTP from the nucleotide pool. This depletion allows for the insertion of dUTP and another 5-FU metabolite, 5-deoxyuridine triphosphate (FdUTP), into DNA (Figure 1A), (Geng et al. 2011; Ghoshal and Jacob 1997; Peters et al. 2002). The DNA damage caused by dUTP and FdUTP triggers Ataxia-telangiectasia mutated and Rad3-

related (ATR) kinase cascade resulting in cell cycle arrest and apoptosis (Figure 1B and C) (Flynn and Zou 2011; Woods and Turchi 2013).

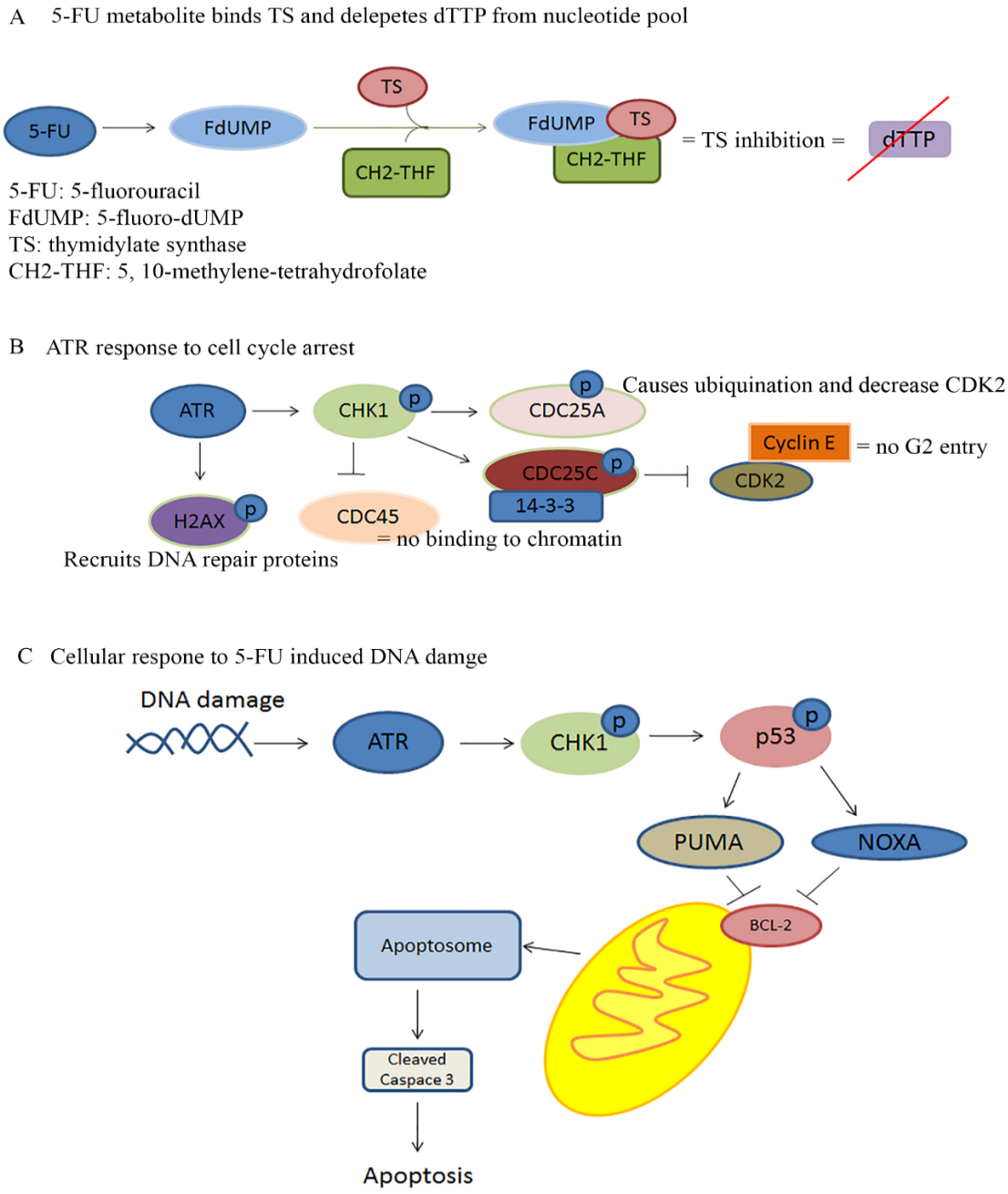

Figure 1. Mechanism of action of 5-fluorouracil. (A) A metabolite of 5-FU (FdUMP) binds TS to delete dTTP from the nucleotide pool. (B) Ataxia-telangiectasia mutated and Rad3-related ATR response to DNA damage. (C) Cellular response to 5-FU induced DNA damage leading to apoptosis.

Unfortunately, the activity of 5-FU is not cancer cell specific, resulting in several side effects and only has a 10-20% response rate in colon cancer patients (Gu et al. 2013; Longley et al. 2003; Rashid et al. 2014; Zhang et al. 2008). One method to try to improve the effectiveness of 5-FU is to include a secondary drug with the treatment (Cheah et al. 2014; Gonzalez-Vallinas et al. 2013; Wang et al. 2014a).

The two isomeric flavonoids, flavone A, and flavone B which are isolated from *Gnaphalium elegans* and *Achyrocline bogotensis,* have been shown by our laboratory to have differential antineoplastic activity against colon cancer (Thomas et al. 2012). Flavone A is cytotoxic to more differentiate CaCo 2 colon cancer cells, while flavone B is effective against the poorly differentiate HCT 116 colon cancer cells. In this chapter, we investigate the mechanisms by which the flavones may cause synergistic effects on colon cancer cell lines when used in combination with 5-FU *in vitro* and *in vivo.*

Methods

Chemicals

Flavone A and flavone B were obtained as previously described (Thomas et al. 2012). Briefly, flavone A was extracted from *G. elegans* dried flowers using $CHCl_3$ then concentrated by dry vacuum. Methanol and filtering were used to remove fats and hydrocarbons from the residue. The concentrated residue was reconstituted in C_6H_6 and eluted by silica gel chromatography using C_6H_6:Me_2CO (19:1) as a mobile phase. The flavonoid was purified by crystallizations in hexane. Physical and spectroscopic properties of 5,7 dihydroxy-3,6,8 trimethoxyflavone, were used for identification of the compound. Flavone B was extracted by soaking fresh leaves of *A. bogotensis* in $CHCl_3$ followed by filtration and concentration. The residue dissolved in hot methanol. Fats and hydrocarbons were filtered out of the sample before

reconcentration. Hexane was used to dissolve and recrystallize the purified flavonoid. Physical and spectroscopic properties as 3,5-dihydroxy-6,7,8-trimethoxyflavone were used to identify the compound. Stock solutions of flavones were prepared using dimethyl sulfoxide to yield a maximum final concentration of 0.01% in the treated well (Sigma-Aldrich, St. Louis, MO). 5-fluorouracil (5-FU) was purchased from Sigma Aldrich (St Louis, MO).

Cell culture

Colon cancer cells lines HCT 116 and CaCo 2 were purchased from American Tissue Type Culture Collection (ATCC; Manassas, VA). HCT 116 cells were culture in McCoy's media and CaCo 2 cells cultured in DMEM/F12 media (GIBCO/Invitrogen, Carlsbad, CA). Media was supplemented with 10% fetal bovine serum (GIBCO/Invitrogen, Carlsbad, CA) and 1% penicillin/streptomycin (Hyclone, Logan, UT). DMEM/F12 was also supplemented with 1% sodium pyruvate (Hyclone, Logan, UT).

Cell viability assay

HCT 116 and CaCo 2 cells were seeded in 48 well plates and grown until ~75% confluent. CaCo 2 cells were treated with either dissolution vehicle (DMSO), flavone A (5-80 µM), 5-FU (5-80 µM) (Cheah et al. 2014; Hwang et al. 2005; Riahi-Chebbi et al. 2015), or combination (5-FU 5-80 µM and 40 µM flavone A). HCT 116 cells were treated with either vehicle, flavone B (5-80 µM), 5-FU (5-80 µM), or combination (5-FU 5-80 µM and 40 µM flavone B). Cells were incubated at 37 ºC for 48-72 hours. 3-(4, 5-methyl-thiazol-2-yl)-2, 5-diphenyl-tetrazolium bromide (MTT) was added at 10% per volume and incubated for 3 hours (Invitrogen). Formazan crystals were solubilized with acidified 2-propanol and optical density was measured at 570 nm using a Biotek PowerWave XS2 plate reader (Winooski, VT).

Statistical analysis was performed using One-way ANOVA (Tukey) on Graph Pad v5. Combination index was determined using CompuSyn.

$$\text{Effect} = 100 - \text{viability} \quad (1)$$

$$CI = [a]/[A] + [b]/[B] \quad (2)$$

a = concentration of individual drug 1 to achieve X effect. A = concentration of drug 1 in combination to achieve effect X. b = concentration of individual drug 2 to achieve X effect. B = concentration of drug 2 in combination to achieve effect X.

Apoptosis assay

Cells were plated on coverslips and grown until ~75% confluent. CaCo 2 cells were treated with vehicle, 40 µM flavone A, 80 µM 5-FU, or combination. HCT 116 cells were treated with vehicle, 40 µM flavone B, 80 µM 5-FU, or combination. After 24-72 hours of treatment, TUNEL assay (TdT-mediated dUTP nick end labeling) was performed as directed by the manufacturer (Roche; Mannheim, Germany). Briefly, the cells were fixed with 4% paraformaldehyde and permeabilized with 0.1% sodium citrate and 0.1% Triton. TUNEL reagent was then added. Nuclei of the cells were stained with DAPI. Fluorescence microscopy images were obtained using an EVOS microscope (AMG, Bothell, WA).

Cell cycle analysis

CaCo 2 or HCT 116 cells were grown in 6 well plates until ~75% confluent. Cells were treated with flavone (40 µM), 5-FU (80 µM), or combination. Cells were lifted with cell scraper and suspended in binding buffer for cell cycle and apoptosis quantification using an Annexin V-FITC kit from Abcam (Cambridge, MA) according to manufacturer instructions. Briefly, Annexin and propidium iodide were added to suspended cells and incubated in the dark for 5 minutes. A BD Accuri C6 flow cytometer (BD Bioscience, San Jose, CA) was used to obtain cell

count. Data was analyzed with CFLOW Plus (BD Bioscience, San Jose, CA). One-way ANOVA (Tukey) was performed using Graph Pad v5 for statistical analysis.

Comet assay

Caco 2 and HCT 116 cells were plated in 6 well plates and grown until ~75% confluent. CaCo 2 cells were treated with vehicle, flavone A (40 µM), 5-FU (80 µM), or combination. HCT 116 cells were treated with vehicle, flavone B (40 µM), 5-FU (80 µM), or combination. Cells were lifted from the plate using a cell scraper and suspended in 300 µL phosphate buffered saline. Alkaline comet assay (Trevigen, Gaithersburg, MD) was performed per manufacturer's instructions. Briefly, cells were suspended in agarose and plated in comet plates. Cells were lysed with lysing buffer then immersed in alkaline unwinding solution. Samples were washed with deionized water and 70% ethanol. SYBR gold (Life Technologies, Eugene, OR) was used to stain the cells. Fluorescence microscopy images were obtained using an EVOS microscope (AMG, Bothell, WA). Tail moment (tail length * percent tail DNA) (Gyori et al. 2014) was determined using the OpenComet plugin for Image-J (NIH). Tail moments > 5 were used to determine average tail moments for 50 + samples. One-way ANOVA (Tukey) was performed using Graph Pad v5 for statistical analysis.

Antibodies

Antibodies pCHK1 (S345), CHK1, pBAD (S112), BAD, P-p44/42 MAPK (T202), p44/42 MAPK (ERK ½), and BCL-2 were purchased from Cell Signaling (Beverly, MA), ² -actin from Sigma (St. Louis, MO), TS from Santa Cruz (Dallas, TX), ³ -H2AX from Bethyl Laboratories (Montgomery, TX), Cleaved Caspase 3 (Asp 175) (R & D Systems, Minneapolis, MN), and Alexa Fluor 594 goat anti-rabbit IgG (GIBCO/Invitrogen, Carlsbad, CA). Peroxidase-conjugated secondary antibodies were affinity purified with no cross-reactivity with other species and

obtained from Pierce (Rockford, IL), Promega (Madison, WI), and Jackson ImmunoResarch (West Grove, PA).

Immunoblot

HCT 116 and CaCo 2 cells were treated in the same manner as for apoptosis assay and lysed after 4-32 hours using lysis buffer consisting of 20 mM imidazole, 100 mM KCl, 1mM $MgCl_2$, 10mM EGTA, 0.2% Triton X-100, phosphatase, and protease inhibitors (Sigma Aldrich). A protein assay from Cytoskeleton (Denver, CO, USA) was used to measure protein concentrations from cell lysates and the colorimetric reaction was read spectrophotometrically at 590nm (Cary 50; Varian, Palo Alto, CA). The samples were run in SDS-PAGE and then blotted onto nitrocellulose membranes. The signal of the primary antibodies was detected using secondary affinity-purified goat anti-mouse or anti-rabbit immunoglobulins coupled to peroxidase and a chemiluminescent system (Pierce; Grand Island, NY) and images obtained using a gel documentation system (G:Box fromSyngene, Frederick, MD). The intensity of the bands in the images were estimated after subtracting the background and compared against a control using Image J (NIH). One-way ANOVA (Tukey) was performed using Graph Pad v5 for statistical analysis.

Immunofluorescence

HCT 116 and CaCo 2 cells were plated on coverslip until ~75% confluent. HCT 116 cells were treated with vehicle, flavone B (40 µM), 5-FU (80 µM), or combination for 48 hours. CaCo 2 cells were treated with vehicle, flavone A (40 µM), 5-FU (80 µM), or combination for 36 hours. Cells were fixed with 3% paraformaldehyde and incubated with cleaved Caspase 3 (A175) antibody (R & D Systems, Minneapolis, MN). Alexa Fluor 594 goat anti-rabbit IgG

(GIBCO/Invitrogen, Carlsbad, CA) was used as secondary antibody and cells were counted stained with DAPI. Images were taken using an EVOS microscope (AMG, Bothell, WA).

Animals and drug administration

Male NCrNU immunodeficient mice were obtained from Taconic (Hudson, NY) and were housed in a sterile room with a 12 hour light-dark cycle. All experiments were carried out following the guidelines of the Animal Care Committee of East Tennessee State University. Mice were injected in the right flank with 5×10^6 HCT116 cells in matrigel. After tumors reached an average of 5 x 5 mm, mice were divided into 4 groups (n=6). Group 1 was treated with polyethylene glycol 400 given by intratumoral (IT) injection and saline given by intraperitoneal (IP) injection once a day, three days a week. Group 2 was administered 1 mg/kg flavone B in polyethylene glycol 400 by IT once a day, three days a week. Group 3 was administered 12 mg/kg 5-FU in saline by IP once a day, three days a week. Group 4 was administered flavone B via IT and 5-FU via IP once a day, three days a week. The weight of mice and tumor size were measured three times a week. Tumor volume (TV) was calculated using length and width measurement of the tumor.

$$TV = d^2 * D/2 \quad (3)$$

With d being the smaller diameter and D the larger diameter. Relative tumor volume (RTV) was calculated as ratio of tumor volume to average control tumor volume. Animal were euthanized under anesthesia and tumors were collected. Two-way ANOVA (Tukey) was performed using Graph Pad Prism for statistical analysis.

Results

Flavone A and flavone B have synergistic activity on colon cancer cells when used in combination with 5-fluorouracil.

To determine whether the addition of flavone A or flavone B to cells treated with 5–FU will produce an increase in cytotoxicity, colon cancer cells were treated with each agent alone and in combination and analyzed for cell viability. A single dose of flavone in the middle of the concentration consistent to the one used in the previous study which caused loss of cell viability e 50% was used in the combination treatments (Thomas et al. 2012). Caco 2 cells were treated with 0, 5, 10, 20, 40, or 80 µM flavone A, 5-FU, or combination (40 µM flavone A and 5-80 µM 5-FU). After 48 hour MTT assay was performed to determine cell viability. Cells treated with either flavone A or 5-FU individually had cell viability similar to that of the controls. However, the combination treatment was able to decrease cell viability to below 50% (Figure 2A). The combination index (CI) was calculated using CompuSyn to determine if the increased cytotoxicity seen with the combination treatment was additive (CI=1), antagonistic (CI>1), or synergistic (CI<1). The effect for all concentration combinations of flavone A and 5-FU used were found to be synergistic (Figure 2B).

HCT 116 cells were treated with 0, 5, 10, 20, 40, or 80 µM flavone B, 5-FU, or combination (40 µM flavone B and 5-80 µM 5-FU) for 72 hours. Flavone B and 5-FU had similar effects on cell viability with the lowest cell viability around 65% (Figure 2C). The combination treatment was more cytotoxic against HCT 116 cells causing cell viability to decrease to 38% with the highest concentration. All concentration combinations of flavone B and 5-FU were synergistic (Figures 2D).

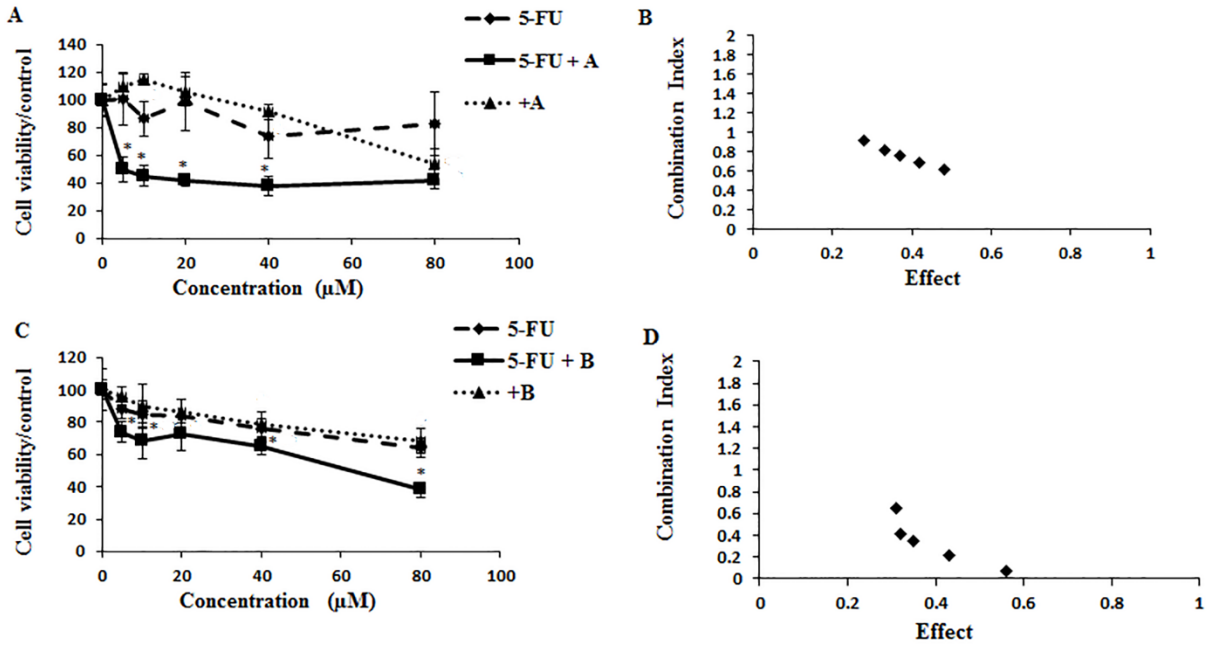

Figure 2. Combination treatment decreases cell viability of colon cancer cells. (A) Cell viability of colon cancer cells, CaCo 2, treated with flavone A, 5-fluorouracil, or combination for 48 hours. (B) Combination index comparing the effect achieved by concentration of drug(s) in combination versus individual treatments of 5-fluorouracil and/or flavone A on CaCo 2 cells. (C) Cell viability of colon cancer cells, HCT 116, treated for 72 hours with flavone B, 5-fluorouracil, or combination. (D) Combination index comparing the effect achieved by concentration of drug(s) in combination versus individual treatments of 5-fluorouracil and/or flavone B on HCT 116 cells. Cell viability was determined using MTT assay. * Significant difference ($p < 0.05$ determined using One-way ANOVA (Tukey).

Combination treatment increases the induction of apoptosis in CaCo 2 cells.

Both flavones and 5-FU have been shown to induce apoptosis (Thomas et al. 2012; Wang et al. 2014a) TUNEL assay was performed to determine if the combination treatment increased the induction of apoptosis versus the individual treatments. CaCo 2 cells were treated with 40 µM flavone A, 80 µM 5-FU, or combination. After 24 or 36 hours, TUNEL assay was

performed. At 24 hours apoptosis could be detected in cells treated with flavone A, but not 5-FU or the combination treatment (Figure 3). Detection of apoptotic activity changed at 36 hours with few apoptotic cells being detected in cells treated with flavone A or 5-FU and several apoptotic cells detected in cells treated in the combination. The difference in the time of apoptotic induction correlates with the change in time of cell death for each treatment. At 24 hours, the antineoplastic activity of flavone A can be detected, however, 5-FU take longer (48 hour) to cause an antineoplastic effect. The combination treatment is similar to 5-FU in the time of apoptosis and cell death induction.

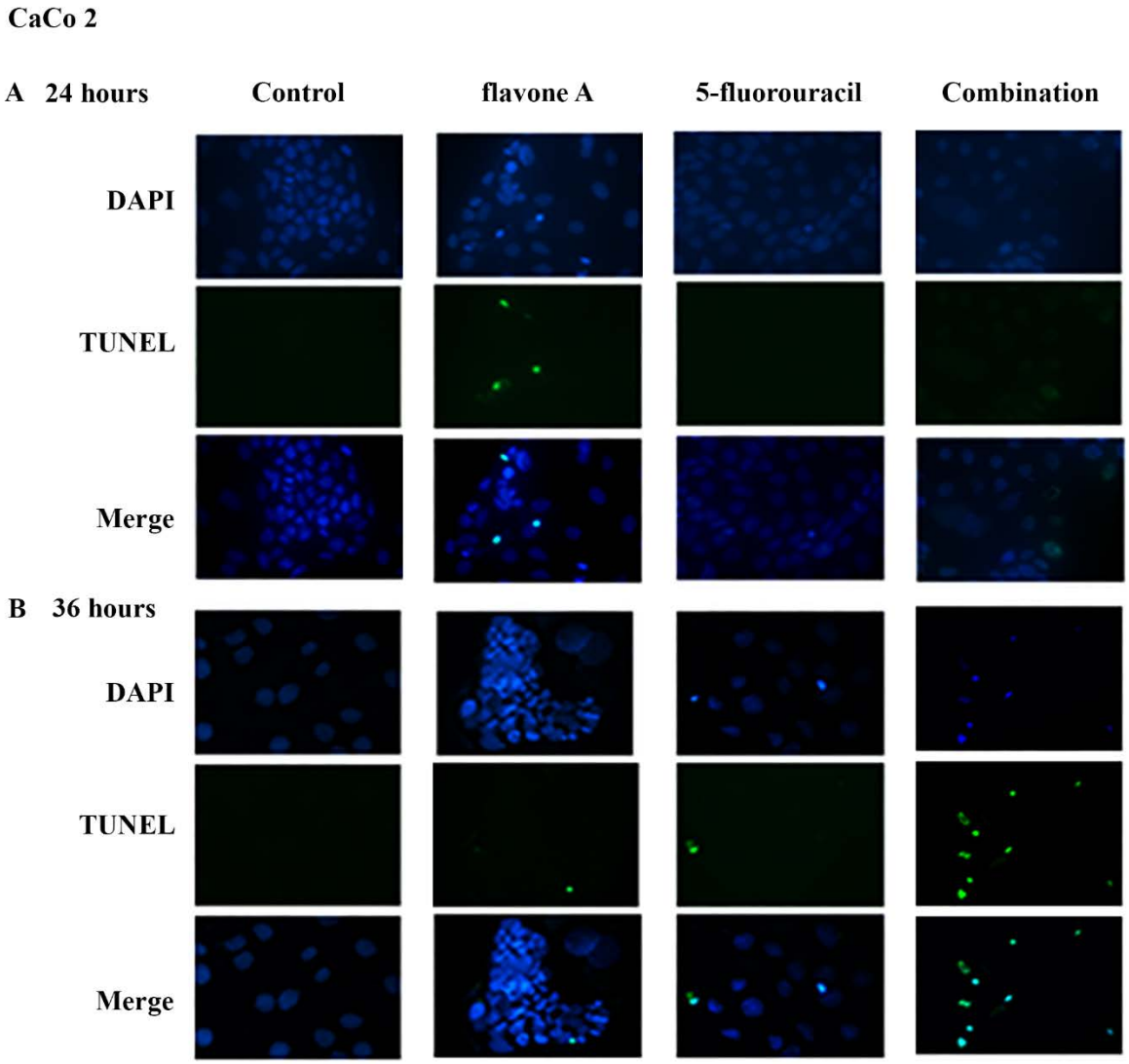

Figure 3. Combination therapy increases the induction of apoptosis in CaCo 2 cells. Caco 2 colon cancer cells were treated with 5-fluorouracil, flavone A, or a combination. TUNEL assay was performed after 24 and 36 hours. The results shown are representative of at least three independent assays.

Combination treatment increases induction of apoptosis in HCT 116 cells.

To determine if a similar change in apoptotic activity occurs when flavone B is used in combination with 5-FU, HCT 116 cells were treated with 40 µM flavone B, 80 µM 5-FU, or combination. TUNEL assay was performed 48 or 72 hours after treatment. At 48 hours, the majority of apoptotic cells were detected in cells treated with 5-FU with some in flavone B treated cells (Figure 4). However, after 72 hours, the majority of apoptotic cells were detected in the combination treatment, while the individual treatments had few apoptotic cells. This differs from CaCo 2 and HCT 116 cells treated with 40 µM flavone A or flavone B, respectively, were apoptosis can be detected as early as 6 hours (LeJeune et al. 2015). These data indicate that flavone B still has some ability to induce apoptosis days after the main effect is seen. However, as with flavone A, the apoptotic and cell death time of induction of the combination treatment is similar to that of 5-FU.

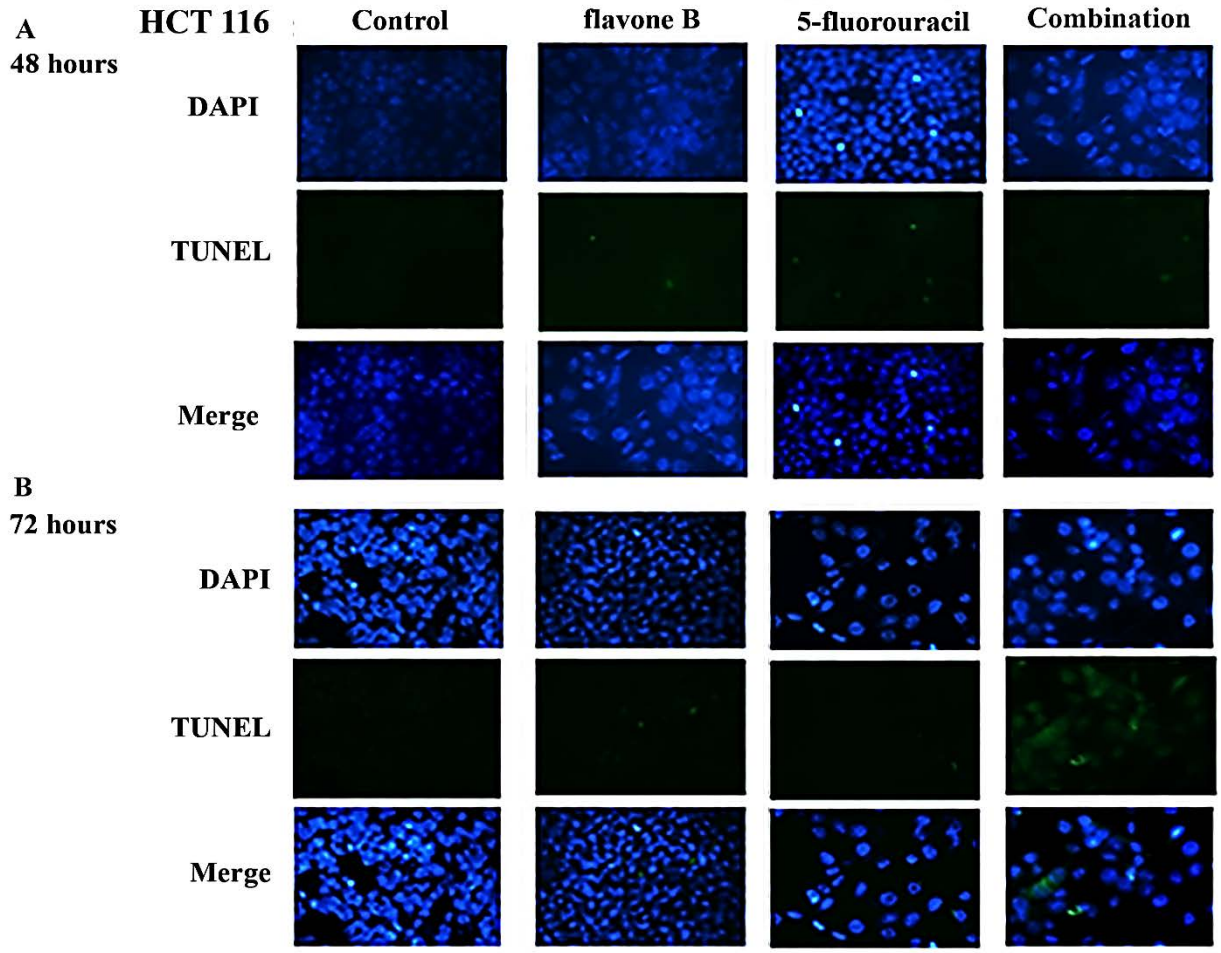

Figure 4. Combination therapy increases the induction of apoptosis in HCT 116 cells. HCT 116 colon cancer cells were treated with 5-fluorouracil, flavone B, or a combination. TUNEL assay was performed after 48 and 72 hours.

5-fluorouracil and the combination treatment increases cells cycle shift to S phase.

Both flavones and 5-FU has been shown to induce S-phase (LeJeune et al. 2015; Robinson et al. 2006; Xiao et al. 2005). To determine if the combination treatment also induces a similar or enhanced cell cycle shift CaCo 2 and HCT 116 cells were treated with flavone A or flavone B, respectively, 5-FU, or combination. Annexin V-FITC and propidium iodide were used to determine the percent of apoptotic cells and which cell cycle cells were in. 5-FU and combination treatment caused a significant shift to S phase in the cell cycle, but did not significantly increase apoptosis in CaCo 2 cells (Figure 5A and B). This could be a result of timing as the flow cytometry was performed at 9 hours which may be long enough to halt the cell cycle, but not long enough to trigger and see the effect of the apoptotic pathway. An increase in apoptosis, as well as a shift to S-phase were seen in HCT 116 cell treated with 5-FU and combination therapy 24 hours post dosing (Figure 5C and D). No change in cell cycle or apoptotic activity was seen in cells dosed with either flavone individually at these time points. However, both flavones were able to induce increases in apoptosis, S, and G2 phases in Panc 28 and HCT 116 cells 9 hours post dosing (LeJeune et al. 2015).

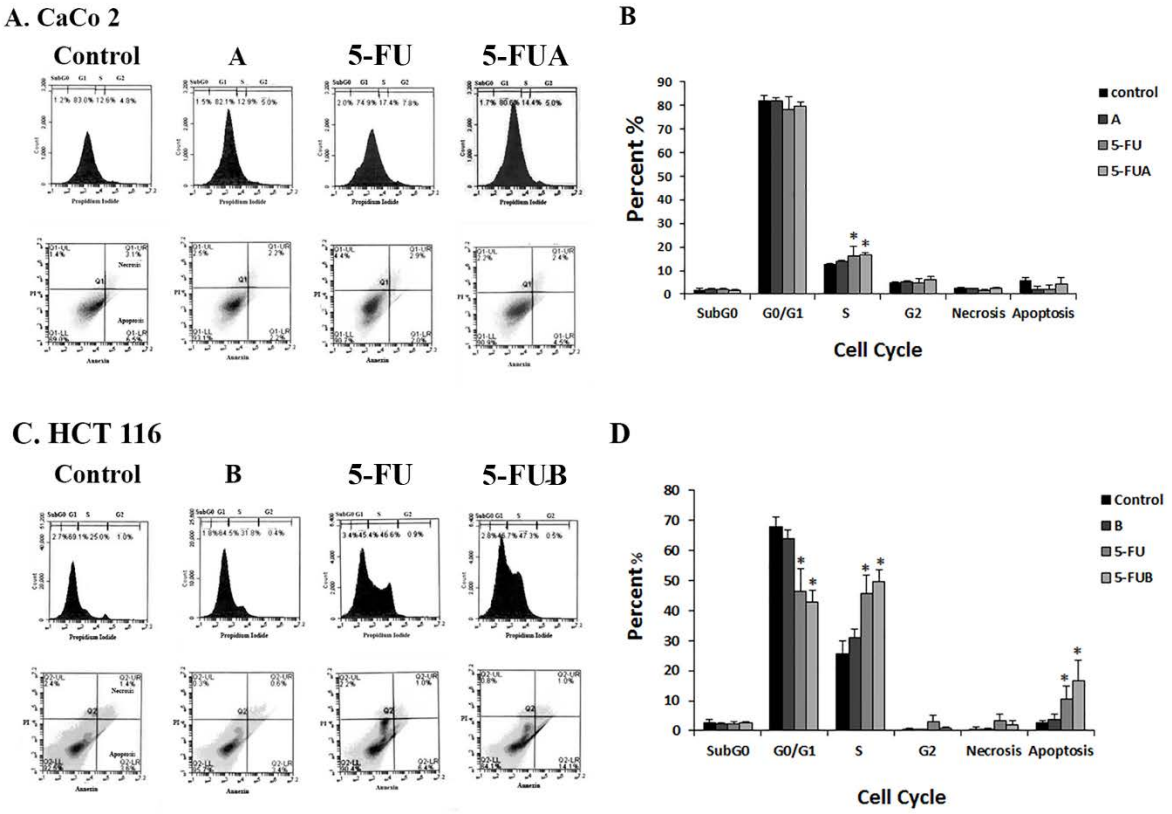

Figure 5. 5-FU and combination treatment cause a cell cycle shift. (A) Caco 2 cells were treated with flavone A, 5-fluorouracil, or combination. Propidium iodide was used to determine cell cycle and annexin was used to determine the percent of apoptotic cells. (B) Graphical representation of the percent of cells in cell cycle or apoptotic cells. (C) HCT 116 cells were treated with flavone B, 5-fluorouracil, or combination. Propidium iodide was used to determine cell cycle and annexin was used to determine the percent of apoptotic cells. (D) Graphical representation of the percent of cells in cell cycle or apoptotic cells. * Significant ($p < 0.05$) from control as determined by One-way ANOVA (Tukey).

<u>The addition of flavone A or flavone B to 5-fluorouracil treatment causes an increase induction of DNA damage.</u>

The shift in time of apoptosis and cell death caused by the addition of 5-FU to the flavone treatment raised the question of if the flavone was enhancing the DNA damage caused by 5-FU resulting in the increase in cell death. Alkaline comet assays were performed on CaCo 2 and

HCT 116 treated with vehicle, 40 µM flavone A or flavone B, respectively, 80 µM 5-FU, or the combination after 24 hours. These assays determined if the combination treatment caused an increase in both ssDNA and dsDNA damage. 5-FU and the combination treatments showed more DNA damage than either the control or flavone treatments for both CaCo 2 and HCT 116 cells (Figure 6A and C). Tail moments (length of tail times percent DNA in the tail) indicates that the combination treatment cause more DNA damage per cell in comparison to the DNA damaged caused by 5-FU alone in both cell lines (Figure 6B and D). The percent of DNA damaged cells per population was not altered in either cell line.

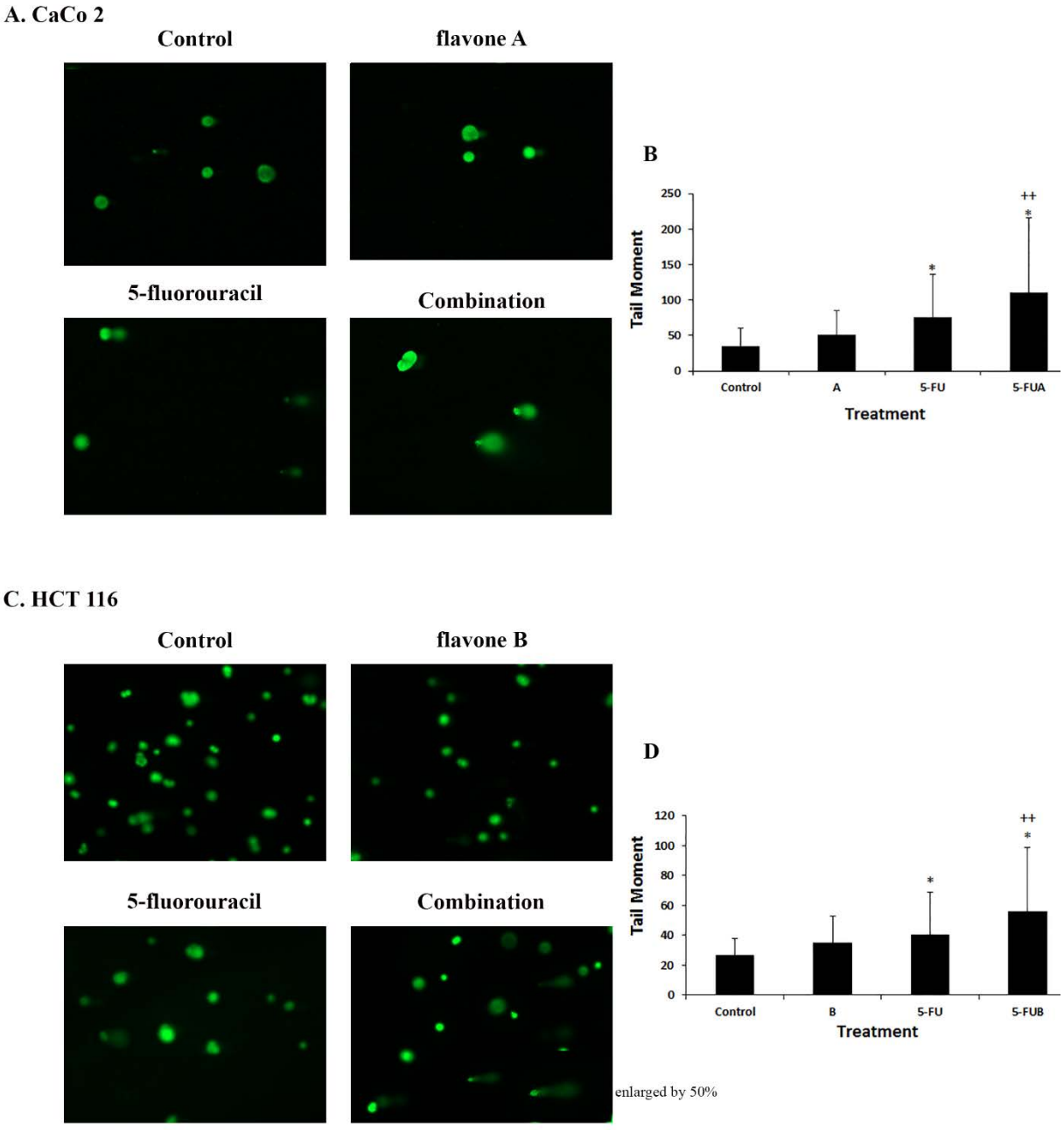

Figure 6. Combination therapy increased the induction of DNA damage. A. Comet assay was performed CaCo 2 cells were treated with flavone A, 5-FU, or the combination for 24 hours. B. Bar graph of the tail moments from CaCo 2 cells treated with flavone A, 5-FU, or combination. C. Comet assay was performed on HCT 116 cells treated with flavone B, 5-FU, or combination for 24 hours. D. Bar graph of the tail moments from HCT 116 cells treated with flavone B, 5-FU, or combination for 24 hours. * Significant ($p < 0.05$) from control as determined by One-way ANOVA (Tukey). ++ Significant ($p < 0.05$) from 5-FU as determined by One-way ANOVA (Tukey).

Flavone A and B enhances the mechanism of action of 5-fluorourail in colon cancer cells.

The complexing of the 5-FU metabolite, FdUMP, with thymidylate synthase (TS) and CH2-THF inhibits the conversion of dUMP to dTMP causing a depletion of dTTP from the nucleotide pool which causes dUTP to be inserted into DNA resulting in DNA damage (Figure 1) (Geng et al. 2011; Ghoshal and Jacob 1997; Peters et al. 2002). Ataxia-telangiectasia mutated and Rad3-related (ATR) kinase response to replication stress in order to start DNA damage repair and has increased levels in cells in response to 5-FU caused DNA damage (Woods and Turchi 2013). ATR activates CHK1 by phosphorylation which in turn arrests the cell by preventing the activation of CDK/cyclins (Flynn and Zou 2011). Histone H2AX is also phosphorylated by ATR in response to DNA replication stress and recruits several DNA repair proteins as well as chromatin remodeling complexes to the chromatin adjacent to the stressed replication fork (Flynn and Zou 2011). When DNA damage is too extensive for repair, CHK1 initiates apoptosis through the activation of tumor-suppressor protein p53 (Wu et al. 2016). Activated p53 induces the transcription of pro-apoptotic proteins BAX, BAK, PUMA, and NOXA and inhibits the transcription of anti-apoptotic protein BCL-2, thus suppressing cell survival (Chipuk et al. 2004; Goldar et al. 2015). The decrease in BCL-2 protein levels causes the release of cytochrome c from the mitochondria allowing to bind to Apf-1 and recruit caspase 9 forming the apoptosome which in turn, cleaves and activates the effector caspase 3 causing the execution apoptosis (Goldar et al. 2015; Pujhari et al. 2014; Zou et al. 1997). To determine if this is the mechanism by which both flavones are able to enhance the amount of DNA damage per cell when used in combination with 5-FU, TS, pCHK1 (Ser 345), ^{3}-H2AX, and BCL-2 levels were examined.

CaCo 2 and HCT 116 cells were treated with 40 µM flavone A or B, respectively, 80 µM 5-FU, or combination. In CaCo 2 cells, the combination treatment increased the concentration of TS by 318% as compared to the control whereas the individual treatments of flavone A and 5-FU caused a 40 and 77% increase, respectively, after 9 hours. In addition, the molecular weight of the band shifted up indicating that the TS was in a complex similar to that seen with 5-FU individual treatment (Figure 7A and B).

After 24 hours, 5-FU treatment increased the percent of pCHK1 by 17% as compared to the control levels whereas the combination treatment increased levels by 68% in Caco 2 cells. Flavone A by itself decreased the expression of pCHK1 by 25% (Figure 7C and D). Combination treatment increased the level of ^{3}-H2AX were expression by 113% over the control and 132% over the flavone A treatment (Figure 7E and F).

After another 5 hours (29 post dosing) changes further down the apoptotic pathway in the form of BCL-2 levels were detected in CaCo 2 cells. Flavone A and the combination treatment significantly decreased the BCL-2 expression to 51 and 54% of control levels, respectively. A similar but not significant decrease in BCL-2 level was seen with 5-FU treatments (60% of the control level (Figure 7G and H). Together, these data indicate that flavone A is able to enhance 5-FU ability to complex with TS, increase DNA damage, and activate the ATR pathway.

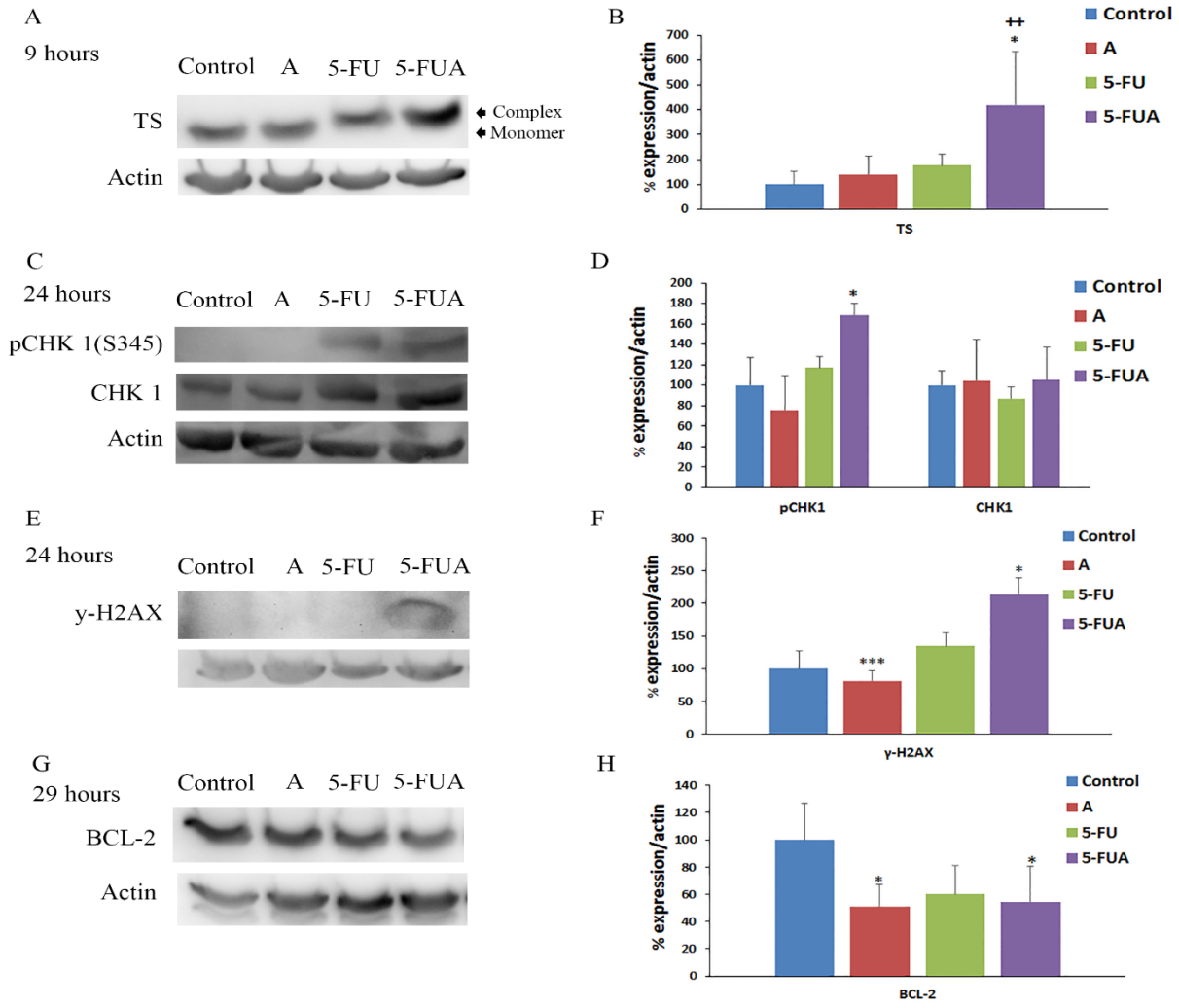

Figure 7. Flavone A enhances 5-FU mechanism of action in CaCo 2 cells. (A) TS levels in CaCo 2 cells treated with vehicle, flavone A (40 µM), 5-fluorouracil (80 µM), or combination for 9 hours. (B) Graphical representation of percent of TS/actin in CaCo 2 cells. (C) pCHK1 and CHK1 levels in CaCo 2 cells were treated with vehicle, flavone A (40 µM), 5-fluorouracil (80 µM), or combination for 24 hours. (D) Graphical representation of percent of pCHK1/actin and CHK1/actin in CaCo 2 cells. (E) ^{3}-H2AX levels in CaCo 2 cells treated with vehicle, flavone A (40 µM), 5-fluorouracil (80 µM), or combination for 24 hours. (F) Graphical representation of percent of ^{3}-H2AX /actin in CaCo 2 cells. (G) BCL-2 levels in CaCo 2 cells treated with vehicle, flavone A (40 µM), 5-fluorouracil (80 µM), or combination for 29 hours. (H) Graphical representation of percent of BCL-2 /actin in CaCo 2 cells. Western blots are representative of experiments performed in triplicate. * Significant ($p < 0.05$) from control as determined by One-way ANOVA (Tukey). ++ Significant ($p < 0.05$) from 5-FU as determined by One-way ANOVA (Tukey). *** Significant ($p < 0.05$) from combination treatment as determined by One-way ANOVA (Tukey).

Flavone B also appears to enhance the mechanism of 5-FU in a similar manner. After 24 hours, the combination treatment increased the levels of TS by 90% over the control levels. In addition, a similar shift in molecular weight was seen, suggesting that both flavones enhance the ability of 5-FU to complex with TS (Figure 8A and B). When used with 5-FU, flavone B was also able to increase the activation of the ATR pathway in a more pronounce manner than flavone A. At 24 hours, pCHK1 levels in HCT 116 cells treated with 5-FU and combination therapies causing an increase of 277 and 400% over control levels, respectively, whereas, flavone B alone caused a 20% increase in pCHK1 (Figure 8C and D). Individual flavone B and 5-FU treatments increased ^{3}-H2AX levels by 38 and 52% over the control. However, the combination treatment increased ^{3}-H2AX levels by 141% over the control (Figure 8E and F).

Effects downstream in the apoptotic pathway could be detected 9 hours later (32 hours post dosing) in BCL-2 levels. The combination treatment significantly decreased BCL-2 levels to 40% of control levels. As seen with CaCo 2 cells, individual flavone B and 5-FU treatments decreases BCL2 levels in a similar fashion (65 and 61% of control, respectively) though these changes were not significant (Figure 8G and H).

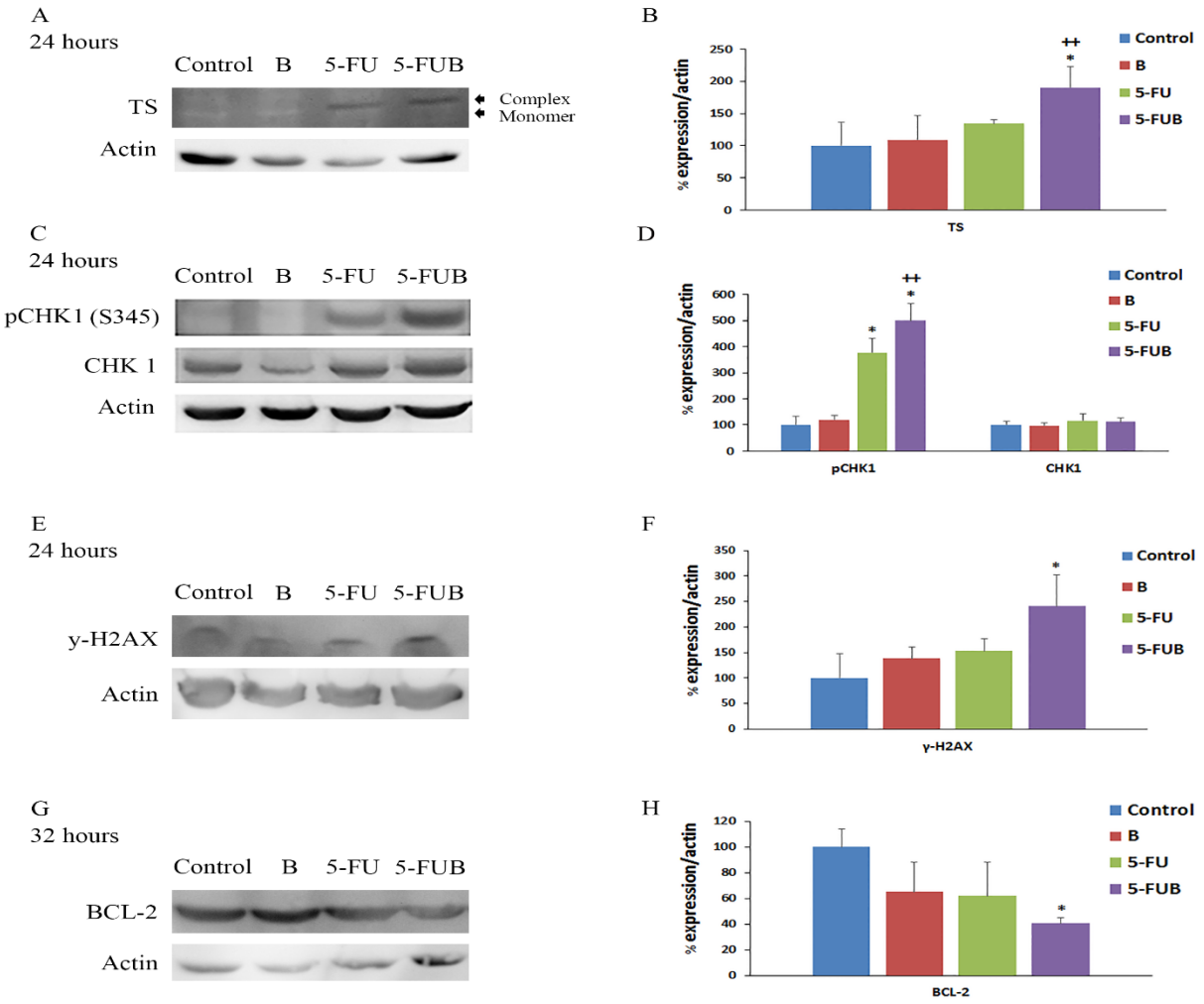

Figure 8. Flavone B enhances 5-FU mechanism of action in HCT 116 cells. (A)TS levels in HCT 116 cells treated with vehicle, flavone B (40 µM), 5-fluorouracil (80 µM), or combination for 24 hours. (B) Graphical representation of percent of TS/actin in HCT 116 cells. (C) pCHK1 and CHK1 levels in HCT 116 cells were treated with vehicle, flavone B (40 µM), 5-fluorouracil (80 µM), or combination for 24 hours. (D) Graphical representation of percent of pCHK1/actin and CHK1/actin in HCT 116 cells. (E) ^{3}-H2AX levels in HCT 116 cells treated with vehicle, flavone B (40 µM), 5-fluorouracil (80 µM), or combination for 24 hours. (F) Graphical representation of percent of ^{3}-H2AX /actin in HCT 116 cells. (G) BCL-2 levels in HCT 116 cells treated with vehicle, flavone B (40 µM), 5-fluorouracil (80 µM), or combination for 32 hours. (H) Graphical representation of percent of BCL-2 /actin in HCT 116 cells. Western blots are representative of experiments performed in triplicate. * Significant ($p < 0.05$) from control as determined by One-

way ANOVA (Tukey). ++ Significant ($p < 0.05$) from 5-FU as determined by One-way ANOVA (Tukey).

Both flavone A and flavone B increase cleavage of Caspase 3 when combined with 5-fluorouracil.

Both flavones and 5-FU cause cell death via apoptosis (Fujinaka et al. 2012; Hwang et al. 2005; LeJeune et al. 2015; Thomas et al. 2012) which is triggered by cleaved effector caspases including caspase 3 (Baig et al. 2016; Olsson and Zhivotovsky 2011). CaCo 2 cells were probed for cleaved caspase 3 7 hours after the decrease in BCL-2 was detected (36 hours post dosing). Cells were treated with vehicle, flavone A (40 µM), 5-FU (80 µM), or combination. A significant increase in the cleavage of caspase 3 was seen in cells treated with the combination versus the control (5.37 vs 0.25%) (Figure 9A and C). Similarly, HCT 116 cells treated with the combination of flavone B (40 µM) and 5-FU (80 µM) had a significant increase in cleaved caspase 3 to 12.88% versus 0.85% seen in the control 56 hours post dosing (Figure 9B and D).

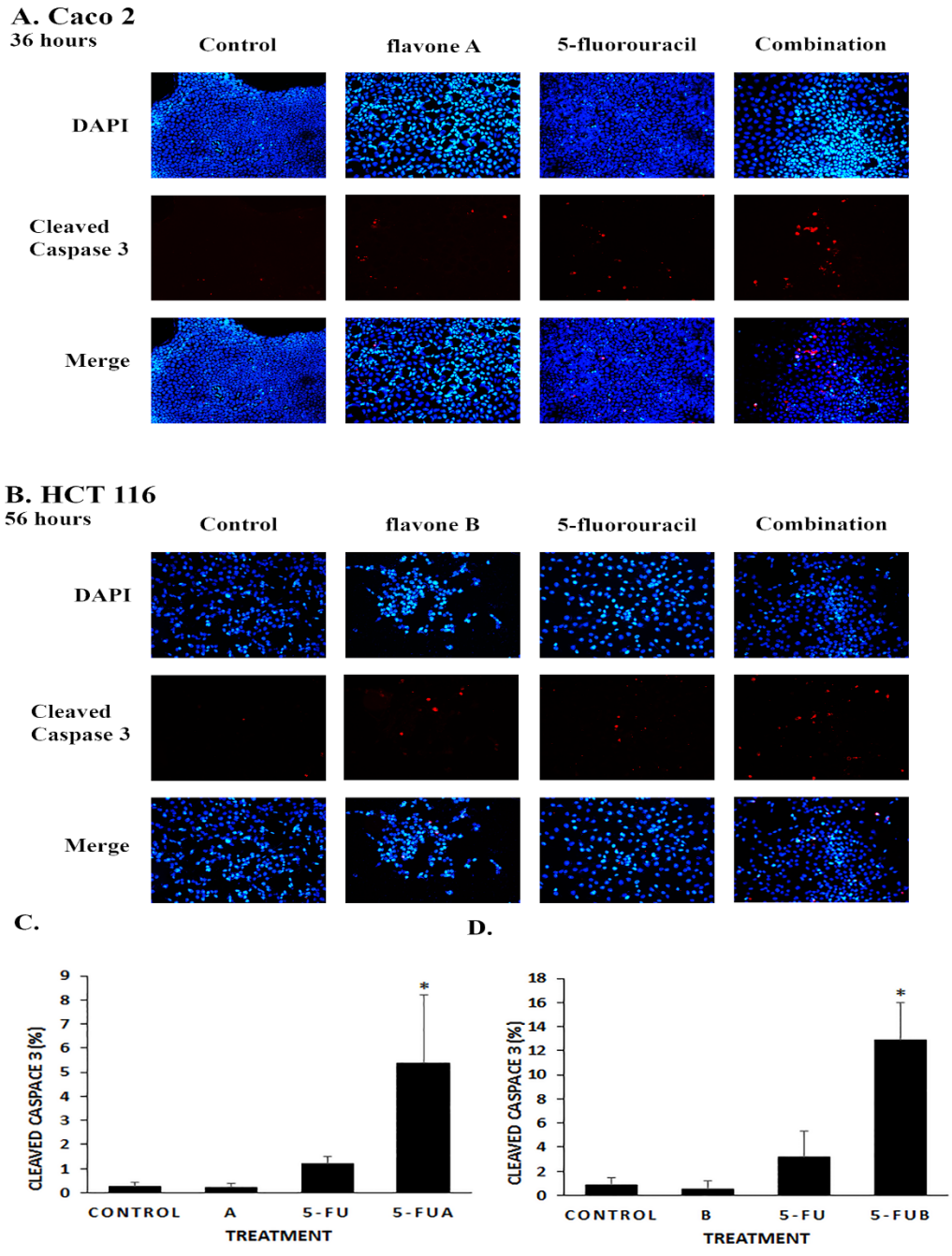

Figure 9. Combination treatment increases cleavage of caspase 3. (A). CaCo 2 cells treated with vehicle, flavone A (40 µM), 5-FU (80 µM), or combination for 36 hours were probed for cleaved caspase 3. (B) HCT 116 cells treated for 56 hours with vehicle, flavone B (40 µM), 5-FU (80 µM), or combination and probed for cleaved caspase 3. (C) Percent of CaCo 2 cell population with cleaved caspace 3. (D) Percent of HCT 116 cell population with cleaved caspace 3. * Significant difference ($p < 0.05$) as determined by One-way ANOVA (Tukey).

5-fluorouracil and combination treatment resulted in large fluid filled tumors.

To determine whether the synergistic activity of flavone B and 5-FU also occurred *in vivo,* 24 male NCruNU mice were inoculated subcutaneously with 5 x 10^6 HCT 116 cells in the right flank and divided into 4 groups; control, flavone B, 5-FU, and combination treatment. Flavone B was administer mixed in polyethylene glycol 400 (PEG 400) via intratumoral injection at a dose of 1 mg/kg. 5-FU was mixed in saline and administered via intraperitoneal injection at a dose of 12 mg/kg. Saline and PEG 400 were used to treat the controls. Treatments were given and tumors measured 3 times a week. Animals were euthanized 12 days post first treatment. At this time final tumor measurements and weight were taken after removal from the animal (Figure 10A &B). Final tumor weight and volume were significantly different for mice treated with the combination at 0.54 ± 0.26 g and 489 ± 354 mm^3, respectively (Figure 10C & D). Our data indicate that relative tumor volume (RTV) increased in mice treated with 5-FU or the combination treatments 12 and 25 fold, respectively, versus the 4 and 3 fold increase that occurred with control and flavone B treated mice, respectively, over the 12 day period (Figure 10E). Unexpectedly, tumors from mice treated with 5-FU or the combination treatment were filled with fluid that was not found in tumors from mice in the control and flavone B treatment groups.

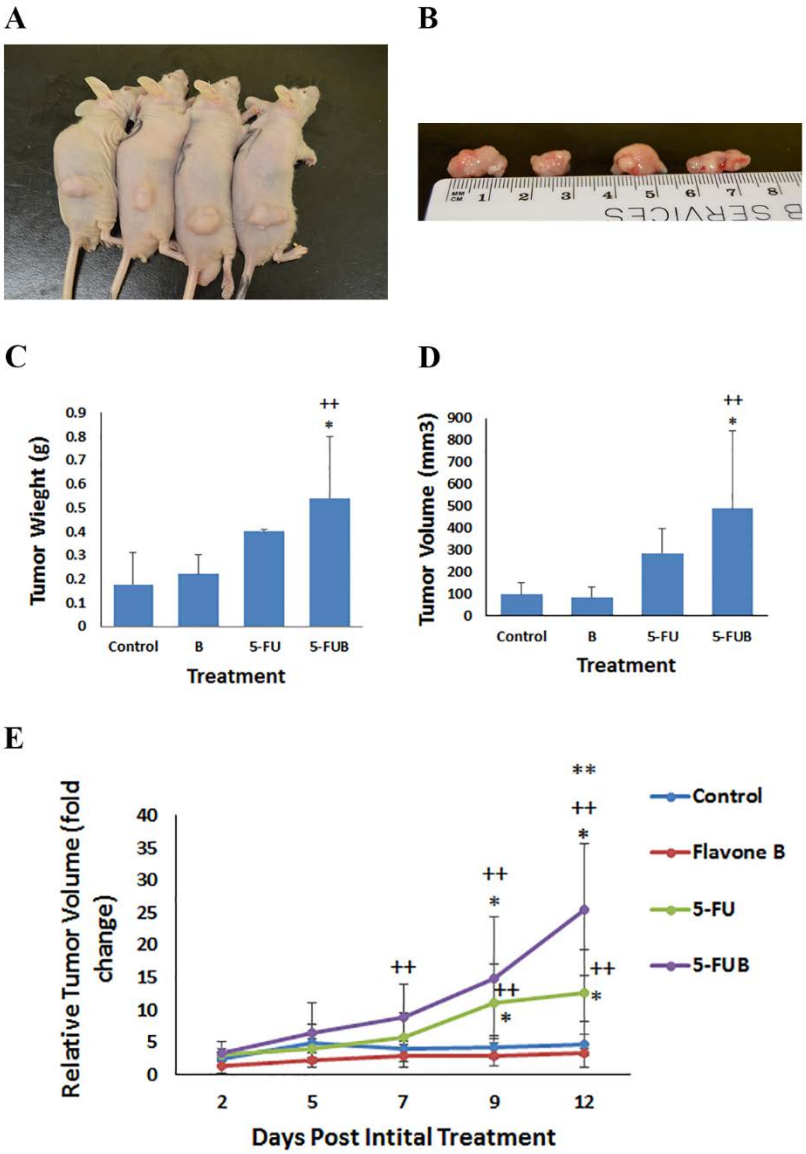

Figure 10. 5-FU and combination treatment increase the rate of tumor growth. Male NCruNU mice with HCT 116 xenografts were treated with vehicle, flavone B (1 mg/kg), 5-FU (12 mg/kg), or combination three times a week for 12 days via intratumoral or intraperitoneal injection. (A) Final tumors in mice treated with control, flavone B, 5-FU, or combination, respectively. (B) Tumors removed from mice treated with control, flavone B, 5-FU, or combination, respectively. (C) Graphical representation of final tumor weight. (D) Graphical representation of final tumor volume. (E) Relative tumor volume change. * Significant ($p < 0.05$) from control as determined by Two-way ANOVA multiple comparison (Tukey). ++ Significant ($p < 0.05$) from flavone B treatment as determined by Two-way ANOVA multiple comparison (Tukey). ** Significant ($p < 0.05$) from 5-FU treatment as determined by Two-way ANOVA multiple comparison (Tukey).

Discussion

Although colon cancer has a 90% 5 year survival rate if the cancer is detected at an early enough stage that it can be removed by surgery, the 5 year survival rate drops to 13% once the cancer has moved to another area (American Cancer Society 2015). Unfortunately, early detection only occurs in 40 % of cases. Common treatment for the other 60% of cases include chemotherapy and radiation. 5-fluorouracil is the most commonly used chemotherapy for the treatment of colon cancer and has a 10-20% response rate (Longley et al. 2003; Zhang et al. 2008). Because 5-FU cases damage to DNA, it is not cancer cell specific and results in several side effects. One strategy to improve the effectiveness of 5-FU and potentially relieve some of the side effects is to add a secondary drug to the therapy.

Our laboratory has previously demonstrated that flavone A and flavone B have differential antineoplastic activity against highly tumorigenic cell lines but not against normal cells *in vitro (Thomas et al. 2012).* This antineoplastic activity is caused by the induction of apoptosis using different mechanisms (LeJeune et al. 2015). Flavone A targets more differentiated cells causing a decrease in the active forms of pro-survival proteins ERK, S6, and BAD triggering the intrinsic apoptotic pathway. Flavone B causes the concomitant increase in phosphorylated ERK and c-JUN in poorly differentiated cells thus triggering an extrinsic apoptotic pathway that is not fully understood. These pathways are activated shortly after dosing causing the majority of effected cells to die within 24 hours.

Our results have shown in no change to cell viability in 24 hours when 5-FU is added to the either flavone treatment (Data not shown). However, CaCo 2 cells treated with flavone A and 5-FU show a decrease in cell viability at 48 hours. HCT 116 treated with flavone B and 5-FU also have a delay in decrease of cell viability which is seen at 72 hours. The effect of 5-FU

individual treatment on cell viability occurred at the same time as combination treatments in both cell lines. This suggested that the addition of 5-FU to each flavone, blocked the mechanism of action of the flavones, possibly favoring the effect of 5-FU. Further investigation into the mechanism via which the combination therapy caused cell death showed an increase in apoptotic activity and shifts in cell cycle showed that these were similar to the 5-FU treatment in the time points of occurrence, whereas, both flavones alone cause on increase in apoptosis and cell cycle shift to the S phase at earlier time points (LeJeune et al. 2015).

5-FU can cause DNA damage by blocking the ability of cells to form dTTP resulting in the incorporation of dUTP into DNA. Specifically, 5-FU can interact and form a complex with thymidylate synthase and 5,10-methylene-tetrahydrofolate (Figure 1) (Geng et al. 2011; Ghoshal and Jacob 1997; Peters et al. 2002). 5-FU induced DNA damage triggers the activation of the ATR pathway which in turn cause an increase in the phosphorylation of histone protein H2AX and CHK1 with the latter halting the cell cycle until the DNA can be repaired. However, if the damage is too extensive, the p53 apoptotic pathway is triggered (Flynn and Zou 2011; Goldar et al. 2015; Woods and Turchi 2013; Wu et al. 2016).

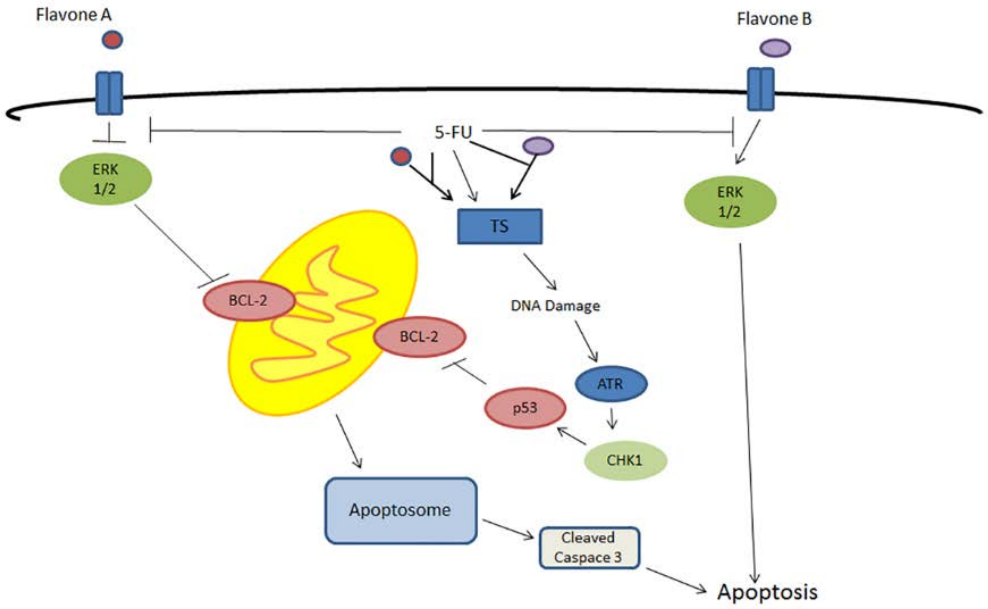

Figure 11. Mechanism of combination therapy**.** Mechanism via which flavone A, flavone B, 5-fluorouracil, and combination therapy induce apoptosis.

The data shown here suggest an increase in the amount of TS in complex and DNA damage when either flavone is used in combination with 5-FU as compared to 5-FU used alone. This results in an increase in activation of the ATR pathway leading to apoptosis in cells treated with combination therapy versus 5-FU treatment alone (Figure 11). On the contrary, the preliminary *in vivo* data do not confirm these observations. Indeed, measurements of tumors on mice with HCT 116 xenografts treated with 5-FU or combination therapy appear to have an increased rate of tumor growth versus control and flavone B treatment (Figure 10). However, the combination therapy appears to cause a significant change in final tumor weight and volume that was not seen with 5-FU alone. When comparing relative tumor volume, the most striking significant differences were seen between flavone B and combination treatment and resulted in the combination treatment being significantly different from all other groups. This suggests that 5-FU and flavone B may be working together *in vivo.* Further analysis of the tumor tissue looking at changes in TS, ^{3}-H2AX, BCL-2, and Caspase 3 expression would be needed to determine if the mechanism is the same *in vivo* as it was observed *in vitro.*

During the extraction of the tumors after euthanasia, several of the tumors treated with 5-FU or the combination treatment were fluid-filled. This buildup of fluid in the hollow center of the tumors may have to be taken into account when analyzing the rate of growth. To determine whether these tumors have higher rates of necrotic cells surrounding the central cavity, histology analysis of the tumor samples will need to be conducted. Tumor sections should be analyzed to determine if there was an increase in cell death either by apoptosis or necrosis around the cavities versus the exterior of the tumor. Although the fluid should have been collected to determine if there was a difference in the type of fluid and volume between 5-FU and combination treatments,

it may be possible to examine the width and diameter of cavities in the tumor sections to determine if there was a size difference in the cavities.

There are many additional factors in the tumor microenvironment in an animal that are not present *in vitro*. HCT 116 colon cancer cells are often used to study some of these factors and their role in the development of resistance to chemotherapy treatments as HCT 116 cells can easily be made resistant to 5-FU (An and Ha 2016; Jin et al. 2016; Liu et al. 2016). Two such factors are the presence of inflammation and the effect of macrophage response. Tumor-associated macrophage (TAMs) respond to tumor cells by being activated to an M2 phenotype which in turn promote tumor development by enhancing proliferation, metastasis, angiogenesis, and immunosuppression (Colegio et al. 2014; Ding et al. 2015; Ghosh et al. 2015; Sousa et al. 2015; Zhou et al. 2015). It has also been shown that in response to 5-FU, TAMs secrete putrescine which makes colon cancer cells, including HCT 116, resistant to chemotherapy *in vitro* and *in vivo* (Zhang et al. 2016). The presence of fluid in the 5-FU and combination treated tumors suggests the presence of inflammation and an increased recruitment of macrophages. Examination of the tumor sections for the presence of TAMs may explain why the 5-FU and combination treatments caused an increase in tumor size or provide insight into the mechanism of resistance.

The increase tumor growth in mice treated with 5-FU or the combination therapy may be the result of low, frequent dose of 5-FU. Previous studies have shown this regimen to have been effective, however, other studies have reported the successful used higher, less frequent dosing regimens (Akindele et al. 2015; Pereira et al. 2016; Shi et al. 2014; Wang et al. 2014b; Zhao et al. 2010). A higher dose given once a week may cause an increase in the rate of cell death thereby limiting the occurrence of inflammation potentially resulting in less accumulation of

TAMs. It is also important to account for technical issues that may have affected the number of cells inoculated into the animals that may explain the occurrence of outliers at the onset of dosing. It is important to note that at this time there was no significant difference in tumor volume.

Flavone B did not show a significant reduction in tumor volume in this study. However, it did have a 48.00 ± 54.10% tumor grow inhibition compared to the control (data not shown). A greater difference between these two groups may have been seen if The experiment was terminated due to the size of the tumors on the 5-FU and combination groups. Furthermore, the examination of hepatic and kidney tissue may suggest the absence of deleterious effects by flavone B, supporting its antitumor or preventive activity in vivo

Further examination of the tissues collected from this study for toxic effects, indications of DNA damage and cells death, as well as, the presence of macrophage are needed before recommendations can be made involving further research with flavone A, flavone B, or the combination treatment.

REFERENCES

American Cancer Society. 2015. Cancer facts & figures 2015. Atlanta: American Caner Society.

American Cancer Society. 2016. Cancer facts & figures 2016. Atlanta: American Cancer Society.

An J, Ha EM. 2016. Combination therapy of lactobacillus plantarum supernatant and 5-fluouracil increases chemosensitivity in colorectal cancer cells. J Microbiol Biotechnol. 26(8):1490-1503.

Baig S, Seevasant I, Mohamad J, Mukheem A, Huri HZ, Kamarul T. 2016. Potential of apoptotic pathway-targeted cancer therapeutic research: Where do we stand? Cell Death Dis. 7:e2058.

Cheah KY, Howarth GS, Bindon KA, Kennedy JA, Bastian SE. 2014. Low molecular weight procyanidins from grape seeds enhance the impact of 5-fluorouracil chemotherapy on caco-2 human colon cancer cells. PloS one. 9(6):e98921.

Colegio OR, Chu NQ, Szabo AL, Chu T, Rhebergen AM, Jairam V, Cyrus N, Brokowski CE, Eisenbarth SC, Phillips GM et al. 2014. Functional polarization of tumour-associated macrophages by tumour-derived lactic acid. Nature. 513(7519):559-563.

Ding L, Liang G, Yao Z, Zhang J, Liu R, Chen H, Zhou Y, Wu H, Yang B, He Q. 2015. Metformin prevents cancer metastasis by inhibiting m2-like polarization of tumor associated macrophages. Oncotarget. 6(34):36441-36455.

Flynn RL, Zou L. 2011. Atr: A master conductor of cellular responses to DNA replication stress. Trends Biochem Sci. 36(3):133-140.

Fujinaka Y, Matsuoka K, Iimori M, Tuul M, Sakasai R, Yoshinaga K, Saeki H, Morita M, Kakeji Y, Gillespie DA et al. 2012. Atr-chk1 signaling pathway and homologous recombinational repair protect cells from 5-fluorouracil cytotoxicity. DNA Repair (Amst). 11(3):247-258.

Geng L, Huehls AM, Wagner JM, Huntoon CJ, Karnitz LM. 2011. Checkpoint signaling, base excision repair, and parp promote survival of colon cancer cells treated with 5-fluorodeoxyuridine but not 5-fluorouracil. PloS one. 6(12):e28862.

Ghosh S, Mukherjee S, Choudhury S, Gupta P, Adhikary A, Baral R, Chattopadhyay S. 2015. Reactive oxygen species in the tumor niche triggers altered activation of macrophages and immunosuppression: Role of fluoxetine. Cell Signal. 27(7):1398-1412.

Ghoshal K, Jacob ST. 1997. An alternative molecular mechanism of action of 5-fluorouracil, a potent anticancer drug. Biochem Pharmacol. 53(11):1569-1575.

Goldar S, Khaniani MS, Derakhshan SM, Baradaran B. 2015. Molecular mechanisms of apoptosis and roles in cancer development and treatment. Asian Pac J Cancer Prev. 16(6):2129-2144.

Gonzalez-Vallinas M, Molina S, Vicente G, de la Cueva A, Vargas T, Santoyo S, Garcia-Risco MR, Fornari T, Reglero G, Ramirez de Molina A. 2013. Antitumor effect of 5-fluorouracil is enhanced by rosemary extract in both drug sensitive and resistant colon cancer cells. Pharmacological research : the official journal of the Italian Pharmacological Society. 72:61-68.

Gu C, Qiao J, Zhu M, Du J, Shang W, Yin W, Wang W, Han M, Lu W. 2013. Preliminary evaluation of the interactions of panax ginseng and salvia miltiorrhiza bunge with 5-fluorouracil on pharmacokinetics in rats and pharmacodynamics in human cells. The American journal of Chinese medicine. 41(2):443-458.

Gyori BM, Venkatachalam G, Thiagarajan PS, Hsu D, Clement MV. 2014. Opencomet: An automated tool for comet assay image analysis. Redox Biol. 2:457-465.
Herrington MB, Takahashi I. 1973. Mutagenesis of bacteriophage pbs 2. Mutat Res. 20(2):275-278.
Hwang JT, Ha J, Park OJ. 2005. Combination of 5-fluorouracil and genistein induces apoptosis synergistically in chemo-resistant cancer cells through the modulation of ampk and cox-2 signaling pathways. Biochemical and biophysical research communications. 332(2):433-440.
Jin Y, Jiang Z, Guan X, Chen Y, Tang Q, Wang G, Wang X. 2016. Mir-450b-5p suppresses stemness and the development of chemoresistance by targeting sox2 in colorectal cancer. DNA Cell Biol. 35(5):249-256.
LeJeune TM, Tsui HY, Parsons LB, Miller GE, Whitted C, Lynch KE, Ramsauer RE, Patel JU, Wyatt JE, Street DS et al. 2015. Mechanism of action of two flavone isomers targeting cancer cells with varying cell differentiation status. PloS one. 10(11):e0142928.
Liu H, Yin Y, Hu Y, Feng Y, Bian Z, Yao S, Li M, You Q, Huang Z. 2016. Mir-139-5p sensitizes colorectal cancer cells to 5-fluorouracil by targeting notch-1. Pathol Res Pract. 212(7):643-649.
Longley DB, Harkin DP, Johnston PG. 2003. 5-fluorouracil: Mechanisms of action and clinical strategies. Nature reviews Cancer. 3(5):330-338.
Lonn U, Lonn S, Nylen U, Winblad G. 1989. 5-fluoropyrimidine-induced DNA damage in human colon adenocarcinoma and its augmentation by the nucleoside transport inhibitor dipyridamole. Cancer research. 49(5):1085-1089.
Olsson M, Zhivotovsky B. 2011. Caspases and cancer. Cell Death Differ. 18(9):1441-1449.
Peters GJ, Backus HH, Freemantle S, van Triest B, Codacci-Pisanelli G, van der Wilt CL, Smid K, Lunec J, Calvert AH, Marsh S et al. 2002. Induction of thymidylate synthase as a 5-fluorouracil resistance mechanism. Biochimica et biophysica acta. 1587(2-3):194-205.
Pujhari S, Baig TT, Zakhartchouk AN. 2014. Potential role of porcine reproductive and respiratory syndrome virus structural protein gp2 in apoptosis inhibition. BioMed research international. 2014:160505.
Rashid S, Ali N, Nafees S, Hasan SK, Sultana S. 2014. Mitigation of 5-fluorouracil induced renal toxicity by chrysin via targeting oxidative stress and apoptosis in wistar rats. Food and chemical toxicology : an international journal published for the British Industrial Biological Research Association. 66:185-193.
Riahi-Chebbi I, Haoues M, Essafi M, Zakraoui O, Fattouch S, Karoui H, Essafi-Benkhadir K. 2015. Quince peel polyphenolic extract blocks human colon adenocarcinoma ls174 cell growth and potentiates 5-fluorouracil efficacy. Cancer Cell Int. 16:1.
Schuetz JD, Wallace HJ, Diasio RB. 1984. 5-fluorouracil incorporation into DNA of cf-1 mouse bone marrow cells as a possible mechanism of toxicity. Cancer research. 44(4):1358-1363.
Sousa S, Brion R, Lintunen M, Kronqvist P, Sandholm J, Monkkonen J, Kellokumpu-Lehtinen PL, Lauttia S, Tynninen O, Joensuu H et al. 2015. Human breast cancer cells educate macrophages toward the m2 activation status. Breast Cancer Res. 17:101.
Srimuangwong K, Tocharus C, Tocharus J, Suksamrarn A, Chintana PY. 2012. Effects of hexahydrocurcumin in combination with 5-fluorouracil on dimethylhydrazine-induced colon cancer in rats. World journal of gastroenterology : WJG. 18(47):6951-6959.

Thomas CM, Wood RC, 3rd, Wyatt JE, Pendleton MH, Torrenegra RD, Rodriguez OE, Harirforoosh S, Ballester M, Lightner J, Krishnan K et al. 2012. Anti-neoplastic activity of two flavone isomers derived from gnaphalium elegans and achyrocline bogotensis. PloS one. 7(6):e39806.
Wang F, Dai W, Wang Y, Shen M, Chen K, Cheng P, Zhang Y, Wang C, Li J, Zheng Y et al. 2014. The synergistic in vitro and in vivo antitumor effect of combination therapy with salinomycin and 5-fluorouracil against hepatocellular carcinoma. PloS one. 9(5):e97414.
Woods D, Turchi JJ. 2013. Chemotherapy induced DNA damage response: Convergence of drugs and pathways. Cancer Biol Ther. 14(5):379-389.
Wu F, Chen WJ, Yan L, Tan GQ, Li WT, Zhu XJ, Ge XC, Liu JW, Wang BL. 2016. Mus81 knockdown improves chemosensitivity of hepatocellular carcinoma cells by inducing s-phase arrest and promoting apoptosis through chk1 pathway. Cancer Med. 5(2):370-385.
Zhang N, Yin Y, Xu SJ, Chen WS. 2008. 5-fluorouracil: Mechanisms of resistance and reversal strategies. Molecules. 13(8):1551-1569.
Zhang X, Chen Y, Hao L, Hou A, Chen X, Li Y, Wang R, Luo P, Ruan Z, Ou J et al. 2016. Macrophages induce resistance to 5-fluorouracil chemotherapy in colorectal cancer through the release of putrescine. Cancer letters. 381(2):305-313.
Zhou W, Ke SQ, Huang Z, Flavahan W, Fang X, Paul J, Wu L, Sloan AE, McLendon RE, Li X et al. 2015. Periostin secreted by glioblastoma stem cells recruits m2 tumour-associated macrophages and promotes malignant growth. Nat Cell Biol. 17(2):170-182.

CHAPTER 5

DISSCUSSION

The isomeric flavones, 5,7-dihydroxy-3,6,8-trimethoxy-2-phenyl-4H-chromen-4-one (5, 7–dihydroxy- 3, 6, 8 trimethoxy flavone/ flavone A) and 3,5-dihydroxy-6,7,8-trimethoxy-2-phenyl-4H-chromen-4-one (3, 5–dihydroxy-6, 7, 8–trimethoxy flavone/ flavone B), from G*naphalium elegans* and *Achyrocline bogotensis* have previously been shown to have antineoplastic activity against highly tumorigenic cancers of the colon, breast, prostate, and pancreas dependent on their differentiation status, while sparing normal cells *in vitro* (Thomas et al. 2012). The hydroxyl on carbon 7 and methoxy on the carbon 3 make flavone A more cytotoxic to better differentiated tumor cells whereas the reverse of these R groups makes flavone B more cytotoxic to more poorly differentiated tumor cells (Chapter 1, Figure 1). These series of studies investigated how these simple structural changes effects the pharmacokinetic, distribution, synergistic activity, and *in vivo* antitumor effects of these flavones.

In order to determine the pharmacokinetics of flavone A and flavone B, methods had to be developed to extract them from rat plasma. This was successfully done using acetonitrile as an organic solvent with recoveries for various concentrations ranging from 84-116% (Whitted et al. 2015). Reverse-phase high performance liquid chromatography quantification methods were developed that used different ratios of acetonitrile and water with acetic acid and triethylamine, as well as the selection of different internal standards (celecoxib and diclofenac). In order to obtain linear ($r^2 > 0.99$) calibration curves, the concentrations were divided into 2 sections for both flavones with ranges of 250-2,500 ng/mL and 2,500-100,000 ng/mL. Quantification was

good with inter-day coefficient of variation being d 22.44 and d 16.18 for flavone A and flavone B, respectively, and accuracies 83-111%.

These methods were used to determine the pharmacokinetics of a single 20 mg/kg IV bolus dose of either flavone A or flavone B. It was found that flavone A has a shorter half-life (83 vs 108 minutes) than flavone B, but both were found to have typical half-lives (< 120 minutes) as reported for flavonoids (Talbi et al. 2014; Yang et al. 2014; Zhang et al. 2014; Zhu et al. 2015). Flavone B did have a much higher volume of distribution (11463 mL/kg) than flavone A (986 mL/kg) which corresponded with its higher clearance (81 vs 13 mL/min/kg) and lower area under the curve (289 vs 2492 µg*min/mL).

The difference in pharmacokinetics was partially explained when colon and pancreatic tissues were examined for flavone A or flavone B. Filtration of the supernatant from centrifuged tissue homogenate by a polyvinylidene fluoride (PDVF) filter (0.45 µm) allowed for the extraction of either flavone. The HLPC methods developed for plasma resulted in good quantification of flavone A and flavone B from colon tissue homogenate (CV 0.88 -24.03 and 1.62-33.56, respectively) using one linear (r^2 >0.99) calibration curve, 250 – 100000 ng/g and 1000 – 25000 ng/g, respectively. However, the quantification method did not yield good CVs when quantifying flavone A or flavone B from pancreatic tissue homogenate (data not shown). The data did show that flavone B distributed to both the colon and the pancreas whereas flavone A only distributed to the colon, which could account for some of the difference in volume of distribution. These data indicated that both flavone A and flavone B would be viable candidates for *in vivo* colon cancer assays. However, only flavone B would be a good candidate for *in vivo* pancreatic cancer assays.

With both colon and pancreatic cancer having low 5 year survival rates reported by the American Cancer Society (American Cancer Society 2016) and having low response rates to current chemotherapies (Longley et al. 2003; Zhang et al. 2008), new or improved treatments are urgently needed. One way to improve the current treatment is to add a secondary therapy. Both flavone A and flavone B were tested for decreased cell viability when used in combination with gemcitabine or 5-fluorouracil (5-FU) against pancreatic cancer. This resulted in cell death similar to that seen with chemotherapy treatment alone.

However, when flavone A or flavone B were combined with 5-FU against colon cancer, there was a decrease in cell viability that was synergistic when compared to either treatment alone. Investigation into the mechanism via which the combination treatment increased cell death revealed that both flavone A and flavone B are capable of enhancing the amount of DNA damage caused by 5-FU by increase the amount of thymidylate synthase in complex preventing the conversion of dUMP to dTMP, thereby depleting dTTP from the nucleotide pool. This results in increase caspase 3 activation and apoptosis in cells treated with both 5-FU and flavone A/flavone B than those given an individual therapy.

Our data suggests that the synergistic effect observed in vitro, is not apparent in *in vivo,* when tumor volume is considered. However, this effect may be apparent in a different manner. As it has been shown in the previous chapter, when HCT 116 xenograft mice were treated with 5-FU or 5-FU plus flavone B, the tumor grew at an increased rate instead of the expected diminishing in size. This resulted in the combination treatment mice having significantly larger tumors in weight and volume. A possible explanation is that the synergistic effect could have resulted in increased inflammation involving tumor associated macrophages which have been previously shown to cause resistance of colon cancer cells to 5-FU and tumor proliferation as a

result of the low dose of 5-FU used (Colegio et al. 2014; Ding et al. 2015; Ghosh et al. 2015; Sousa et al. 2015; Zhang et al. 2016; Zhou et al. 2015). Further examination of the tumor tissue for DNA damage, cell death, and inflammation marker such as TAMs are needed to determine if there is indeed a synergistic effect by the combination these two agents in colon tumors

In the case of Flavone B our data suggest a slight decrease in tumor growth as compared to the control, that may have been clearly apparent if the experiment was not terminated due to high tumor size in 5-FU and the combination groups. The possible absence of renal or hepatic damage by histological examination in mice treated with flavone B alone, may warrant extending the HCT 116 xenograft experiment using just control and flavone B treated groups. Similarly, this experiments can be conducted to if flavone A has any antitumor activity against CaCo 2 xenografts.

In conclusion, based on our pharmacokinetics and tissue distribution studies, flavone A and flavone B are good candidates as individual treatments for colon cancer and flavone B maybe a good candidate for the treatment of pancreatic cancer. The fact that flavone A and flavone B target cells of varying differential status may provide an advantage for using them in combination *in vivo*. The results obtained *in vivo* in colon cancer warrant further exploration of using these as secondary therapies to 5-FU. Since the tumors in the 5-FU and combination groups are fluid filled, adjustment in the dose of 5-FU in combination with flavone A or flavone B may demonstrate a synergistic effect on colon tumors.

REFERENCES

Akindele AJ, Mahajan G, Wani ZA, Sharma S, Satti NK, Adeyemi OO, Mondhe DM, Saxena AK. 2015. Anticancer activity of the phytomedicine das-77. Integr Cancer Ther. 14(1):57-64.

American Cancer Society. 2014. Cancer facts & figures 2014. Altanta: American Cancer Society.

American Cancer Society. 2015. Cancer facts & figures 2015. Atlanta: American Caner Society.

American Cancer Society. 2016. Cancer facts & figures 2016. Atlanta: American Cancer Society.

An J, Ha EM. 2016. Combination therapy of lactobacillus plantarum supernatant and 5-fluouracil increases chemosensitivity in colorectal cancer cells. J Microbiol Biotechnol. 26(8):1490-1503.

Baig S, Seevasant I, Mohamad J, Mukheem A, Huri HZ, Kamarul T. 2016. Potential of apoptotic pathway-targeted cancer therapeutic research: Where do we stand? Cell Death Dis. 7:e2058.

Becher OJ, Holland EC. 2006. Genetically engineered models have advantages over xenografts for preclinical studies. Cancer research. 66(7):3355-3358, discussion 3358-3359.

Benariba N, Djaziri R, Bellakhdar W, Belkacem N, Kadiata M, Malaisse WJ, Sener A. 2013. Phytochemical screening and free radical scavenging activity of citrullus colocynthis seeds extracts. Asian Pacific Journal of Tropical Biomedicine. 3(1):35-40.

Boatright KM, Salvesen GS. 2003. Mechanisms of caspase activation. Curr Opin Cell Biol. 15(6):725-731.

Bonarska-Kujawa D, Cyboran S, Zylka R, Oszmianski J, Kleszczynska H. 2014. Biological activity of blackcurrant extracts (ribes nigrum l.) in relation to erythrocyte membranes. BioMed research international. 2014:783059.

Cai H, Verschoyle RD, Steward WP, Gescher AJ. 2003. Determination of the flavone tricin in human plasma by high-performance liquid chromatography. Biomedical chromatography : BMC. 17(7):435-439.

Chattopadhyay A, Chiang CW, Yang E. 2001. Bad/bcl-[x(l)] heterodimerization leads to bypass of g0/g1 arrest. Oncogene. 20(33):4507-4518.

Cheah KY, Howarth GS, Bindon KA, Kennedy JA, Bastian SE. 2014. Low molecular weight procyanidins from grape seeds enhance the impact of 5-fluorouracil chemotherapy on caco-2 human colon cancer cells. PloS one. 9(6):e98921.

Chiang LC, Ng LT, Lin IC, Kuo PL, Lin CC. 2006. Anti-proliferative effect of apigenin and its apoptotic induction in human hep g2 cells. Cancer letters. 237(2):207-214.

Chipuk JE, Kuwana T, Bouchier-Hayes L, Droin NM, Newmeyer DD, Schuler M, Green DR. 2004. Direct activation of bax by p53 mediates mitochondrial membrane permeabilization and apoptosis. Science. 303(5660):1010-1014.

Choudhary MI, Hareem S, Siddiqui H, Anjum S, Ali S, Atta Ur R, Zaidi MI. 2008. A benzil and isoflavone from iris tenuifolia. Phytochemistry. 69(9):1880-1885.

Choudhury D, Ganguli A, Dastidar DG, Acharya BR, Das A, Chakrabarti G. 2013. Apigenin shows synergistic anticancer activity with curcumin by binding at different sites of tubulin. Biochimie. 95(6):1297-1309.

Cohen GM. 1997. Caspases: The executioners of apoptosis. Biochem J. 326 (Pt 1):1-16.

Colegio OR, Chu NQ, Szabo AL, Chu T, Rhebergen AM, Jairam V, Cyrus N, Brokowski CE, Eisenbarth SC, Phillips GM et al. 2014. Functional polarization of tumour-associated macrophages by tumour-derived lactic acid. Nature. 513(7519):559-563.

Das S, Das J, Samadder A, Boujedaini N, Khuda-Bukhsh AR. 2012. Apigenin-induced apoptosis in a375 and a549 cells through selective action and dysfunction of mitochondria. Exp Biol Med (Maywood). 237(12):1433-1448.

Ding L, Liang G, Yao Z, Zhang J, Liu R, Chen H, Zhou Y, Wu H, Yang B, He Q. 2015. Metformin prevents cancer metastasis by inhibiting m2-like polarization of tumor associated macrophages. Oncotarget. 6(34):36441-36455.

Doleckova I, Rarova L, Gruz J, Vondrusova M, Strnad M, Krystof V. 2012. Antiproliferative and antiangiogenic effects of flavone eupatorin, an active constituent of chloroform extract of orthosiphon stamineus leaves. Fitoterapia. 83(6):1000-1007.

Dole•ková I, Rárová L, Grúz J, Vondrusová M, Strnad M, Kryatof V. 2012. Antiproliferative and antiangiogenic effects of flavone eupatorin, an active constituent of chloroform extract of orthosiphon stamineus leaves. Fitoterapia. 83(6):1000-1007.

Flynn RL, Zou L. 2011. Atr: A master conductor of cellular responses to DNA replication stress. Trends Biochem Sci. 36(3):133-140.

Fujinaka Y, Matsuoka K, Iimori M, Tuul M, Sakasai R, Yoshinaga K, Saeki H, Morita M, Kakeji Y, Gillespie DA et al. 2012. Atr-chk1 signaling pathway and homologous recombinational repair protect cells from 5-fluorouracil cytotoxicity. DNA Repair (Amst). 11(3):247-258.

Geng L, Huehls AM, Wagner JM, Huntoon CJ, Karnitz LM. 2011. Checkpoint signaling, base excision repair, and parp promote survival of colon cancer cells treated with 5-fluorodeoxyuridine but not 5-fluorouracil. PloS one. 6(12):e28862.

Geybels MS, Verhage BA, Arts IC, van Schooten FJ, Goldbohm RA, van den Brandt PA. 2013. Dietary flavonoid intake, black tea consumption, and risk of overall and advanced stage prostate cancer. American journal of epidemiology. 177(12):1388-1398.

Ghosh S, Mukherjee S, Choudhury S, Gupta P, Adhikary A, Baral R, Chattopadhyay S. 2015. Reactive oxygen species in the tumor niche triggers altered activation of macrophages and immunosuppression: Role of fluoxetine. Cell Signal. 27(7):1398-1412.

Ghoshal K, Jacob ST. 1997. An alternative molecular mechanism of action of 5-fluorouracil, a potent anticancer drug. Biochem Pharmacol. 53(11):1569-1575.

Goldar S, Khaniani MS, Derakhshan SM, Baradaran B. 2015. Molecular mechanisms of apoptosis and roles in cancer development and treatment. Asian Pac J Cancer Prev. 16(6):2129-2144.

Gonzalez-Vallinas M, Molina S, Vicente G, de la Cueva A, Vargas T, Santoyo S, Garcia-Risco MR, Fornari T, Reglero G, Ramirez de Molina A. 2013. Antitumor effect of 5-fluorouracil is enhanced by rosemary extract in both drug sensitive and resistant colon cancer cells. Pharmacological research : the official journal of the Italian Pharmacological Society. 72:61-68.

Gu C, Qiao J, Zhu M, Du J, Shang W, Yin W, Wang W, Han M, Lu W. 2013. Preliminary evaluation of the interactions of panax ginseng and salvia miltiorrhiza bunge with 5-fluorouracil on pharmacokinetics in rats and pharmacodynamics in human cells. The American journal of Chinese medicine. 41(2):443-458.

Gyori BM, Venkatachalam G, Thiagarajan PS, Hsu D, Clement MV. 2014. Opencomet: An automated tool for comet assay image analysis. Redox Biol. 2:457-465.

Ha US, Bae WJ, Kim SJ, Yoon BI, Hong SH, Lee JY, Hwang TK, Hwang SY, Wang Z, Kim SW. 2015. Anthocyanin induces apoptosis of du-145 cells in vitro and inhibits xenograft growth of prostate cancer. Yonsei Med J. 56(1):16-23.

Herreros-Villanueva M, Hijona E, Cosme A, Bujanda L. 2012. Mouse models of pancreatic cancer. World journal of gastroenterology : WJG. 18(12):1286-1294.

Hwang JT, Ha J, Park OJ. 2005. Combination of 5-fluorouracil and genistein induces apoptosis synergistically in chemo-resistant cancer cells through the modulation of ampk and cox-2 signaling pathways. Biochemical and biophysical research communications. 332(2):433-440.

Ito C, Itoigawa M, Tan HT, Tokuda H, Yang Mou X, Mukainaka T, Ishikawa T, Nishino H, Furukawa H. 2000. Anti-tumor-promoting effects of isoflavonoids on epstein-barr virus activation and two-stage mouse skin carcinogenesis. Cancer letters. 152(2):187-192.

Jin Y, Jiang Z, Guan X, Chen Y, Tang Q, Wang G, Wang X. 2016. Mir-450b-5p suppresses stemness and the development of chemoresistance by targeting sox2 in colorectal cancer. DNA Cell Biol. 35(5):249-256.

Kale A, Gawande S, Kotwal S. 2008. Cancer phytotherapeutics: Role for flavonoids at the cellular level. Phytother Res. 22(5):567-577.

Kandaswami C, Lee LT, Lee PP, Hwang JJ, Ke FC, Huang YT, Lee MT. 2005. The antitumor activities of flavonoids. In vivo. 19(5):895-909.

Khan N, Afaq F, Syed DN, Mukhtar H. 2008. Fisetin, a novel dietary flavonoid, causes apoptosis and cell cycle arrest in human prostate cancer lncap cells. Carcinogenesis. 29(5):1049-1056.

Killion JJ, Radinsky R, Fidler IJ. 1998. Orthotopic models are necessary to predict therapy of transplantable tumors in mice. Cancer Metastasis Rev. 17(3):279-284.

Konate K, Yomalan K, Sytar O, Zerbo P, Brestic M, Patrick VD, Gagniuc P, Barro N. 2014. Free radicals scavenging capacity, antidiabetic and antihypertensive activities of flavonoid-rich fractions from leaves of trichilia emetica and opilia amentacea in an animal model of type 2 diabetes mellitus. Evidence-based complementary and alternative medicine : eCAM. 2014:867075.

Lambert JD. 2013. Does tea prevent cancer? Evidence from laboratory and human intervention studies. The American journal of clinical nutrition. 98(6 Suppl):1667S-1675S.

LeJeune TM, Tsui HY, Parsons LB, Miller GE, Whitted C, Lynch KE, Ramsauer RE, Patel JU, Wyatt JE, Street DS et al. 2015. Mechanism of action of two flavone isomers targeting cancer cells with varying cell differentiation status. PloS one. 10(11):e0142928.

Lin YT, Wu YH, Tseng CK, Lin CK, Chen WC, Hsu YC, Lee JC. 2013. Green tea phenolic epicatechins inhibit hepatitis c virus replication via cycloxygenase-2 and attenuate virus-induced inflammation. PloS one. 8(1):e54466.

Liu H, Yin Y, Hu Y, Feng Y, Bian Z, Yao S, Li M, You Q, Huang Z. 2016. Mir-139-5p sensitizes colorectal cancer cells to 5-fluorouracil by targeting notch-1. Pathol Res Pract. 212(7):643-649.

Liu HL, Jiang WB, Xie MX. 2010. Flavonoids: Recent advances as anticancer drugs. Recent patents on anti-cancer drug discovery. 5(2):152-164.

Longley DB, Harkin DP, Johnston PG. 2003. 5-fluorouracil: Mechanisms of action and clinical strategies. Nature reviews Cancer. 3(5):330-338.

Lopez-Lazaro M. 2002. Flavonoids as anticancer agents: Structure-activity relationship study. Curr Med Chem Anticancer Agents. 2(6):691-714.

Middleton E, Jr., Kandaswami C, Theoharides TC. 2000. The effects of plant flavonoids on mammalian cells: Implications for inflammation, heart disease, and cancer. Pharmacological reviews. 52(4):673-751.
Mota KS, Dias GE, Pinto ME, Luiz-Ferreira A, Souza-Brito AR, Hiruma-Lima CA, Barbosa-Filho JM, Batista LM. 2009. Flavonoids with gastroprotective activity. Molecules. 14(3):979-1012.
Nagata S. 1997. Apoptosis by death factor. Cell. 88(3):355-365.
Niedergethmann M, Alves F, Neff JK, Heidrich B, Aramin N, Li L, Pilarsky C, Grutzmann R, Allgayer H, Post S et al. 2007. Gene expression profiling of liver metastases and tumour invasion in pancreatic cancer using an orthotopic scid mouse model. British journal of cancer. 97(10):1432-1440.
Olsson M, Zhivotovsky B. 2011. Caspases and cancer. Cell Death Differ. 18(9):1441-1449.
Pantavos A, Ruiter R, Feskens E, C Ed, Hofman A, B HS, O HF, J CK-d. 2014. Total dietary antioxidant capacity, individual antioxidant intake and breast cancer risk: The rotterdam study. International journal of cancer Journal international du cancer.
Park MH, Hong JE, Park ES, Yoon HS, Seo DW, Hyun BK, Han SB, Ham YW, Hwang BY, Hong JT. 2015. Anticancer effect of tectochrysin in colon cancer cell via suppression of nf-kappab activity and enhancement of death receptor expression. Mol Cancer. 14:124.
Pawlikowska-Pawlega B, Misiak LE, Jarosz-Wilkolazka A, Zarzyka B, Paduch R, Gawron A, Gruszecki WI. 2014. Biophysical characterization of genistein-membrane interaction and its correlation with biological effect on cells - the case of eypc liposomes and human erythrocyte membranes. Biochimica et biophysica acta. 1838(8):2127-2138.
Pereira DM, Simoes AE, Gomes SE, Castro RE, Carvalho T, Rodrigues CM, Borralho PM. 2016. Mek5/erk5 signaling inhibition increases colon cancer cell sensitivity to 5-fluorouracil through a p53-dependent mechanism. Oncotarget. 7(23):34322-34340.
Peters GJ, Backus HH, Freemantle S, van Triest B, Codacci-Pisanelli G, van der Wilt CL, Smid K, Lunec J, Calvert AH, Marsh S et al. 2002. Induction of thymidylate synthase as a 5-fluorouracil resistance mechanism. Biochimica et biophysica acta. 1587(2-3):194-205.
Pujhari S, Baig TT, Zakhartchouk AN. 2014. Potential role of porcine reproductive and respiratory syndrome virus structural protein gp2 in apoptosis inhibition. BioMed research international. 2014:160505.
Rashid S, Ali N, Nafees S, Hasan SK, Sultana S. 2014. Mitigation of 5-fluorouracil induced renal toxicity by chrysin via targeting oxidative stress and apoptosis in wistar rats. Food and chemical toxicology : an international journal published for the British Industrial Biological Research Association. 66:185-193.
Record IR, Broadbent JL, King RA, Dreosti IE, Head RJ, Tonkin AL. 1997. Genistein inhibits growth of b16 melanoma cells in vivo and in vitro and promotes differentiation in vitro. International journal of cancer Journal international du cancer. 72(5):860-864.
Riahi-Chebbi I, Haoues M, Essafi M, Zakraoui O, Fattouch S, Karoui H, Essafi-Benkhadir K. 2015. Quince peel polyphenolic extract blocks human colon adenocarcinoma ls174 cell growth and potentiates 5-fluorouracil efficacy. Cancer Cell Int. 16:1.
Robinson HM, Jones R, Walker M, Zachos G, Brown R, Cassidy J, Gillespie DA. 2006. Chk1-dependent slowing of s-phase progression protects dt40 b-lymphoma cells against killing by the nucleoside analogue 5-fluorouracil. Oncogene. 25(39):5359-5369.
Rossi M, Edefonti V, Parpinel M, Lagiou P, Franchi M, Ferraroni M, Decarli A, Zucchetto A, Serraino D, Dal Maso L et al. 2013. Proanthocyanidins and other flavonoids in relation to

endometrial cancer risk: A case-control study in italy. British journal of cancer. 109(7):1914-1920.
Shargel L, Wu-Pong S, Yu ABC. 2005. Applied biopharmaceutics & pharmacokinetics. New York: Appleton & Lange Reviews/McGraw-Hill, Medical Pub. Division.
Shi DB, Li XX, Zheng HT, Li DW, Cai GX, Peng JJ, Gu WL, Guan ZQ, Xu Y, Cai SJ. 2014. Icariin-mediated inhibition of nf-kappab activity enhances the in vitro and in vivo antitumour effect of 5-fluorouracil in colorectal cancer. Cell Biochem Biophys. 69(3):523-530.
Song H, Bao J, Wei Y, Chen Y, Mao X, Li J, Yang Z, Xue Y. 2015. Kaempferol inhibits gastric cancer tumor growth: An in vitro and in vivo study. Oncol Rep. 33(2):868-874.
Sousa S, Brion R, Lintunen M, Kronqvist P, Sandholm J, Monkkonen J, Kellokumpu-Lehtinen PL, Lauttia S, Tynninen O, Joensuu H et al. 2015. Human breast cancer cells educate macrophages toward the m2 activation status. Breast Cancer Res. 17:101.
Srimuangwong K, Tocharus C, Tocharus J, Suksamrarn A, Chintana PY. 2012. Effects of hexahydrocurcumin in combination with 5-fluorouracil on dimethylhydrazine-induced colon cancer in rats. World journal of gastroenterology : WJG. 18(47):6951-6959.
Surichan S, Androutsopoulos VP, Sifakis S, Koutala E, Tsatsakis A, Arroo RR, Boarder MR. 2012. Bioactivation of the citrus flavonoid nobiletin by cyp1 enzymes in mcf7 breast adenocarcinoma cells. Food and chemical toxicology : an international journal published for the British Industrial Biological Research Association. 50(9):3320-3328.
Talbi A, Zhao D, Liu Q, Li J, Fan A, Yang W, Han X, Chen X. 2014. Pharmacokinetics, tissue distribution, excretion and plasma protein binding studies of wogonin in rats. Molecules. 19(5):5538-5549.
Thomas CM, Wood RC, 3rd, Wyatt JE, Pendleton MH, Torrenegra RD, Rodriguez OE, Harirforoosh S, Ballester M, Lightner J, Krishnan K et al. 2012. Anti-neoplastic activity of two flavone isomers derived from gnaphalium elegans and achyrocline bogotensis. PloS one. 7(6):e39806.
Torrenegra RD, Escarria S, Raffelsberger B, Achenbach H. 1980. 5,7-dihydroxy-3,6,8-trimethoxyflavone from the flowers of gnaphalium elegans. Phytochemistry. (19):2795–2796.
Torrenegra RD, Escarria S, Tenorio E, Achenbach H. 1982. Estudio fitoquimico del achirocline bogotensis. Rev Latinoam Quim. (13):75–76.
Torrenegra RD, Pedrozo P, Rojas C, Carrizosa S. 1987. Plantas colombianas del ge´nero gnaphalium (iv) g. Rufescens y g. Antennarioides. Revista Latinoamericana de Quı´mica. (18):116–118.
Vermeulen E, Zamora-Ros R, Duell EJ, Lujan-Barroso L, Boeing H, Aleksandrova K, Bueno-de-Mesquita HB, Scalbert A, Romieu I, Fedirko V et al. 2013. Dietary flavonoid intake and esophageal cancer risk in the european prospective investigation into cancer and nutrition cohort. American journal of epidemiology. 178(4):570-581.
Wang F, Dai W, Wang Y, Shen M, Chen K, Cheng P, Zhang Y, Wang C, Li J, Zheng Y et al. 2014a. The synergistic in vitro and in vivo antitumor effect of combination therapy with salinomycin and 5-fluorouracil against hepatocellular carcinoma. PloS one. 9(5):e97414.
Wang HK. 2000. The therapeutic potential of flavonoids. Expert Opin Investig Drugs. 9(9):2103-2119.

Wang J, Yang ZR, Guo XF, Song J, Zhang JX, Wang J, Dong WG. 2014b. Synergistic effects of puerarin combined with 5-fluorouracil on esophageal cancer. Molecular medicine reports. 10(5):2535-2541.
Wang Y, Gapstur SM, Gaudet MM, Peterson JJ, Dwyer JT, McCullough ML. 2014c. Evidence for an association of dietary flavonoid intake with breast cancer risk by estrogen receptor status is limited. The Journal of nutrition. 144(10):1603-1611.
Wesolowska O, Wisniewski J, Duarte N, Ferreira MJ, Michalak K. 2007. Inhibition of mrp1 transport activity by phenolic and terpenic compounds isolated from euphorbia species. Anticancer research. 27(6B):4127-4133.
Whitted CL, Palau VE, Torrenegra RD, Harirforoosh S. 2015. Development of reversed-phase high performance liquid chromatography methods for quantification of two isomeric flavones and the application of the methods to pharmacokinetic studies in rats. J Chromatogr B Analyt Technol Biomed Life Sci. 1001:150-155.
Woods D, Turchi JJ. 2013. Chemotherapy induced DNA damage response: Convergence of drugs and pathways. Cancer Biol Ther. 14(5):379-389.
Wu CP, Calcagno AM, Hladky SB, Ambudkar SV, Barrand MA. 2005. Modulatory effects of plant phenols on human multidrug-resistance proteins 1, 4 and 5 (abcc1, 4 and 5). The FEBS journal. 272(18):4725-4740.
Wu F, Chen WJ, Yan L, Tan GQ, Li WT, Zhu XJ, Ge XC, Liu JW, Wang BL. 2016. Mus81 knockdown improves chemosensitivity of hepatocellular carcinoma cells by inducing s-phase arrest and promoting apoptosis through chk1 pathway. Cancer Med. 5(2):370-385.
Xiao Q, Park Y, Hollenbeck AR, Kitahara CM. 2014. Dietary flavonoid intake and thyroid cancer risk in the nih-aarp diet and health study. Cancer epidemiology, biomarkers & prevention : a publication of the American Association for Cancer Research, cosponsored by the American Society of Preventive Oncology. 23(6):1102-1108.
Xiao Z, Xue J, Sowin TJ, Rosenberg SH, Zhang H. 2005. A novel mechanism of checkpoint abrogation conferred by chk1 downregulation. Oncogene. 24(8):1403-1411.
Yang CS, Landau JM, Huang MT, Newmark HL. 2001. Inhibition of carcinogenesis by dietary polyphenolic compounds. Annual review of nutrition. 21:381-406.
Yang F, Song L, Wang H, Wang J, Xu Z, Xing N. 2015. Combination of quercetin and 2-methoxyestradiol enhances inhibition of human prostate cancer lncap and pc-3 cells xenograft tumor growth. PloS one. 10(5):e0128277.
Yang YF, Li Z, Xin WF, Wang YY, Zhang WS. 2014. Pharmacokinetics and brain distribution differences of baicalin in rat underlying the effect of panax notoginsenosides after intravenous administration. Chinese journal of natural medicines. 12(8):632-640.
Zamora-Ros R, Agudo A, Lujan-Barroso L, Romieu I, Ferrari P, Knaze V, Bueno-de-Mesquita HB, Leenders M, Travis RC, Navarro C et al. 2012. Dietary flavonoid and lignan intake and gastric adenocarcinoma risk in the european prospective investigation into cancer and nutrition (epic) study. The American journal of clinical nutrition. 96(6):1398-1408.
Zamora-Ros R, Fedirko V, Trichopoulou A, Gonzalez CA, Bamia C, Trepo E, Nothlings U, Duarte-Salles T, Serafini M, Bredsdorff L et al. 2013. Dietary flavonoid, lignan and antioxidant capacity and risk of hepatocellular carcinoma in the european prospective investigation into cancer and nutrition study. International journal of cancer Journal international du cancer. 133(10):2429-2443.
Zamora-Ros R, Sacerdote C, Ricceri F, Weiderpass E, Roswall N, Buckland G, St-Jules DE, Overvad K, Kyro C, Fagherazzi G et al. 2014. Flavonoid and lignan intake in relation to

bladder cancer risk in the european prospective investigation into cancer and nutrition (epic) study. British journal of cancer.
Zandi K, Teoh BT, Sam SS, Wong PF, Mustafa MR, Abubakar S. 2012. Novel antiviral activity of baicalein against dengue virus. BMC Complement Altern Med. 12:214.
Zhang N, Yin Y, Xu SJ, Chen WS. 2008. 5-fluorouracil: Mechanisms of resistance and reversal strategies. Molecules. 13(8):1551-1569.
Zhang WM, Li RF, Sun M, Hu DM, Qiu JF, Yan YH. 2014. Uplc-ms/ms method for determination of avicularin in rat plasma and its application to a pharmacokinetic study. J Chromatogr B Analyt Technol Biomed Life Sci. 965:107-111.
Zhang X, Chen Y, Hao L, Hou A, Chen X, Li Y, Wang R, Luo P, Ruan Z, Ou J et al. 2016. Macrophages induce resistance to 5-fluorouracil chemotherapy in colorectal cancer through the release of putrescine. Cancer letters. 381(2):305-313.
Zhao L, Chen Z, Wang J, Yang L, Zhao Q, Wang J, Qi Q, Mu R, You QD, Guo QL. 2010. Synergistic effect of 5-fluorouracil and the flavanoid oroxylin a on hepg2 human hepatocellular carcinoma and on h22 transplanted mice. Cancer chemotherapy and pharmacology. 65(3):481-489.
Zheng X, Wang W, Piao H, Xu W, Shi H, Zhao C. 2013. The genus gnaphalium l. (compositae): Phytochemical and pharmacological characteristics. Molecules. 18(7):8298-8318.
Zhou W, Ke SQ, Huang Z, Flavahan W, Fang X, Paul J, Wu L, Sloan AE, McLendon RE, Li X et al. 2015. Periostin secreted by glioblastoma stem cells recruits m2 tumour-associated macrophages and promotes malignant growth. Nat Cell Biol. 17(2):170-182.
Zhu S, Yan H, Niu K, Zhang S. 2015. Simultaneous determination of seven components from hawthorn leaves flavonoids in rat plasma by lc-ms/ms. J Chromatogr Sci. 53(6):909-914.
Zou H, Henzel WJ, Liu X, Lutschg A, Wang X. 1997. Apaf-1, a human protein homologous to c. Elegans ced-4, participates in cytochrome c-dependent activation of caspase-3. Cell. 90(3):405-413.

APPENDIX

Elsevier Copyright Policy

http://www.elsevier.com/about/company-information/policies/copyright/personal-use

As this is a retained right, no written permission from Elsevier is necessary.

As outlined in our permissions licenses, this extends to the posting to your university's digital repository of the thesis provided that if you include the published journal article (PJA) version, it is embedded in your thesis only and not separately downloadable:

19. Thesis/Dissertation: If your license is for use in a thesis/dissertation your thesis may be submitted to your institution in either print or electronic form. Should your thesis be published commercially, please reapply for permission. These requirements include permission for the Library and Archives of Canada to supply single copies, on demand, of the complete thesis and include permission for Proquest/UMI to supply single copies, on demand, of the complete thesis. Should your thesis be published commercially, please reapply for permission. Theses and dissertations which contain embedded PJAs as part of the formal submission can be posted publicly by the awarding institution with DOI links back to the formal publications on ScienceDirect.

Chapter 2: Crystal Whitted, Victoria Palau, Ruben Torrenegra, and Sam Harirforoosh. 2015. Development of reversed-phase high performance liquid chromatography methods for quantification of two isomeric flavones and the application of the methods to pharmacokinetic studies in rats. J*ournal of Chromatography B* http://dx.doi.org/10.1016/j.jchromb.2015.07.039

VITA

CRYSTAL WHITTED

Education:

B.S. Ecology and Evolutionary Biology, University of Tennessee, Knoxville, Tennessee 2002

M.S. Biology, New York University, New York, New York 2006

Ph. D Biomedical Science, East Tennessee University, Johnson City, Tennessee 2016

Experience:

Thesis Research, East Tennessee State University, Johnson City, Tennessee 2012-2016

Graduate Teaching Assistant, East Tennessee State University, Johnson City, Tennessee 2013-2015

Graduate Teaching Assistant, New York University, New York, New York 2005

Volunteer Laboratory Research, New York University, New York, New York 2004-2005

Office Manager, Whitted Excavation, Sevierville, Tennessee 2006-2008

Publications:

Crystal L. Whitted, Brian M. Cartwright, Zachary Walls, Yue Zou[2], Ruben D. Torrenegra, and Victoria E. Palau. Two isomeric flavones and 5-fluorouracil have synergistic activity against colon cancer *in vitro.* (IN PROGRESS)

Crystal L. Whitted, Victoria E. Palau, Ruben D. Torrenegra, Oscar E. Rodriguez, and Sam Harirforoosh. 2016 Quantification of two isomeric flavones in rat colon tissue using reverse phase high performance liquid chromatography. BMC (IN REVIEW)

Timothy M. LeJeune, Hei Yin Tsui, Laura B. Parsons, Gerald E. Miller, Crystal Whitted, Kayla E. Lynch, Robert E. Ramsauer, Jasmine U. Patel, Jarrett E.Wyatt, Doris S. Street, Carolyn B. Adams, Brian McPherson, Hei Man Tsui, Julie A. Evans, Christopher Livesay, Ruben D. Torrenegra, Victoria E. Palau. 2015 Mechanism of Action of Two Flavone Isomers Targeting Cancer Cells with Varying Cell Differentiation Status. PLOSONE|DOI:10.1371/journal.pone.0142928

Crystal Whitted, Victoria Palau, Ruben Torrenegra, and Sam Harirforoosh. 2015. Development of reversed-phase high performance liquid chromatography methods for quantification

of two isomeric flavones and the application of the methods to pharmacokinetic studies in rats. J*ournal of Chromatography B* http://dx.doi.org/10.1016/j.jchromb.2015.07.039

Abstracts

Crystal L. Whitted, Victoria E. Palau, Ruben D. Torrenegra, Oscar E. Rodriguez, and Sam Harirforoosh. 2016. The Use of Reverse Phase High Performance Liquid Chromatography to Determine 5, 7–dihydroxy-3, 6, 8–trimethoxy Flavone and 3, 5–dihydroxy-6, 7, 8–trimethoxy Flavone Concentrations in Rat Colon Tissue. Poster presentation at American Association of Pharmaceutical Scientists; Denver, CO,

Crystal Whitted, Michael Cartwright, Zachary Walls, Yue Zou, Ruben Torrenegra, and Victoria Palau. 2016 Two Isomeric Flavonoids Have a Synergistc Effect in Colon Cancer Cells When Used in Combination with 5-fluorouracil Due to Increased DNA Damage. Poster presentation at Appalachian Research Forum; Johnson City, TN

Beatrice Turner, Lilian Ikele, Ya Chang Liu, Matthew Abbott, Crystal Whitted, Ruben D. Torrenegra, Jeanet Rodriguez, and Victoria E. Palau. 2016. Effect of Gnaphalin on Cell Adhesion Proteins in Pancreatic and Colon Cancer. Poster presentation at Appalachian Research Forum; Johnson City, TN

John M. Jarrett, Joel K. Annor-Gyamfi, Crystal Whitted, Victoria E. Palau, Abbas G. Shilabin. 2016. Synthesis and *In-Vitro* Cell Viability/Cytotoxicity Studies of Novel Pyrrolobenzodiazepines. Poster presentation at The Capitol Event; Nashville, TN

Crystal L. Whitted, Angela V. Hanley, Kenneth W. Bullins, Derek E. Murrell, Victoria E. Palau, Ruben Torrenegra, and Sam Harirforoosh. 2015. Pharmacokinetics of 5,7-dihydroxy-3,6,8-trimethoxy-2-phenyl-4Hchromen-4-one in Rats. Poster presentation at American Association of Pharmaceutical Scientists; Orlando, FL

Turner, B., Ikele, L., Whitted, **C**., Torrenegra, R., Palau, VE. 2015. Gnaphalin a Flavonoid from *Gnaphalium gracile H.B.K.* has a Differential Apoptotic Effect on Pancreatic Cell Lines. Poster presentation at Appalachain Research Forum; Johnson City, TN

Ya Chang Liu, Cody Irick, Crystal Whitted, Ruben Torrenegra, Victoria Palau. 2015. Gnaphalin a Flavonoid Derived from *Gnaphlium gracile H.B.K.* has a Differential Cytotoxic Effect on Colon Cancer Cell Lines. Poster presentation at Appalachian Research Forum; Johnson City, TN

Erika Bowen, Shea Davis, Emily Dixon, Morgan Corbin, Crystal Whitted, Ruben Torrenegra, Victoria Palau. 2015. Evaluation of Flavone P on Pancreatic Cancer Cell Lines. Poster presentation at Appalachain Research Forum; Johnson City, TN